



UNIVERSITÀ DEL PIEMONTE ORIENTALE

Università degli Studi del Piemonte Orientale

Department of Health Sciences

Ph.D. Program

in Medical Sciences and Biotechnology

XXXIV cycle

**Two convergent ways for a better molecular
characterization and prediction to chemoradiation
in patients affected by IDH-wildtype glioblastoma**

Academic Discipline [SSD (Settore Scientifico Disciplinare)]:

MED/08 – Anatomia Patologica

Coordinator: Prof.ssa Marisa GARIGLIO

Tutor: Prof. Renzo Luciano BOLDORINI

PhD student: Dr. Paolo SPINA

Academic year 2023 – 2024

*A Domenico:
con te, è tutto più bello.*

INDEX

LIST OF ABBREVIATIONS	4
SUMMARY	7
RIASSUNTO	10
INTRODUCTION	13
AIM OF THE THESIS	37
PATIENTS AND METHODS	39
RESULTS	58
DISCUSSION	78
CONCLUSION AND FUTURE PERSPECTIVES	85
REFERENCES	87
RINGRAZIAMENTI	99

LIST OF ABBREVIATIONS

11C-MET	11C-methionine
18F-FDG	18F-fluorodeoxyglucose
18F-FDOPA	18F-fluorophenylalanine
18F-FET	18F-fluoroethyl-L-tyrosine
5-ALA	5-aminolevulinic acid
5hmC	5-hydroxymethylcytosine
5mC	5-methylcytosine
ADC	Apparent diffusion coefficient
C	Cytosine
CBV	Cerebral blood volume
CCNU	Lomustine
CDK4	Cyclin-dependent kinase 4
CDKN2A	Cyclin-dependent kinase inhibitor 2A
CDKN2B	Cyclin-dependent kinase inhibitor 2B
CI	Confidence interval
CLL	Chronic lymphocytic leukemia
CNS	Central Nervous System
CSF	Cerebrospinal fluid
Ct	Threshold cycle
ctDNA	circulating tumor DNA
DSC	Dynamic susceptibility contrast
EGFR	Epidermal growth factor receptor

EGFRvIII	Epidermal growth factor receptor variant III
EOC	Ente Ospedaliero Cantonale
FFPE	formalin-fixed paraffin-embedded
FISH	Fluorescent in situ hybridization
GBM	Glioblastoma
GFAP	Glial fibrillary acidic protein
GTR	Gross total resection
IDH	Isocitrate dehydrogenase
IHC	Immunohistochemistry
INA	Intercalating nucleic acid
IOSI	Oncology Institute of Southern Switzerland
IPN	Intercalating pseudo-nucleotide
iSTR	incomplete subtotal resection
LGG	Low-grade glioma
LOB	Limit of blank
LOD	Limit of detection
MGMT	O-6-methylguanine-DNA methyltransferase
MGMT-M	methylated MGMT
MGMT-UM	unmethylated MGMT
miRNA	microRNA
MMR	Mismatch repair
MRI	Magnetic resonance imaging
MRS	Magnetic resonance spectroscopy
MS-MLPA	Methyl-specific multiplex ligation-dependent probe amplification

MSP	Methylation-specific PCR
MSRE	Methylation-sensitive restriction enzyme
NF1	Neurofibromatosis type 1
NTC	No-template control
OS	Overall survival
PD-1	Programmed cell death protein-1
PDGFRA	Platelet-derived growth factor alpha
PET	Positron emission tomography
PFS	Progression-free survival
PTEN	Phosphatase and tensin homolog
RFU	Relative fluorescence unit
RTK	Receptor tyrosine kinase
STR	Subtotal resection
TAPS	TET-assisted pyridine borane sequencing
TERT	Telomerase reverse transcriptase
TET	Ten-eleven translocation
T _m	Melting temperature
TMZ	Temozolomide
U	Uracil
WHO	World Health Organization

SUMMARY

Introduction

Glioblastoma (GBM), the most common malignant brain tumor in adults, presents a challenging prognosis with a median survival of 12 to 15 months. Anticipating the effectiveness of treatments, especially chemotherapy and radiotherapy, is critical in GBM management.

Temozolomide (TMZ) is effective in GBM patients with MGMT promoter hypermethylation, found in about 40% of cases. For this type of molecular diagnosis, DNA methylation analysis faces challenges with standard PCR approaches, prompting the use of sodium bisulfite treatment, a time-consuming process with potential bias and DNA damage issues.

In addition, while MGMT promoter methylation is a crucial prognostic factor, it does not fully describe the disease's behavior. Emerging data suggest that altered miRNA expression may contribute to MGMT gene silencing, adding complexity to GBM molecular dynamics.

Aim of the thesis

This thesis is divided into two sections. The first explores specific miRNAs' impact on MGMT and prognosis in GBM patients, aiming to validate associations with TMZ treatment response. The second section introduces the novel EpiDirect[®] assay, developed in collaboration with a Danish company, for bisulfite-free DNA methylation analysis. The new assay is compared to existing bisulfite-dependent assays to assess sensitivity, specificity, and clinical utility.

Patients and methods

In the first part, MGMT expression, promoter methylation, and miRNA expression were analyzed in 112 GBMs using immunohistochemistry (IHC), methylation-specific PCR and real-time PCR experiments, respectively.

The second part focused on testing EpiDirect[®], a novel quantitative PCR (qPCR) platform. It utilizes the synergistic interaction between cytosine methylation and the DNA analog platform INA[®] to discriminate between methylated and unmethylated cytosines without pre-

treatment. The assay's performance was compared to two bisulfite-dependent methods for methyl-specific PCR using 42 brain tumor samples.

Results

In the first section of the study, MGMT promoter methylation was observed in 36.1% of assessable cases, and MGMT protein expression was absent in 44.9% of cases. Noteworthy, miRNA expressions included robust overexpression of miR-21 and miR-196b and downregulation of miR-767.3. Statistical analyses revealed significant associations between low miRNA expression and MGMT protein positivity in unmethylated cases, as well as associations with MGMT promoter methylation in methylated cases. Improved overall survival (OS) was noted in cases with negative MGMT protein expression, methylated patients, and with specific miRNA expressions. Additionally, superior progression-free survival (PFS) was linked to MGMT methylation and gross total resection.

In the second part, EpiDirect[®] demonstrated a sensitivity of 0.82 and specificity of 0.84 compared to the first method as a reference. When compared to the second method as a reference, sensitivity was 0.75, and specificity was 0.76. Notably, EpiDirect[®] identified 5 methylated samples missed by the comparator methods. EpiDirect[®] provided results in less than 2 hours, contrasting with the over 5 hours required by the comparator methods after DNA extraction, emphasizing its efficiency and speed.

Discussion

In the first section, the study focused on seven miRNAs and their role in modulating MGMT expression. Significant correlations were found between reduced expression of four miRNAs (miR-181c, miR-195, miR-648, and miR-767.3p) and MGMT protein expression, aligning with prior research indicating their downregulation in poor TMZ treatment responders. This emphasizes the potential of these miRNAs in influencing glioblastoma treatment responses and guiding therapeutic strategies. Another key finding is the confirmed correlation between miRNA expression, particularly miR-648, and MGMT methylation, highlighting the intricate relationship between miRNA expression and the epigenetic status of the MGMT gene.

Regarding clinical relevance, the study reaffirmed positive correlations between improved OS and PFS with MGMT promoter hypermethylation. Patients with negative IHC results also exhibited better clinical outcomes. Furthermore, four miRNAs (miR-21, miR-195, miR-

196b, and miR-648) demonstrated statistically significant associations with OS, suggesting their potential prognostic value in GBM patients.

In the second part, the challenges associated with existing MGMT methylation analysis methodologies were discussed, emphasizing the need for a balance between sensitivity, specificity, and practicality, especially when dealing with limited DNA samples. EpiDirect[®] was introduced as an innovative qPCR-based platform that eliminates the need for pre-treatment steps, offering a simplified and streamlined approach to DNA methylation analysis. The clinical validation revealed variations between methods, particularly in cases with low methylation levels, underscoring the importance of careful interpretation and validation, especially in such scenarios.

Conclusions and future perspectives

Our study, one of the first aimed to investigate multiple miRNAs in the same GBM cohort, highlights the potential of miRNA expression as an alternative method for assessing promoter methylation and regulating MGMT expression. If validated in larger GBM series, miRNA expression could become a diagnostic tool for predicting the efficacy of chemoradiation, offering more personalized therapeutic strategies.

EpiDirect[®], an innovative quantitative PCR-based DNA methylation analysis platform, is a breakthrough that streamlines the process by eliminating pre-treatment steps. Integrating EpiDirect[®] into diagnostics could save time, streamline workflows, and facilitate methylation analysis in resource-limited settings, promoting the adoption of advanced molecular techniques.

RIASSUNTO

Introduzione

Il glioblastoma (GBM), tumore cerebrale maligno primitivo più comune nell'adulto, ha una prognosi infausta, con una sopravvivenza mediana di 12-15 mesi. La previsione dell'efficacia dei trattamenti, in particolare della chemioterapia e della radioterapia, è fondamentale nella presa a carico del paziente affetto da GBM.

La terapia con temozolomide (TMZ) è efficace nei pazienti affetti da GBM con ipermetilazione del promotore di MGMT, riscontrata in circa il 40% dei casi. Per tale diagnosi molecolare, l'analisi della metilazione del DNA può essere particolarmente difficoltosa attraverso gli approcci standard delle analisi PCR, richiedendo l'uso del trattamento con bisolfito di sodio, un processo che richiede molto tempo e che può danneggiare il DNA.

Inoltre, sebbene la metilazione del promotore di MGMT sia un fattore prognostico cruciale, tale variabile non è completamente in grado di predire il comportamento della malattia. Dati emergenti suggeriscono che l'espressione alterata dei miRNA può contribuire al silenziamento del gene MGMT, aggiungendo complessità alle dinamiche molecolari del GBM.

Scopo della tesi

La tesi è divisa in due sezioni. La prima esplora l'impatto di specifici miRNA su MGMT e prognosi in pazienti affetti da GBM, con l'obiettivo di valutare l'associazione con la risposta al trattamento con TMZ. La seconda sezione prende in esame EpiDirect[®], una nuova metodica sviluppata in collaborazione con un'azienda danese per l'analisi della metilazione senza pretrattamento del DNA, confrontandola con test esistenti dipendenti dal bisolfito, per valutarne sensibilità, specificità e utilità clinica.

Pazienti e metodi

Nella prima parte, l'espressione di MGMT, la metilazione del promotore e l'espressione di miRNA sono state analizzate in 112 GBM rispettivamente mediante analisi immunohistochimica (IHC), PCR metilazione-specifica e real-time PCR.

La seconda parte si è concentrata sulla sperimentazione di EpiDirect[®], una nuova piattaforma di PCR quantitativa (qPCR). Essa utilizza l'interazione sinergica tra la metilazione della citosina e la piattaforma analoga del DNA INA[®] per discriminare tra citosine metilate e non metilate senza pretrattamento. Le prestazioni del test sono state confrontate con due metodi bisolfito-dipendenti per la PCR metil-specifica utilizzando 42 campioni di tumori cerebrali.

Risultati

Nella prima sezione dello studio, la metilazione del promotore di MGMT è stata osservata nel 36,1% dei casi valutabili e l'espressione della proteina MGMT era assente nel 44,9% dei casi. Le espressioni di miRNA degne di nota includevano una forte sovraespressione di miR-21 e miR-196b e l'iporegolazione di miR-767.3. Le analisi statistiche hanno rivelato associazioni significative tra la bassa espressione dei miRNA e la positività della proteina MGMT nei casi non metilati, nonché associazioni con la metilazione del promotore di MGMT nei casi metilati. È stata osservata una migliore sopravvivenza globale (OS) nei casi con espressione negativa della proteina MGMT, nei pazienti metilati e in quelli con espressione di specifici miRNA. Inoltre, una maggior sopravvivenza libera da progressione di malattia (PFS) era legata alla metilazione di MGMT e alla resezione tumorale completa.

Nella seconda parte, EpiDirect[®] ha dimostrato una sensibilità di 0,82 e una specificità di 0,84 rispetto al primo metodo di riferimento; rispetto al secondo metodo di riferimento, la sensibilità è stata di 0,75 e la specificità di 0,76. In particolare, EpiDirect[®] ha identificato 5 campioni metilati non individuati dai metodi di confronto. EpiDirect[®] ha fornito risultati in meno di 2 ore, a differenza delle oltre 5 ore richieste dai metodi di confronto dopo l'estrazione del DNA, sottolineando così la sua efficienza e velocità.

Discussione

Nella prima sezione, lo studio si è concentrato su 7 miRNA e sul loro ruolo nella modulazione di MGMT. Sono state riscontrate correlazioni significative tra la ridotta espressione di 4 miRNA (miR-181c, miR-195, miR-648 e miR-767.3p) e l'espressione della proteina MGMT, in linea con le ricerche precedenti che indicavano la loro iporegolazione nei pazienti con scarsa risposta al trattamento con TMZ. Questi dati sottolineano le potenzialità di tali miRNA nell'influenzare le risposte al trattamento del GBM e nel guidare le strategie terapeutiche. Un altro dato fondamentale è la conferma della correlazione tra l'espressione dei miRNA, in particolare di miR-648, e la metilazione di MGMT,

evidenziando la relazione tra l'espressione dei miRNA e lo stato epigenetico del gene MGMT.

Per quanto riguarda la rilevanza clinica, lo studio ha ribadito le correlazioni positive tra il miglioramento di OS e PFS e l'ipermetilazione del promotore di MGMT. Anche i pazienti con IHC negativa hanno mostrato esiti clinici migliori. Inoltre, 4 miRNA (miR-21, miR-195, miR-196b e miR-648) hanno dimostrato associazioni statisticamente significative con l'OS, suggerendone il potenziale valore prognostico nei pazienti con GBM.

Nella seconda parte sono state discusse le sfide associate alle attuali metodologie di analisi della metilazione di MGMT, sottolineando la necessità di un equilibrio tra sensibilità, specificità e praticità, soprattutto quando si ha a che fare con campioni di DNA limitati. EpiDirect[®] rappresenta una piattaforma innovativa basata su qPCR che elimina la necessità di fasi di pre-trattamento, offrendo un approccio semplificato e snello all'analisi della metilazione del DNA. La validazione clinica ha rivelato variazioni tra i metodi, in particolare nei casi con bassi livelli di metilazione, sottolineando l'importanza di un'attenta interpretazione e validazione dei dati, soprattutto in tali contesti.

Conclusioni e prospettive future

Il nostro studio, uno dei primi a indagare più miRNA nella stessa coorte di GBM, evidenzia il potenziale dell'espressione dei miRNA come metodo alternativo per valutare la metilazione del promotore e la regolazione dell'espressione di MGMT. Se convalidata in serie più ampie di GBM, l'espressione dei miRNA potrebbe diventare uno strumento diagnostico per prevedere l'efficacia della chemioradioterapia, offrendo strategie terapeutiche maggiormente personalizzate.

EpiDirect[®], un'innovativa piattaforma per l'analisi della metilazione del DNA basata su PCR quantitativa, costituisce un'innovazione che semplifica tale processo eliminando le fasi di pre-trattamento. L'integrazione di EpiDirect[®] nella pratica diagnostica potrebbe far risparmiare tempo, snellire i flussi di lavoro e facilitare l'analisi della metilazione in ambienti con risorse limitate, promuovendo al contempo l'adozione di tecniche molecolari avanzate.

INTRODUCTION

1. GLIOBLASTOMA

1.1. Epidemiology

Around 85,000 individuals receive a diagnosis of a primary brain tumor in the United States each year, with approximately 29% of them being classified as malignant [Schaff et al., 2023]. Among adults, roughly 80% to 85% of malignant brain tumors are gliomas, which have the characteristic of infiltrating the brain tissue extensively. In the fifth edition of the World Health Organization's (WHO) classification for Central Nervous System (CNS) tumors, which serves as the global standard for categorizing brain and spinal cord tumors, this category is referred to as "adult-type diffuse gliomas" [Louis et al., 2021]. In this group, glioblastoma (GBM), the most prevalent malignant primary brain tumor in adults, is responsible for the majority of fatalities among individuals with primary brain tumors. It tends to occur more frequently after the age of 40 and reaches its peak incidence in individuals aged 75 to 84 years [Wen et al., 2020]. Survival rates are negatively correlated with age: only 5% of all individuals diagnosed with GBM manage to survive for five years, and this percentage drops to 2% among patients aged 65 years or older [Ostrom et al., 2021]. Despite advancements in our comprehension of the biology underlying these tumors, we still need substantial enhancements in treatments or patient outcomes.

Fewer than 5% of adults diagnosed with malignant brain tumors have a reported family history of brain tumors or a predisposition syndrome for malignancy. Approximately 5% of all gliomas are considered familial, and there are several rare Mendelian inherited syndromes linked to adult glioma and GBM [Vijapura et al., 2017]. Interestingly, the occurrence of germline variants appears to be higher than expected, with as many as 13% of glioma patients carrying at least one harmful or likely harmful genetic alteration in their germline [Jonsson et al., 2019].

Through genome-wide association studies focused on genetic risk factors, researchers have confirmed the presence of 25 single nucleotide polymorphisms associated with an increased risk of glioma, including 11 that are specific to GBM. While the precise biological implications of these associations are still being investigated, this comprehensive genetic approach has identified regions containing key glioma-related genes, such as telomerase

reverse transcriptase (*TERT*), *RTEL1*, epidermal growth factor receptor (*EGFR*), and cyclin-dependent kinase inhibitor 2B (*CDKN2B*) [Melin et al., 2017]. Notably, most of these regions are associated with well-defined molecular subtypes of glioma [Labreche et al., 2018].

Previous exposure to ionizing radiation targeted at the central nervous system, typically as part of malignancy treatment, such as in the case of childhood leukemia, is a known risk factor for brain tumors [Braganza et al., 2012]. However, there is no established link between exposure to low-frequency electromagnetic fields and the development of brain tumors [International Agency for Research on Cancer Working Group on the Evaluation of Carcinogenic Risks to Humans; World Health Organization, 2023]. Additionally, there is a lack of high-quality evidence to support an association between cellular telephone use and the occurrence of brain tumors [Weed, 2022].

1.2. Molecular pathogenesis, genomics and characterization

The latest WHO classification has seen an expansion in the practice of genotyping for GBM [Louis et al., 2021]. The increasing prevalence of molecular profiling and the application of machine learning techniques have contributed to more precise prognostic assessments and tailored treatment strategies. The identification of novel mutations within GBM opens up opportunities for the development of new drugs targeting these mutations, while the correlation of mutations within tumors with distinct clinical courses enhances our ability to diagnose and predict disease severity.

In 2017, the establishment of cIMPACT-NOW (Consortium to Inform Molecular and Practical Approaches to central nervous system (CNS) Tumor Taxonomy) was announced. This consortium's purpose is to assess and propose revisions to the WHO classification of brain tumors, reflecting the evolving understanding of these tumors at the molecular level and their practical implications in clinical practice [Louis et al., 2017].

The latest WHO criteria and nomenclature introduced in 2021 have further emphasized the importance of molecular genetics in the diagnosis of GBM:

- a. Astrocytoma, *IDH*-mutant: previously, *IDH*-mutant tumors could be classified as diffuse astrocytoma, anaplastic astrocytoma, or GBM. However, the latest

classification now groups them together as a single type of *IDH*-mutant astrocytoma, graded 2, 3, or 4.

- b. Grading criteria: grading of *IDH*-mutant diffuse astrocytic tumors is no longer solely based on histology. It also considers the presence of the *CDKN2A/B* homozygous deletion mutation. This mutation leads to a CNS WHO grade of 4, even if microvascular proliferation or necrosis is absent.
- c. GBM, *IDH*-wildtype: the classification recognizes specific molecular markers for this tumor, included the presence of a *TERT* promoter mutation, *EGFR* gene amplification, and combined gain of the entire chromosome 7 and loss of the entire chromosome 10 (+7/-10). If any of these markers are present in an *IDH*-wildtype diffuse and astrocytic glioma in adults, the diagnosis should be GBM, *IDH*-wildtype.
- d. Pediatric patients: the diagnostic criteria for *IDH*-wildtype diffuse astrocytomas differ, and different types of pediatric-type gliomas are used for diagnosis [Louis et al., 2021].

IDH-wildtype GBMs are characterized by the absence of mutations in *IDH1* codon 132 and *IDH2* codon 172. They also do not carry mutations in H3 p.K28X (previously known as p.K27X) or H3 p.G35X (previously known as p.G34X) [Leske et al., 2021]. In patients aged 55 years or older at the time of diagnosis, who have a histologically classic GBM not located in midline structures and no history of a pre-existing lower-grade glioma, the absence of immunoreactivity for *IDH1* p.R132H is sufficient for the diagnosis of *IDH*-wildtype GBM [Louis et al., 2016]. Further DNA sequencing is not necessary in this case because the probability of non-canonical *IDH* mutations is very low, less than 1%, in GBMs from patients aged 55 years or older [Chen et al., 2014].

However, in patients aged less than 55 years, or in those with a history of lower-grade glioma and/or tumors that show immunohistochemical loss of nuclear ATRX expression, negative *IDH1* p.R132H immunostaining should be followed by DNA sequencing to check for less common *IDH1* or *IDH2* mutations. If no *IDH* mutations are detected by sequencing, these tumors are classified as GBM, *IDH*-wildtype [Capper et al., 2018a].

Tumors located in midline structures should also be evaluated for H3 p.K28M (previously known as K27M) mutation to exclude the possibility of diffuse midline glioma, H3 p.K27X-altered. In hemispheric tumors, especially in younger patients, it is important to rule out H3 p.G34X-mutant diffuse hemispheric gliomas through immunohistochemistry for H3.3

p.G35R (previously known as p.G34R) or H3.3 p.G35V (previously known as p.G34V) mutation or by sequencing of *H3-3A* (*H3F3A*) [Leske et al., 2021]. This comprehensive approach ensures an accurate diagnosis and appropriate classification of GBMs based on the presence or absence of specific genetic mutations.

Frequent and diagnostically relevant molecular alterations in *IDH*-wildtype GBMs include:

- a. *TERT* promoter mutations are commonly found in *IDH*-wildtype glioblastomas. These mutations are associated with increased telomerase activity and are important for tumor cell immortalization.
- b. Amplification of the *EGFR* is a hallmark genetic alteration in GBMs. It leads to overexpression of *EGFR*, which plays a crucial role in tumor growth and progression.
- c. The +7/−10 genotype refers to alterations involving chromosomes 7 and 10, typically involving gains of genetic material on chromosome 7 and losses on chromosome 10. These genetic changes are frequently observed in *IDH*-wildtype GBMs and contribute to their aggressive nature [Stichel et al., 2018].

The presence of at least one of these molecular aberrations in an *IDH*- and H3-wildtype diffuse glioma is sufficient for the diagnosis of *IDH*-wildtype GBM, even in the absence of microvascular proliferation and/or necrosis [Louis et al., 2020].

In addition to these genetic alterations, DNA methylation profiling has emerged as a valuable tool for diagnosing and stratifying GBMs. A significant calibrated score for the DNA methylation profile of *IDH*-wildtype GBM is sufficient for diagnosis. DNA methylation profiles can further classify GBMs into molecular subgroups, with the RTK1, RTK2/classic, and mesenchymal subgroups being the most common in adult patients [Capper et al., 2018b]. While the clinical relevance of methylation-based subgroups in adult patients is somewhat limited, high-grade gliomas in children and adolescents may exhibit less common DNA methylation profiles that are associated with significantly longer survival [Korshunov et al., 2017].

Overall, DNA methylation profiling can assist in diagnosing challenging cases and differentiating GBM from histologically similar entities, enhancing our understanding of the molecular diversity within this aggressive brain tumor [Capper et al., 2018a].

Molecular profiling has allowed researchers to identify common genetic mutations and core pathways shared among sporadic glioblastomas. Through analysis of gene expression and DNA methylation, leading to the identification of three primary GBM subgroups. Each subgroup is characterized by specific genetic alterations.

- a. Proneural Group is marked by proneural gene expression patterns and receptor tyrosine kinase (*RTK*) I/LGm6 DNA methylation profiles. It is often associated with amplifications of genes like cyclin-dependent kinase 4 (*CDK4*) and platelet-derived growth factor alpha (*PDGFRA*). This subgroup is more common among relatively younger adults.
- b. Classical Group exhibits classical gene expression patterns and classic-like *RTK II* DNA methylation profiles. It is characterized by a high frequency of *EGFR* amplifications and the loss of *CDKN2A/B* genes.
- c. Mesenchymal Group (mesenchymal/mesenchymal-like subtype) is enriched for tumors with neurofibromatosis type 1 (*NFI*) loss and increased tumor infiltration by macrophages [Wang et al., 2017].

These three distinct subgroups, along with mixed entities that exhibit characteristics from more than one subgroup, account for the majority of GBM. All of these subgroups are associated with mutations in the *TERT* promoter. While molecular classification has provided valuable insights and a framework for research, its clinical utility in GBM treatment remains uncertain. None of the GBM subtypes can reliably predict responses to current therapies. Additionally, assigning a specific subtype can be challenging in some cases, as tumors may exhibit multiple subtypes simultaneously, and subtypes may change over the course of the disease [Capper et al., 2018a].

Currently, the only predictive biomarker for treatment response to TMZ is the presence of MGMT-mediated DNA repair silencing. This silencing typically occurs due to *MGMT* promoter methylation and the loss of the second allele of chromosome 10 [Stupp et al., 2009; Reifenberger et al., 2014].

MGMT promoter methylation status is routinely assessed in *IDH*-wildtype GBMs because it provides valuable clinical information regarding the response to chemotherapy and patient survival [Weller et al., 2009]. Specifically, it helps predict how patients will respond to treatment with drugs like TMZ or TMZ plus lomustine (CCNU) [Hegi et al., 2005; Taal e

al., 2014; Weller et al., 2015]. In elderly patients, *MGMT* promoter methylation status can guide treatment decisions, helping determine whether chemotherapy or radiotherapy is the more appropriate course of action [Wick et al., 2012; Malmström et al., 2012].

Gene expression patterns have been extensively studied in gliomas and can be used to distinguish different types of brain tumors, such as GBM from pilocytic astrocytoma, other malignant astrocytomas, and oligodendroglioma. Additionally, gene expression patterns can help differentiate *IDH*-mutant gliomas from *IDH*-wildtype gliomas, regardless of grade and histology [Tandel et al., 2019].

Despite the wealth of information provided by gene expression profiles, they have not yet gained clear significance in routine clinical diagnostics for GBM. While they offer valuable insights into tumor biology and heterogeneity, their translation into routine clinical practice has been limited, and more research is needed to establish their clinical utility in guiding treatment decisions and predicting patient outcomes.

While the clinical utility of these glioblastoma subtypes is still being investigated, using the classifier to confirm a glioblastoma diagnosis can be beneficial in selected cases, especially in situations with unusual histopathology or when patients have experienced long-term survival, which may raise diagnostic uncertainties [Louis et al., 2017].

On the other hand, the presence of mutations in *IDH1/2* in adult diffuse gliomas is associated with extended patient survival. A quick and cost-effective initial screening method for *IDH* mutation is mutation-specific immunohistochemistry for the most common variant, *IDH1* p.R132H, which accounts for well over 90% of all *IDH* mutations in GBM. If this immunohistochemistry test is positive, it confirms the presence of an *IDH* mutation [Louis et al., 2021].

In cases where the initial immunohistochemistry is negative (i.e., “antibody-negative” GBM), further testing, such as targeted sequencing, may be considered. However, the decision to perform additional testing depends on various factors, including the patient’s age. *IDH* mutations, especially non-canonical ones, are exceptionally rare in older patients (more than 55 years). Additionally, GBMs that contain microthrombi and/or clear pseudopalisading necrosis upon initial diagnosis are very unlikely to have an *IDH* mutation [DeWitt et al., 2017].

Genomic profiling has significantly enhanced our comprehension of the molecular mechanisms underlying GBM and has uncovered potential avenues for developing targeted therapies tailored to specific groups of patients. Despite this progress, the overall treatment outcomes for individuals with GBM have not seen substantial improvements.

1.3. Clinical presentation

Headache is a common symptom, affecting nearly 50% of individuals newly diagnosed with a brain tumor [Schaff et al., 2023]. In cases of rapidly growing tumors, patients may experience increased intracranial pressure, leading to nausea, vomiting, and fatigue.

Depending on the tumor's location, patients may develop focal neurological deficits. Frontal tumors, in particular, can lead to personality changes and mood disorders, which are sometimes mistaken for psychogenic disorders or natural age-related changes, potentially delaying diagnosis.

Sensorimotor deficits are the initial symptom in approximately 20% of all GBM patients, while about 5% of patients present with aphasia, primarily when tumors arise in the speech-dominant hemisphere (typically the left side). Epilepsy can also mimic aphasia or sensorimotor deficits due to tissue damage post-seizure, and it is more common in GBMs affecting the temporal lobe. Epilepsy can either be a presenting symptom (in 24–68% of cases) or develop later in the disease course (in 19–38%). When epilepsy is a presenting symptom, it tends to be associated with longer survival, possibly because it is linked to younger age, cortical location, smaller tumor size (indicating better surgical options), and earlier diagnosis.

Interestingly, headaches are the initial symptom in less than one-third of all GBM patients. These headaches are usually dull in nature and tend to occur at night or upon waking. Other signs of increased intracranial pressure, such as nausea, vomiting, dizziness, fatigue, and cognitive impairment, tend to appear more as the disease progresses but can also be present at the time of diagnosis [Wirsching et al., 2016].

1.4. Diagnosis and imaging

The diagnostic tool of choice for GBM is a contrast-enhanced magnetic resonance imaging (MRI) scan. These tumors typically appear as an enhancing, necrotic-looking mass surrounded by non-enhancing signal abnormalities that consist of edema and infiltrative tumor. Hemorrhage, cystic changes, or multicentric enhancement are also frequently observed. When combined with the patient's clinical history, radiologists can often confidently diagnose GBM based on these MRI findings. However, challenges can arise because other intra-axial neoplasms, such as metastases, some lower-grade gliomas, and occasionally lymphomas, may exhibit similar imaging characteristics. Non-neoplastic neurological conditions like abscesses or demyelinating lesions can also appear similar on MRI [Ly et al., 2020].

MRI is invaluable for providing detailed anatomical information about the tumor and its relationship with adjacent brain structures, which is essential for surgical planning. When tumors are close to critical brain regions, functional MRI can assist in planning the optimal surgical approach to achieve maximal safe resection of the enhancing tumor, with the goal of improving patient survival [Ellingson et al., 2015].

For consistency and reliability, a standardized brain tumor imaging protocol is recommended for clinical trials and ideally should be incorporated into routine clinical imaging for GBM patients. Advanced MRI techniques are becoming increasingly available to evaluate the physiological and metabolic properties of GBM. Perfusion-weighted imaging, such as dynamic susceptibility contrast (DSC) MRI, measures cerebral blood volume (CBV), which correlates with microvessel density and area. Since increased microvascular proliferation due to tumor-induced angiogenesis is a characteristic of GBM, CBV can help differentiate glioblastoma from other tumor types or histological grades. DSC-MRI may also aid in distinguishing pseudoprogression, a response to radiotherapy and immunotherapies, from true progression, although both false-negative and false-positive results can occur [Gharzeddine et al., 2019].

The apparent diffusion coefficient (ADC), derived from diffusion-weighted MRI, inversely correlates with tumor cell density. ADC values for GBMs are higher than those for lower-grade gliomas but lower than those for lymphoma. Magnetic resonance spectroscopy (MRS) can detect changes in metabolite concentrations within the tumor. GBMs typically exhibit

significantly elevated choline levels due to increased cell proliferation and reduced N-acetyl aspartate due to neuronal loss. However, these changes are sensitive but not specific for GBM, as they can also be observed in other neoplastic or inflammatory conditions [Oz et al., 2014].

Positron emission tomography (PET) can provide additional insights into GBM biology, aid in differential diagnosis, delineate the extent of the tumor for surgical and radiotherapy planning, and monitor post-treatment changes (distinguishing progression from pseudoprogression). Amino acids are preferred PET tracers (such as ¹¹C-MET, ¹⁸F-FET, ¹⁸F-FDOPA) due to their higher specificity and lower signal-to-noise ratio compared to glucose (¹⁸F-FDG) [Law et al., 2019].

1.5. Histopathology and immunophenotype

GBMs are frequently large upon initial diagnosis and have the capacity to occupy a substantial portion of a brain lobe. They typically manifest as unilateral growths, but they can extend across the corpus callosum and affect both hemispheres, forming a characteristic “butterfly lesion”. Most often, hemispheric GBMs are primarily situated within the brain tissue (intraparenchymal) and are centered in the white matter. On rare occasions, they can be superficial, coming into contact with the protective membranes (leptomeninges) and the outermost layer (dura) of the brain, occasionally resembling metastatic growths or meningiomas. The infiltration into the cortical region may lead to the thickening of the overlying tan cortex, which sits atop a necrotic area within the white matter.

GBMs lack well-defined boundaries; when observed on a cut surface, their appearance varies. They often display a peripheral region with shades of greyish to pink masses surrounding central areas characterized by yellowish necrosis. In certain regions, necrotic tissue may abut adjacent brain structures directly, without a noticeable intermediate zone of macroscopically detectable tumor tissue. The central necrotic region can occupy a significant portion, sometimes as much as 80%, of the total tumor mass. GBMs frequently exhibit scattered red and brown areas representing recent and older hemorrhages. Extensive hemorrhages can occur, giving rise to stroke-like symptoms, occasionally serving as the initial indicators of the tumor. When macroscopic cysts are present, they contain a cloudy

fluid comprising liquefied necrotic tumor tissue. These cysts differ from the well-defined cysts found in lower-grade diffuse astrocytomas.

Microscopically, GBM is typically characterized as a diffusely infiltrating glioma with a high cell density. It primarily consists of astrocytic tumor cells that are often poorly differentiated, displaying nuclear abnormalities and significant pleomorphism. Most cases exhibit readily identifiable mitotic activity, often at a brisk pace. Two distinctive diagnostic features of GBM are microvascular proliferation and necrosis, sometimes accompanied by perinecrotic palisading. In the case of an *IDH*- and *H3*-wildtype diffuse glioma, the presence of either microvascular proliferation or necrosis is sufficient for a glioblastoma diagnosis. When examining specimens from patients who have undergone treatment, it becomes essential to differentiate between therapy-induced necrosis, particularly radionecrosis, and the inherent tumor necrosis.

The outdated term “GBM multiforme” highlights the histopathological variability of this tumor. Some lesions display a high degree of variation in cell shape and size, with numerous multinucleated giant cells. Others are highly cellular but relatively uniform in appearance. While the astrocytic nature of the neoplasms can be easily identified in some tumors, it may be challenging to recognize in poorly differentiated lesions.

The distribution of histological features within a GBM can vary, but typically, large necrotic regions are centrally located within the tumor, while viable tumor cells are more commonly found in the outer edges. The region of high cellularity and abnormal blood vessels that encircles the tumor, known as the contrast-enhancing ring, is often the target for biopsy due to its radiological visibility. Microvascular proliferation is a common feature throughout the tumor but is usually most pronounced around areas of necrosis and in the peripheral infiltrative zone.

GBMs exhibit a remarkable degree of morphological diversity, with poorly differentiated cells that may appear fusiform, round, or pleomorphic. However, better-differentiated neoplastic astrocytes can often be identified, at least in some areas. The transition between regions with recognizable astrocytic differentiation and highly anaplastic (small, round, and primitive-looking) cells can occur gradually or suddenly. In gemistocytic lesions, anaplastic tumor cells may be interspersed throughout the tumor, mixed with differentiated gemistocytes. An abrupt change in morphology may indicate the emergence of a distinct

tumor clone, possibly due to subclonal molecular diversification during the evolution of the tumor.

Cellular pleomorphism in GBMs encompasses various cell formations, including small, undifferentiated, spindled, lipidized, granular, epithelioid, and/or giant cells. In certain tumors, these patterns can become dominant, such as in regions with bipolar, fusiform cells arranged in intersecting bundles and fascicles, resembling a spindle cell sarcoma. The accumulation of epithelioid tumor cells characterized by well-defined plasma membranes and the absence of cell processes, as seen in epithelioid GBMs, can resemble metastatic carcinoma or melanoma [Louis et al., 2021].

Additionally, some GBMs exhibit well-recognized patterns that are characterized by a predominance of a particular cell type. These subtypes include:

- a. Giant cell GBM, distinguished by the presence of numerous giant cells within the tumor.
- b. Gliosarcoma, which contains both gliomatous and sarcomatous components, often showing spindle cell features.
- c. Epithelioid GBM, with an accumulation of epithelioid tumor cells with distinctive features, resembling epithelial cells.
- d. Small Cell GBM, which is characterized by the prevalence of small, densely packed tumor cells.
- e. GBM with a primitive neuronal component, with elements reminiscent of primitive neuronal cells.
- f. Granular cell GBM, identified by the presence of granular cells within the tumor.

These distinctive patterns and cell types contribute to the histological diversity observed in GBMs.

By definition, *IDH*-wildtype GBMs do not exhibit immunostaining for IDH1 p.R132H and do not show positivity with mutation-specific antibodies against H3 p.K28M, H3.3 p.G35R, or H3.3 p.G35V. The nuclear immunostaining for ATRX is usually retained in the majority of these tumors, while widespread nuclear positivity for p53 is observed in approximately

25-30% of cases. Nuclear p53 positivity is notably more frequent in the giant cell GBM subtype.

GBMs often express the glial fibrillary acidic protein (GFAP), but the degree of reactivity can vary significantly among cases. For instance, gemistocytic areas within the tumors are frequently strongly positive for GFAP, while primitive cellular components often lack GFAP expression. Expression of S100 protein is also common in GBMs.

OLIG2 is a highly specific marker for gliomas and can be diagnostically useful. It is more commonly strongly positive in astrocytomas and oligodendrogliomas than in ependymomas and non-glial tumors.

Cytokeratin positivity may primarily indicate cross-reactivity with GFAP. Immunostaining with the keratin antibody cocktail AE1/AE3 is often positive, particularly in contrast to most other keratins. However, GBMs with epithelial metaplasia may express epithelial markers, including cytokeratins, in the epithelial component.

In gliosarcomas, the sarcomatous components typically do not express glial markers but are positive for vimentin. In rare cases, they may express markers indicating differentiation along myogenic or other mesenchymal lineages.

Stem cell biomarkers such as CD133, CD44, SOX2, OCT4, and nestin may be present in GBMs but have limited diagnostic significance. Notably, intratumoral heterogeneity for immunohistochemical positivity is common in GBMs, with differential expression of markers like nestin, MAP2, and GFAP within different regions of the same tumor. Expression of EGFR is frequent in *IDH*-wildtype GBMs, especially in tumors with *EGFR* amplification [Louis et al., 2021].

1.6. Further molecular characterization

The genetic landscape of *IDH*-wildtype GBMs is complex, and various molecular alterations are associated with specific histological or morphological subtypes. Here are some key genetic findings related to different subtypes and patterns of *IDH*-wildtype GBMs:

- a. BRAF p.V600E mutation is relatively rare in *IDH*-wildtype GBMs but is detectable in up to 50% of GBMs with epithelioid histology. It is found in a high percentage

(79%) of pleomorphic xanthoastrocytoma-like tumors, 35% of adult-type *IDH*-wildtype GBMs, but not in pediatric RTK1 tumors [Korshunov et al., 2018].

- b. *TP53* mutations are detectable in approximately 25% of all *IDH*-wildtype GBMs. However, they are found in more than 80% of giant cell GBMs, which less commonly carry *EGFR* amplification and *TERT* promoter mutations.
- c. *EGFR* amplification appears to be frequent in small cell GBMs, which represent a distinct histological subtype within GBMs. *EGFR* is an important driver of cell growth and division in these tumors.
- d. *MYC* or *MYCN* amplification has been linked to primitive neuronal components within GBMs. These amplifications are associated with the presence of primitive neuronal features.
- e. Gliosarcomas, a rare subtype of GBM, typically do not demonstrate *EGFR* amplification or other distinguishing genetic alterations. Their genetic profile may be more similar to conventional GBMs [Oh et al., 2016].

It is important to note that none of these genetic alterations is specific or sufficient for defining the respective morphological subtypes or patterns of GBMs. The molecular characterization of these tumors is complex, and multiple genetic changes can occur within individual GBMs.

Following the initial treatment, which typically involves surgical resection, radiation therapy, and chemotherapy, distinct subgroups of tumor cells may emerge, exhibiting unique characteristics. For instance, approximately 10% of recurrent GBMs, occurring after treatment with temozolomide (TMZ), exhibit a significantly higher mutation rate [Körber et al., 2019].

This phenomenon of DNA “hypermutation” is often linked to underlying genetic deficiencies in DNA mismatch repair (MMR) genes. Furthermore, hypermutation can develop as a result of exposure to DNA alkylating agents, particularly in gliomas that have O6-methylguanine-DNA methyltransferase (*MGMT*) methylation, including those with isocitrate dehydrogenase (*IDH*) mutations [Touat et al., 2020].

When comparing tumor samples obtained at the time of diagnosis with those from recurrence, it is observed that roughly 80% of mutations and copy-number variations remain

consistent between the primary and recurrent tumors. Mutations in genes such as *PIK3CA*, *TERT*, and *EGFR* amplification that are found in the primary tumor typically persist in the recurrent tumor. In contrast, genetic events like amplifications of *PDGFRA*, mutations in *EGFR*, and the presence of the *EGFR* variant III (*EGFRvIII*) rearrangement are more likely to be lost. The most common genetic changes acquired in recurrent tumors include mutations in *TP53*, *EGFR*, and phosphatase and tensin homolog (*PTEN*) [Barthel et al., 2019].

Emerging sequencing technologies provide a deeper insight into intratumoral heterogeneity and the evolution of GBMs. Single-cell transcriptomics have revealed that glioblastomas are composed of cells representing each of the three gene expression subtypes, rather than fitting neatly into a single category. This supports earlier findings from bulk gene expression profiling of multiple tumor sectors.

Single-cell DNA profiling has confirmed previous observations made through fluorescent in situ hybridization (FISH), demonstrating that many GBMs consist of mixtures of subclones, each characterized by the amplification of a different RTK, such as *EGFR*, *PDGFRA* or *MET* [Wen et al., 2020].

Moreover, sequencing the circulating tumor DNA (ctDNA) present in cerebrospinal fluid (CSF) can provide a genetically accurate snapshot of the glioma genome in up to 50% of patients. This advancement may potentially eliminate the need for repeat tumor biopsies in certain cases. With ongoing technological advancements, it may also become feasible to evaluate plasma ctDNA in the future [Miller et al., 2019].

Furthermore, ongoing research is exploring novel predictive biomarkers for molecularly targeted therapies in subsets of GBM patients. These potential biomarkers include a high tumor mutation burden, BRAF p.V600E mutation, *NTRK* or *FGFR* gene family fusions, and *MET* amplification or fusions. These markers hold promise for tailoring therapeutic approaches in specific GBM subgroups and improving treatment outcomes.

2. TREATMENT OF GLIOBLASTOMA

Current treatment methods for GBM involve a combination of surgical procedures, radiotherapy, and chemotherapy. Notably, the addition of TMZ, an alkylating chemotherapy

agent, to the treatment regimen has represented a significant advancement. Additionally, the identification of specific gene mutations within tumor cells has become highly valuable for predicting outcomes and guiding targeted therapies.

However, it is important to note that GBM remains an incurable malignancy. It is the most aggressive form among diffuse gliomas of the astrocyte lineage, and in the majority of cases, patients face a median survival of less than 15 months. The primary goal of medical management is to diagnose the tumor through biopsy, extend and enhance the patient's quality of life.

Treatment typically involves a multimodal approach. Symptomatic treatment is crucial for addressing symptoms caused by local pressure damage to brain centers, which can include epilepsy, neurological deficits, hydrocephalus, and increased intracranial pressure.

Surgical intervention remains a central component of patient care and management. However, due to the difficulty of distinguishing tumor cells from healthy surrounding tissue and the phenomenon of tumor shedding, local recurrence can still occur despite achieving complete macroscopic resection of the tumor.

Surgical removal of all contrast-enhancing tumor tissue, known as gross total resection (GTR), has been associated with improved progression-free survival and overall survival in the treatment of GBM. One technique that has proven beneficial in aiding surgeons in achieving GTR is the use of 5-aminolevulinic acid (5-ALA), an optical imaging agent. 5-ALA helps in the visualization of malignant tissue during surgery, enhancing the ability of surgeons to distinguish tumor tissue from healthy one. This improved visualization has led to higher rates of GTR and has been linked to improved outcomes, including a better 6-month progression-free survival (PFS) rate [Molinaro et al., 2020].

The challenge of achieving clear surgical margins in GBM surgery is attributed to the presumed spread of tumor cells along neuronal fibers (neuropils) without noticeable macroscopic changes. This makes it difficult for surgeons to achieve microscopic resectability and completely cure the patient through surgery alone. Extensive resection is limited by the potential damage it can cause to critical nerve centers and pathways, which can significantly diminish the patient's quality of life and overall well-being [Hottinger et al., 2014; Kirstein et al., 2020].

Currently, the standard of care following surgical resection is fractionated adjuvant radiotherapy. This involves administering radiation therapy in fractions over a specified period. It is a crucial part of the treatment regimen.

Another important aspect of GBM treatment is chemotherapy. In 2005, a study led by Stupp et al. demonstrated the greater efficacy of combined treatment involving fractionated radiotherapy (administered in daily fractions of 2 Gy over 5 days per week for 6 weeks, totaling 60 Gy) along with concurrent TMZ administration (at a daily dose of 75 mg per square meter of body surface area, taken every day from the start to the end of radiotherapy). This was followed by six cycles of adjuvant TMZ (administered at a dose of 150 to 200 mg per square meter for 5 days during each 28-day cycle) compared to radiotherapy alone.

This combined approach demonstrated improved outcomes compared to radiotherapy alone, highlighting the importance of chemotherapy as a part of GBM treatment.

In the mentioned study, the effectiveness of TMZ was found to be greater when the *MGMT* promoter in GBM cells was methylated. Subsequent adjuvant chemotherapy with TMZ combined with radiotherapy (TMZ/RT → TMZ) significantly improved median survival, as well as 2- and 5-year survival rates. This approach is currently the standard of care for GBM patients who are under 70 years of age or even over 70 years old if they are in good physical condition. TMZ is typically administered daily during radiotherapy and then for 5 days every 4 weeks for six cycles as maintenance (adjuvant) therapy following the completion of radiotherapy. The methylation status of the *MGMT* gene promoter is a strong predictive marker, and patients with this mutation appear to derive the greatest benefit from chemotherapy.

However, it is worth noting that in rare cases, TMZ may lead to the development of myelodysplastic syndrome, acute myeloid leukemia, or even acute lymphoblastic leukemia. This risk underscores the importance of closely monitoring patients undergoing this treatment [Stupp et al., 2017].

Recurrence of GBM is unfortunately inevitable, typically occurring with a median PFS of approximately 7 months. To address this challenge, many patients undergo a second tumor resection, followed by additional chemotherapy with agents like nitrosoureas or TMZ. In the United States, bevacizumab is often used to manage symptoms caused by vasogenic oedema.

Despite ongoing research and development, many new drugs have not demonstrated efficacy in late-stage clinical trials, highlighting the difficulties in early clinical drug development for GBM. Unlike some other intracranial tumors that respond to small molecule inhibitors targeting oncogenic signaling pathways, such as everolimus, selumetinib, vemurafenib, ibrutinib, or belzutifan, GBMs have largely remained unresponsive to molecularly targeted therapy.

Immunotherapies like antibodies targeting the immune checkpoint inhibitor programmed death protein -1 (PD-1), such as pembrolizumab or nivolumab, have also not shown significant improvement in overall survival in phase 3 trials, despite their ability to modify the tumor microenvironment [Schaff et al., 2023].

Current research efforts are exploring alternative approaches, such as generating antitumor immunity through intratumoral injection of genetically engineered viruses like herpes simplex virus type 1, adenovirus, or poliovirus. These novel therapies aim to harness the immune system's potential to combat GBM, representing a promising avenue for future treatments.

Currently, there is no screening tool or test available to detect GBM before the onset of clinical symptoms. The gold standard for imaging studies to visualize GBM is MRI, which is crucial for diagnosis and treatment planning.

In summary, while advances have been made in the treatment of GBM, it remains a formidable challenge, and efforts are focused on prolonging patient survival and improving their quality of life.

3. *MGMT* GENE: ROLE, METHYLATION AND ANALYSIS IN GBM

MGMT gene is located on chromosome 10q26 and encodes a protein responsible for DNA repair. It plays a crucial role in removing alkyl groups from the O6 position of guanine, which is a critical site for DNA alkylation. *MGMT* function includes preventing the cross-linking of double-stranded DNA caused by alkylating agents. The expression levels of *MGMT* in gliomas can influence how patients respond to alkylating agents. The regulation of *MGMT* expression is primarily controlled by promoter methylation, an epigenetic

modification of the DNA, which leads to epigenetic silencing of the *MGMT* gene. Up to 45% of glioma patients exhibit *MGMT* promoter methylation [Hegi et al., 2005].

MGMT promoter methylation has significant clinical implications, particularly for GBM patients. Those with methylated *MGMT* tend to benefit from treatment with TMZ, while patients without methylation do not experience the same benefits. This phenomenon is consistent across different age groups. Additionally, the double inactivation of *MGMT* through promoter methylation and loss of chromosome 10q results in increased sensitivity to TMZ compared to either promoter methylation or 10q loss alone. The combination of *IDH* mutations and *MGMT* promoter methylation is associated with the most favorable response rates to TMZ and radiotherapy [Malmström et al., 2012].

However, some studies [Vuong et al 2020] have suggested that not all GBM patients with *MGMT* promoter methylation may benefit from TMZ therapy. They propose that only GBM patients who also have *TERT* mutations in addition to *MGMT* methylation may exhibit sensitivity to TMZ.

Furthermore, *MGMT* not only serves as a positive predictive factor for TMZ therapy but also functions as a positive prognostic marker. Several studies have reported that *MGMT* methylation predicts longer overall survival (OS) in GBM patients. Patients with both *IDH1* mutations and *MGMT* methylation tend to have longer survival times than those with only an *IDH1* mutation. PFS is also extended in patients with *MGMT* promoter methylation who receive TMZ [Mansouri et al., 2019; Radke et al., 2019].

Additionally, some research [Shah et al, 2011] has indicated that methylation at different sites within the *MGMT* promoter may have varying effects on PFS, highlighting the complexity of *MGMT* role in glioma prognosis and treatment response.

DNA methylation, particularly the methylation of cytosine, involves the addition of a methyl group to the fifth carbon of cytosine, resulting in the formation of 5-methylcytosine (5mC). Analyzing DNA methylation is a complex task due to several challenges associated with its detection.

One of the primary challenges is that DNA methylation cannot be directly analyzed using standard PCR techniques because methylation patterns are not preserved during the amplification process. To address this issue, the most commonly used methods for

methylation analysis involve a chemical conversion step called sodium bisulfite treatment before PCR, characterised by:

- a. Conversion of unmethylated cytosines (C) into uracils (U), while 5mC remains unchanged. This conversion introduces a sequence difference between unmethylated and methylated DNA at the cytosine positions.
- b. After bisulfite treatment, the modified DNA can be subjected to various analytical techniques to distinguish methylated from unmethylated cytosines. Two commonly used methods are:
 - Methyl-specific PCR (MSP) uses primers designed to specifically amplify either methylated or unmethylated DNA, allowing for the differentiation of methylation status [Herman et al., 1996].
 - Pyrosequencing is a quantitative method that can provide detailed information about the degree of methylation at specific cytosine sites [Colella et al., 2003].

It is important to note that different bisulfite conversion kits from various manufacturers may exhibit variations in recovery, conversion efficiency, and conversion specificity. These differences can potentially affect the precision and accuracy of methylation analysis, making it essential to choose appropriate kits and controls for research or clinical applications [Kint et al., 2018].

Lastly, because bisulfite treatment can be harsh on DNA and may introduce artifacts, efforts have been made to develop bisulfite-free methods for DNA methylation analysis. These alternative methods aim to provide more reliable and less damaging approaches for studying DNA methylation patterns.

Bisulfite-free methods for DNA methylation analysis are valuable alternatives to bisulfite-based approaches, as they can be less damaging to DNA and offer different advantages and limitations. One commonly used bisulfite-free method involves enzymatic digestion by methylation-sensitive restriction enzymes (MSREs) followed by methyl-specific multiplex ligation-dependent probe amplification (MS-MLPA). Here are some key points about this method and a newer technique called TET-assisted pyridine borane sequencing (TAPS):

- a. MSRE followed by MS-MLPA:

- Enzymatic digestion: MSREs are used to selectively cleave DNA at sites that are sensitive to methylation status. These enzymes recognize specific DNA sequences and cleave them only if they are unmethylated.
- MS-MLPA: after enzymatic digestion, the resulting DNA fragments can be analyzed using MS-MLPA, a method that combines multiplex ligation-dependent probe amplification with methylation-specific probes. This allows for the quantification of methylation levels at specific loci.
- Advantages: this approach is less harsh on DNA compared to bisulfite treatment and can provide valuable methylation information. However, it is limited to regions containing the recognition sites for the MSREs [Nygren et al., 2005].

b. TAPS:

- TAPS leverages the action of the enzyme TET (ten-eleven translocation) to oxidize 5mC to 5-hydroxymethylcytosine (5hmC) and further to unmodified cytosine. Then, pyridine borane treatment converts 5hmC to uracil (T) while leaving unmodified cytosine unchanged. Sequencing can then identify the presence of T (indicating 5mC or 5hmC) or C (indicating unmodified cytosine) at specific sites.
- Advantages and limitations: TAPS provides high-resolution methylation information at the base level but can be time-consuming and involves multiple steps, making it labor-intensive [Liu et al., 2019].

Each of these bisulfite-free methods has its own strengths and weaknesses, and the choice between them depends on the specific research goals and constraints of a given study. Researchers often select the method that best suits their needs in terms of precision, efficiency, and coverage of target regions.

4. miRNA

microRNAs (miRNAs) are small non-coding RNA molecules consisting of 19-22 nucleotides first described in *Caenorhabditis elegans* in 1993. Lee et al. discovered them and they proposed the existence of a class of regulatory genes producing small antisense RNAs influencing gene expression later to be known as microRNAs.

In 2001, the word microRNA was first introduced by Lagos-Quintana et al. who could show that many miRNAs are expressed in several species and are highly conserved. The main role of miRNAs is post-transcriptional regulation by sequence-specific repression of mRNAs. To date, more than 2000 miRNAs have been discovered in the human genome, which each regulates hundreds of targets including genetic pathways, indicating their role in gene regulation, disease development and also tumorigenesis.

Dysregulation of miRNAs due to gene deletions, amplifications and translocations or defects in the miRNA biogenesis machinery seem to be the mechanisms contributing to the malignant cell types eventually leading to malignancy.

In 2002, Calin et al. were the first to discover an association between miRNA dysregulation and malignancy: a deletion on chromosome 13q14 coding for the miR15 and miR16 genes was observed in more than half of the B-cell chronic lymphocytic leukemia (CLL) and deletions or down-regulations of miR-15 and miR-16 were observed in 68% of the CLL.

Further, in 2004, they published that miRNAs are either tumor suppressive or oncogenic depending on their location; located at regions of loss of heterozygosity suggests tumor suppressors, while located at regions of amplifications suggests oncogenes. miRNAs are commonly found at tumor-associated regions, in which loss of heterozygosity regions may contain tumor suppressor genes and amplifications harbor oncogenes or the other way around.

Another mechanism for dysregulation of miRNAs in malignancy apart from deletions and amplifications is the control of the transcription factors. The dysregulation of transcription factors regulating, for example, cell cycle progression, apoptosis, autophagy, invasion, and neoangiogenesis is tightly linked to tumor development.

Consequently, miRNAs also represent an innovative treatment option as prognostic and diagnostic biomarkers as well as therapeutic targets in malignancy therapy.

The most common upregulated miRNA in many malignancies is miR-21. miR-21 is an oncogenic miRNA inhibiting key regulator of apoptotic genes. It was first found to be significantly upregulated in human glioblastoma and its inhibition leads to increased caspase activation followed by apoptotic cell death. Therefore, miR-21 is an example of an oncogenic miRNA, in which upregulation is associated with tumorigenesis [Bautista-Sánchez et al., 2020]. Various bioinformatics and experimental studies have tried to identify a set of de-regulated miRNAs in GBM that are responsible for this tumor.

The following table (Fig. 1) gives an overview of some miRNAs already discovered in GBM, their targets (if known) and their prognostic value (if available).

microRNA	Regulation	Type	Target	Function	Prognosis
miR-10b	up	oncogenic	uPAR, RhoC	↑invasion ↑apoptosis, ↓cell	
miR-7	down	tumor suppressor	EGFR	proliferation, ↓migration, ↓invasion	
miR-17	up	oncogenic	DFFA, PI2KCA, E2F3m VEGFA, ATG7	↑autophagy	
miR-21	up	oncogenic	HNRPK, TAp63, PTEN, EGFR, E2F3, PDCD4, WNT5A	↓apoptosis, ↓autophagy, ↑invasion	
miR-26a	up	oncogenic	PTEN	↑tumor growth ↑angiogenesis	high level = longer OS and PFS with carmustine ↑TMZ resistance
miR-34a	down	tumor suppressor	E2F3, PI2KCA, EGFR, DFFA, CSL2, BAX, c-Met, Notch	↑cell cycle arrest, ↓invasion ↓migration ↓cell proliferation	
miR-92b-3p	up	oncogenic	PTEN	↑migration, ↑invasion ↓apoptosis	low level = shorter OS
miR-124	down	tumor suppressor	CDK6	↓cell cycle progression	
miR-125b	up	oncogenic	p53, p38MAPK, Bmf	↑proliferation, ↑cell cycle progression,	high level = higher grade
miR-128	down	tumor suppressor	RTKs, EGFR, PDGF-R, E2F3a	↓proliferation, ↑differentiation, ↓migration	
miR-130a	up	tumor suppressor	E2F8	ROS production	high level = extended survival without progression predictor for TMZ response
miR-137	down	tumor suppressor	CDK6	↓cell cycle progression	

microRNA	Regulation	Type	Target	Function	Prognosis
miR-142-3p	down	tumor suppressor	IL-6, HMGA2	↓cell viability	high levels = low MGMT low levels = high MGMT
miR-155	up	oncogenic	FOXO3a	↑proliferation, ↑migration, ↑invasion	low level = long OS
miR-181a	down	tumor suppressor	Bcl-2	↑apoptosis	
miR-181b	down	tumor suppressor	SALL4	↓proliferation, ↓migration, ↓invasion	
miR-181d	down	tumor suppressor	MGMT, Bcl-2, KRAS	↓proliferation, ↓cell cycle progression, ↑apoptosis	high level = improved OS
miR-210	up	oncogenic	SIN3A	↑proliferation, ↓apoptosis ↓invasion,	low level = long OS
miR-218	down	tumor suppressor	IKK-β, LEF1, Bmi1	↓migration, ↓proliferation, ↑apoptosis	
miR-221/222	up	oncogenic	p27, AKT, TIMP-3, PTEN, E2F3	↑proliferation, ↑invasion	up in short-term, down in long-term survivors, ↑TMZ sensitivity ↓long-term survival high level = extended survival without progression
miR-326	down	tumor suppressor	WNT5A, TOM34		
miR-335	up	oncogenic	DAAM1, PAX6	↑proliferation, ↑invasion	
miR-339	up	oncogenic		↑migration, ↑invasion ↓apoptosis	
miR-370-3p	down and up	tumor suppressor	β-catenin, FOXM1	↓cell proliferation ↓cell cycle progression	upregulation = inhibition of GBM growth long upregulation = longer survival
miR-409	down	tumor suppressor	HMGN5, cyclin D1, MMP2	↑invasion, ↑proliferation	
miR-451	down	tumor suppressor	Cyclin D1, p27, Bcl-2, MMP-2, MMP-9	↓cell cycle ↓cell growth ↑apoptosis ↓cell growth	
miR-603	up	oncogenic	WIF1, CTNNBIP1	↑proliferation, ↑cell cycle progression	

Figure 1. miRNAs in GBM: their targets, functions, and prognostic value (↓ = decreased, ↑ = increased) [Kirstein et al., 2020].

AIM OF THE THESIS

As already mentioned, one of the most important prognostic-predictive factors in GBM is methylation of the *MGMT* gene promoter. We also know this alone is not sufficient to describe the behaviour of the disease and its response to therapy: some studies have shown that patients with unmethylated tumors may experience an unexpected favorable outcome after radio-chemotherapy.

This seemingly paradoxical phenomenon can be explained in at least two ways:

1. on the one hand, since the discovery of the importance of the *MGMT* promoter methylation status in GBM therapy outcome, it is now known that the promoter methylation is not the only deterministic factor for *MGMT* protein expression;
2. on the other hand, the sensitivity of the techniques currently used to test for methylation of *MGMT* can result in false-negative results, so we consider tumours that are actually methylated to be unmethylated; moreover, different methods potentially leading to differences in precision between them.

For the first point, some studies have shown that mRNA expression was found to be low. One of this mechanisms affecting mRNA expression seems to be represented by miRNA expression. There are now data suggesting how changes in miRNA expression may lead to the degradation of *MGMT* mRNA, with the result of *MGMT* gene silencing. Indeed, these miRNAs affect GBM phenotype transition and malignant progression targeting more than 500 targets responsible for various biological processes such as cell proliferation, division, growth, and intercellular communication. The following table (Fig. 2) gives an overview of those miRNAs regulating *MGMT* expression, which were identified experimentally and which exhibit significant effects in cell lines:

microRNA	Regulation	Type	Prognosis
miR-142-3p	down	tumor suppressor	suppression of MGMT protein ↑TMZ sensitivity
miR-181d	down	tumor suppressor	degradation of MGMT mRNA; high level = improved OS
miR-221/222	up	oncogenic	suppression of MGMT; ↑TMZ sensitivity
miR-370-3p	down and up	tumor suppressor	regulatory effects on MGMT; ↑TMZ sensitivity
miR-409-3p	up	oncogenic	repression of MGMT
miR-603	up	oncogenic	suppression of MGMT ↑TMZ sensitivity
miR-648	up	tumor suppressor	inhibition of MGMT protein translation
miR-767-3p	up	tumor suppressor	degradation of MGMT mRNA

Figure 2. miRNAs involved in MGMT regulation in GBM (↓ = decreased, ↑ = increased) [Kirstein et al., 2020].

For this reason, one part of this thesis focuses on the influence of specific miRNAs (i.e., miR-21, miR-195, miR-767-3p, miR-196b, miR-648, miR-181d, miR-181c) on *MGMT* and consequently on prognosis, leading to investigate the pattern of miRNA expression and its correlation to TMZ sensitivity by analyzing a large cohort of GBM patients, comprehensive of patients' clinical outcome. The primary objective of this part of the study is to verify whether a pattern of miRNA expression correlates with response to the treatment with TMZ and its clinical efficacy, while the secondary objective is to verify if a cumulative panel of markers may identify a group of patients experiencing a better outcome after the administration of standard TMZ therapy combined with radiotherapy.

As for the second part, in collaboration with a Danish company, we set-up and validated a new assay, based on a bisulfite-free analysis method, called EpiDirect[®], that allows for direct PCR quantification of DNA methylations using untreated DNA compared to two bisulfite-relying, methyl-specific PCR assays, in order to evaluate its sensitivity, specificity, and clinical utility.

PATIENTS AND METHODS

1. ABOUT miRNA EXPRESSION AND ITS CORRELATION WITH RESPONSE TO STANDARD THERAPY

Retrospective data were gathered from two prominent neurosurgical centers located in two European countries: the Service of Neurosurgery at the Neurocenter of Southern Switzerland, EOC, Switzerland, and the Department of Neurosurgery at Insubria University Hospital, Italy. This data collection spanned over a ten-year period, from 2004 to 2013. The study was conducted in full compliance with the established protocol, the most recent Declaration of Helsinki, the ICH-GCP (Good Clinical Practice) guidelines, and ISO EN 14155, whenever applicable. Additionally, the study adhered to all national legal and regulatory requirements. Data and specimens were collected and analyzed solely for the purposes of this study after receiving the necessary approvals from the Cantonal Ethics Committee in Bellinzona, Switzerland (Reference: CE 3086-2016-01108).

For each patient, the collected data encompassed information such as gender, age, the type of surgical procedure performed, postoperative outcomes, postoperative complications, and their overall follow-up until the time of their demise. All data were sourced from the electronic medical records of the two respective institutions.

Inclusion criteria comprised patients aged over 18 years, confirmed histological diagnosis of *IDH*-wildtype GBM, WHO grade 4, treatment following the Stupp scheme (comprising 60 Gray radiotherapy and concomitant TMZ chemotherapy, followed by six cycles of maintenance TMZ), death resulting from GBM, and the availability of tissue, preserved in the archives, for biomolecular analyses.

Exclusion criteria encompassed individuals with an unclear GBM diagnosis or those with low-grade gliomas (LGGs), pediatric patients under the age of 18, patients who followed treatment schemes outside the Stupp protocol, and those whose demise was attributed to causes other than GBM.

The OS, defined as the duration from the surgical procedure to the date of death, and PFS, defined as the time from the initiation of the first radio-chemotherapy treatment to the date

of clinical or radiological progression in accordance with the RANO criteria, were subjected to analysis. Concerning the type of surgery, three categories were established based on the postoperative MRI performed within the initial 72 hours: Gross Total Resection (GTR, characterized by the absence of contrast-enhancing residual tissue visible on T1-injected MRI sequences), incomplete Subtotal Resection (iSTR, marked by evidence of contrast-enhancing residual tumor), and Biopsy.

1.1. Histological and molecular analysis

The pathological assessment was carried out by two expert pathologists at the Institute of Pathology, EOC, in Locarno, Switzerland. Each sample underwent an evaluation of *MGMT* promoter methylation, *MGMT* immunohistochemistry (IHC), and miRNA expression analysis.

1.1.1 MGMT promoter methylation

Genomic DNA for *MGMT* methylation analyses was extracted from three 8 µm thick formalin-fixed, paraffin-embedded (FFPE) tumor sections using an automated extraction method (Maxwell system, Promega, Madison, WI, USA). Approximately 100 ng of DNA from each sample underwent bisulfite treatment, which was accomplished using the EZ DNA Methylation-Gold™ kit (Zymo Research, Irvine, CA, USA).

Subsequently, the methylation status was determined through PCR-pyrosequencing employing the MGMTPlus kit, following the recommended protocol (Diatech Pharmacogenetics, Jesi, Italy). This assay assessed the methylation of six consecutive cytosines within the *MGMT* promoter (located at chr10:131,265,507–131,265,556). The presence of methylation was ascertained using a threshold of 10%. This threshold value was established by calculating the limit based on negative controls, specifically DNA samples from 15 FFPE healthy brain tissues. The calculation involved the mean of the methylation ratio, adding twice the standard deviation, assuming a Gaussian distribution of the raw signal from the negative samples.

1.1.2 MGMT immunohistochemistry

To prepare the tissue samples for IHC analysis, three sections, each measuring 1–2 μm in thickness, were obtained from whole FFPE tissue. These sections were subjected to a deparaffinization and rehydration process. Subsequently, they were pretreated with citrate buffer at a $\text{pH} = 6$ in a microwave oven for a duration of 20 minutes. Following this, the sections were treated overnight with the primary antibody, anti-MGMT (clone MT3.1, Chemicon International, Temecula, CA, USA), and diluted at a ratio of 1/400. This was followed by the application of a polymeric detection system (Ultravision DAB Detection System, LabVision, Fremont, CA, USA), following the manufacturer's instructions.

In line with existing literature, MGMT IHC positivity was determined when more than 5% of neoplastic cells displayed intense nuclear staining [Brell et al., 2011; Cao et al., 2009]. Two pathologists independently assessed and scored the IHC results.

1.1.3 miRNA analysis

For miRNA extraction, three 10 μm thick FFPE tumor sections were processed using the RecoverAll™ Total Nucleic Acid Isolation Kit for FFPE, following the manufacturer's instructions (ThermoFisher Scientific, Waltham, MA, USA).

Specifically, miRNA-specific reverse transcription was carried out using the TaqMan® MicroRNA Reverse Transcription Kit and 5X primers included in inventoried TaqMan MicroRNA assays (Life Technologies). The miRNAs analyzed included miR-21, miR-195, miR-767-3p, miR-196b, miR-648, miR-181d, miR-181c, and RNU6B (utilized as an endogenous control). Each sample underwent analysis in triplicate using Universal Master Mix and assays from TaqMan MicroRNA assays (Life Technologies) as per the manufacturer's recommendations.

As calibration samples, 12 normal brain specimens from patients with cerebral arteriovenous malformations were chosen. The relative miRNA expression levels were calculated using the Livak method.

1.2. Statistical analysis

At first, mean and median values were calculated to summarize the results of each variable. The relative chi-square, $\text{CHI}_{\text{rel}}^2$, describes the statistical association existing among pairs of variables:

$$x_{\text{rel}}^2 = \frac{1}{x_{\text{max}}^2} \sum_i \sum_j \frac{(n_{i,j} - \hat{n}_{i,j})^2}{\hat{n}_{i,j}}$$

where $n_{i,j}$ indicates the number of patients observed in row i and column j of the contingency table, \hat{n} is the expected value of counts given the statistical independence of the two considered variables, and with

$$x_{\text{max}}^2 = N \cdot \min(m_R - 1, m_C - 1)$$

the maximum value taken by the chi-square statistic when the sample size is N and the contingency tables has m_R rows and m_C columns. The relative chi-square takes values in $[0, 1]$, with 0 indicating the lack of statistical association.

OS and PFS curves for censored data were obtained using the Kaplan–Meier estimator.

$$\hat{S}(t) = \prod_{i:t_i \leq t} \left(1 - \frac{d_i}{n_i}\right)$$

which is the estimate of the probability that life is longer than t ; furthermore, t_i is a time when at least one event (death) was observed, d_i is the number of events (deaths) that happened at time t_i , and n_i represents the individuals known to have survived up to time t_i . Comparisons of curves given different molecular characterizations were performed by logrank tests. PFS curves were also estimated and tested within strata defined by the variable of surgery.

Log-rank tests were conducted to assess whether there were significant differences among the survival curves of groups defined by an explanatory variable [Bogaerts et al, 2018]. All the analyses, as well as the creation of graphs and reports, were carried out using the R software and the following R packages: “bootstrap” and “survival”.

Regarding miRNA expression, it is important to note that there are no established and validated cut-off values for GBM, or for that matter, in other diseases, especially in real-time experiments. Therefore, three different cut-off values for evaluating positive cases were

applied based on similar studies found in the literature: Cut-off > 3, Cut-off > 1, and Cut-off > the median value. In this study, we present results using a cut-off > 3, which is considered a robust approach for evaluating miRNA expression and is a cut-off value that we have previously published in a different paper [Forcella et al., 2018; Cardia et al., 2023]. Using a cut-off > 1 only considers slight deviations as clinically relevant, while employing a cut-off equal to the median values might produce results that are too dependent on the specific patient cohort.

2. ABOUT DIRECT PCR QUANTIFICATION OF METHYLATIONS USING UNTREATED DNA

In this study, we have harnessed the physicochemical characteristics of 5mC to develop a qPCR platform for DNA methylation analysis without the need for any prior DNA treatment. We achieve this by employing a DNA analog platform known as Intercalating Nucleic Acid (INA[®]), which impacts the π -stacking interactions within DNA.

In brief, the stability of double-stranded DNA results from the combination of Watson-Crick base-pairing and base-stacking interactions. It has been established that the latter, base-stacking, is the primary stabilizing force in the DNA double helix. This effect arises from the interactions between the π -electrons and is consequently referred to as π -stacking. Notably, even though 5mC doesn't participate in Watson-Crick base-pairing, it has been observed to influence the thermal stability of DNA duplexes.

INA[®] incorporates at least one nucleobase analog, referred to as an intercalating pseudo-nucleotide (IPN), which consists of a flat, conjugated aromatic or heteroaromatic ring system. This IPN is strategically linked to the phosphodiester backbone at predetermined positions within a synthetically designed oligonucleotide. The IPN effectively stacks alongside adjacent nucleobases, enhancing the π -stacking energy of the DNA helix and consequently raising the melting temperature (T_m). The properties of INA[®] have found various applications, including the sensitive detection of single-point mutations in DNA.

We introduce a novel property of INA[®] which involves a noticeable distinction in the stacking behavior when it interacts with 5mC as opposed to cytosine. This distinction is

reflected in the increased thermal stability of methylated DNA compared to non-methylated DNA. We have harnessed this effect to develop a new qPCR platform for the direct detection and quantification of DNA methylation, eliminating the need for any prior treatment of the template DNA. We have named this method EpiDirect[®].

EpiDirect[®] relies on a unique primer design, referred to as an “EpiPrimer[®]”, which enables the selective amplification of methylated DNA while discriminating against unmethylated DNA.

2.1 MGMT region for the study

The study focused on a DNA sequence containing four CpG sites situated in exon 1 of the *MGMT* promoter. These specific CpG sites are positioned on chromosome 10, GRCh38.p13, spanning from nucleotide 129,467,250 to 129,467,263 with the sequence "CGTCCCGACGCCG". These CpG sites are denoted as numbers 75 to 78 (numbering according to the study of by Malley et al.). Importantly, previous studies have established a link between these CpG sites and the survival outcomes of patients with glioblastoma [Stupp et al., 2005; Hegi et al., 2005; Yin et al., 2014; Yang et al., 2015; Vaubel et al., 2020; Śledzińska et al., 2021]. According to the feasibility of the regions for using the melting temperature approach, we used the CpG islands identified as clinically relevant for the assessment of *MGMT* promoter methylation.

2.2 Design of fluorescent oligonucleotides for melt studies

Three distinct oligonucleotides were custom-synthesized to target CpG sites numbered 75 to 78 within the *MGMT* promoter. These oligonucleotides were designed as fluorescent probes, featuring a FAM[®] fluorophore at the 5'-end and a black hole quencher 1 (BHQ[®]-1) at the 3'-end. One probe was constructed using standard DNA chemistry (referred to as "Ref," with sequence ID: P1), while the other two probes were chemically modified by incorporating IPN molecules.

Specifically, two probes were designed with IPN molecules attached to the 5' end of the G of the CpG sites. One of these probes used IPN 1, resulting in the creation of "INA-1"

(sequence ID: P2), and the other used IPN 2, leading to the development of "INA-2" (sequence ID: P3). All oligonucleotide sequences can be found in Table 1.

Sequence ID	Name	Sequence 5' to 3'-end
P1	Ref	FAM-CGTCCCGACGCCCG-BHQ1
P2	INA-1	FAM-C1GTCCC1GAC1GCCC1G-BHQ1
P3	INA-2	FAM-C2GTCCC2GAC2GCCC2G-BHQ1
T1	UM	CGGGCGTCGGGACG
T2	M	mCGGGmCGTmCGGGAmCG
T3	1mC	mCGGGCGTCGGGACG
T4	2mC	CGGGmCGTCGGGACG
T5	3mC	CGGGCGTmCGGGACG
T6	4mC	CGGGCGTCGGGA mCG
T7	1,2mC	mCGGGmCGTCGGGACG
T8	1,2,3mC	mCGGGmCGTmCGGGACG

Table 1. Probes and target sequences used for the analysis of DNA and INA[®] affinities towards unmodified and 5mC modified target sequences. Abbreviations: C = non-methylated cytosine; mC = 5-methylcytosine; 1 = IPN molecule 1; 2 = IPN molecule 2.

2.3 Design of target oligonucleotides for melt studies

A set of eight targets was designed, each corresponding to the sequences identified by the IDs P1-P3. These targets were constructed as follows:

- An oligonucleotide with unmethylated cytosines (denoted as "UM," with sequence ID: T1).
- An oligonucleotide with 5mC amidites at all four CpG sites (referred to as "M," with sequence ID: T2).

For the investigation of the impact of the number of methylated CpG sites and the methylation pattern on the melting temperature (T_m) of the DNA duplex, probes P1-P3 and targets T3-T8 were employed. The targets were designed as follows:

- Four targets were created, each featuring one methylated CpG site at one of the four CpG sites within the MGMT target sequence (identified as T3-T6).
- Additionally, two targets were synthesized with two and three methylated CpG sites (denoted as T7 and T8) to explore the relationship between the number of methylated CpG sites and the resulting T_m .

This design allowed for the investigation of how the T_m of the DNA duplex is influenced by the number and pattern of methylated CpG sites.

2.4 Protocol for melt studies

Probe sequences with the IDs P1-P3 were paired with complementary target sequences having various CpG methylation patterns, identified by the IDs T1-T8. The aim was to determine the melting temperature (T_m) of the duplex formed between these probes and targets. The following procedure was followed:

- a. Each probe sequence was mixed with a corresponding target sequence in individual PCR tubes.
- b. In each tube, a 20 μ L buffer was added, which contained 0.02 M Na_2HPO_4 , 0.02 M NaCl, and 2 mM EDTA, known as the TM buffer.
- c. The PCR tubes received 2.5 μ L of the probe (resulting in a working concentration of 2 μ M) and 2.5 μ L of the target (with a concentration of 4 μ M).
- d. The mixtures were subjected to a melting analysis using a BaseTyper48.4 Quiet HRM Real-Time PCR System (PentaBase A/S, Odense, Denmark).
- e. The analysis was initiated with a pre-melt hold at 95°C for 60 seconds, followed by a hold at 40°C for 60 seconds.
- f. The melting phase started from 40°C and gradually increased to 95°C with a ramping rate of 0.5°C per second.
- g. Fluorescence measurements were taken at each 0.5 °C interval during the melting process.

This experimental setup allowed for the determination of T_m values for the probe-target duplexes and the assessment of how they varied based on the CpG methylation patterns in the target sequences. The experiments were conducted in triplicates for each probe-target pair.

2.5 Design of EpiDirect[®] MGMT Methylation qPCR Assay

The assay was specifically developed to assess the methylation status of the four CpG sites that were previously examined in the melt studies, which are located within the MGMT promoter at positions 75 to 78. The oligonucleotide sequences employed in this assay are detailed in Table 2.

Gene	Oligo type	Sequence 5' to 3'-end	IPN*	Working conc. [nM]
<i>MGMT</i>	Fw primer	CGACCCGACGCCCGAGCGCTTCAC TGAGACA GGTCCTCGC	4	900
<i>MGMT</i>	Rev primer	CGAGGGAGAGCTCCGCACTCTTCC G	0	900
<i>MGMT</i>	Hydrolysis probe	FAM AGGCGACCCAGACTCACCAAG	4	500
<i>TBP</i>	Fw primer	AGGCAGCCATGCCACCTCACTGC	0	400
<i>TBP</i>	Rev primer	AGGTCAGGAGGAACCAAGTGAGC CCCA	1	400
<i>TBP</i>	Hydrolysis probe	HEX CACACAGA ACTAATGTGCCTGTGA ACAG ACACCA BHQ1	6	400

*Number of IPN molecules in the sequence. The location of the molecules in the sequence is not shown.

Table 2. Sequence and working concentration of primers and probes used in the EpiDirect® *MGMT* Methylation qPCR Assay. Abbreviations: Fw, primer forward; IPN, Intercalating pseudo-nucleotide; MGMT, O-6-methylguanine-DNA methyltransferase; Rev, primer reverse.

The assay utilized a forward EpiPrimer® and a standard reverse primer to amplify a DNA region spanning 97 base pairs, encompassing positions 129,467,250 to 129,467,346. Notably, the EpiPrimer® incorporated IPN molecule 2 at each of the CpG sites it targeted.

To enable precise detection of the amplification, a HydrolEasy® probe, an INA®-based hydrolysis probe, was designed downstream of the reverse primer. This probe featured a FAM® fluorophore at the 5'-end and a BHQ®-1 quencher at the 3'-end.

In the design of the EpiPrimer®, a single mismatch was intentionally introduced at the third nucleotide from the 5'-end. This was done to reduce the melting temperature (T_m) of the

primer since the targeted region is notably GC-rich. This unique assay design allowed for the accurate analysis of DNA methylation at the specified CpG sites in the *MGMT* promoter.

2.6 PCR set-up

In the assay, a four times concentrated mixture (referred to as 4X) containing the primers and probes detailed in Table 2 was prepared, denoted as the PP mix. The final concentration of each oligonucleotide in the PCR tube can be found in Table 2.

For each PCR setup, 10 μ L of 2X Ampliqueen master mix (PentaBase A/S) was combined with 5 μ L of the 4X PP mix and 5 μ L of purified DNA.

The PCR process was carried out using a CFX Opus 96 Real-time PCR Instrument manufactured (Bio-Rad Laboratories, Inc). It followed the following program:

- a. An initial activation step, consisting of a 120-second hold at 95°C for DNA polymerase activation.
- b. Five pre-cycles, with each cycle involving 60 seconds of denaturation at 100°C, followed by 60 seconds of combined annealing and elongation at 76°C.
- c. Subsequently, 40 cycles were performed, with each cycle consisting of 10 seconds at 98°C and 60 seconds at 76°C.
- d. During the second step of the cycles at 76°C, fluorescence was acquired specifically on the FAM[®] and HEX[®] channels, which allowed for the monitoring of the amplification.

In the verification experiments, two specific DNA samples were employed:

- a. Fully Methylated DNA (cat# D5014, Zymo Research, Irvine, CA, US): this sample was utilized to represent fully methylated DNA, where all relevant CpG sites were methylated.
- b. Unmethylated Human Genomic DNA (cat# G3041, Promega, Madison, WI, US): this sample was used to represent unmethylated DNA, where all relevant CpG sites were unmethylated.

In addition to the test samples, several controls were included in each PCR setup:

- a. No-Template Control (NTC): this is a negative control where no DNA template was added to the PCR reaction. It serves to check for any contamination or background signals.
- b. Positive Control (5 ng): this control consisted of a mixture of fully methylated and unmethylated DNA at a 25% methylation level. It was used to confirm the performance of the assay in detecting a specific level of methylation.
- c. Negative Control (5 ng): this control contained unmethylated DNA and was used to verify the assay's ability to detect unmethylated DNA.

These controls and samples were crucial in assessing the accuracy and reliability of the methylation detection assay by providing references for fully methylated, unmethylated, and intermediate (positive control) DNA methylation levels.

2.7 Assay verification

Two separate linear dynamic range studies were conducted to assess the performance of the assay. The first study focused on methylation calling, while the second evaluated the concentration of DNA. In both studies, five replicates were analyzed for each dilution to ensure the robustness of the results.

Methylation Calling Study:

- A dilution series was prepared, comprising DNA samples with different levels of methylation: 100%, 50%, 25%, 10%, 5%, and 2.5% methylated DNA.
- These samples were diluted to a concentration of 1 ng/μL in TE-buffer (consisting of 500 mM TRIS, 250 nM EDTA, and water).
- The experiment was repeated, resulting in data from two separate PCR runs.
- Data from both runs were used to develop an equation for calculating the methylation percentage based on the ΔC_t (cycle threshold) value.
- ΔC_t values were plotted against the common logarithm of the percent methylation, and linear regression was performed. The linear regression analysis allowed for the estimation of the relationship between ΔC_t and methylation percentage.

DNA Concentration Study:

- In this study, a dilution series was created using a factor of ten dilution, ranging from 10 ng/μL to 0.01 ng/μL.
- These dilutions were prepared using 25% methylated DNA, which corresponded to the positive control.
- Δ Ct values were plotted against the common logarithm of the DNA concentration, and linear regression analysis was conducted. The slope of the linear fit was used to calculate the PCR efficiency (E).

These studies helped validate the assay's ability to accurately detect DNA methylation levels and assess DNA concentration. The linear regression analyses in both studies provided insights into the relationship between Δ Ct values and methylation percentage, as well as DNA concentration, respectively. The PCR efficiency was determined from the slope of the linear fit in the DNA concentration study.

In the evaluation of the assay's performance, two important parameters were determined:

Limit of Blank (LOB):

- To calculate the LOB, twenty replicates of unmethylated DNA were prepared and diluted to a concentration of 1 ng/μL in TE-buffer.
- The LOB is a measure of the assay's background noise, indicating the highest signal or response that can be expected when analyzing blank or negative samples.

Limit of Detection (LOD):

- The LOD represents the lowest level of methylation that the assay can reliably detect.
- To establish the LOD, the LOB data was used as a reference point.
- It was defined as the percentage of methylation at which a minimum of 95% of the replicates could be reliably detected by the assay.
- The LOD was experimentally determined using twenty replicates of 3% methylated DNA, each diluted to a concentration of 1 ng/μL in TE-buffer. This confirmed the assay's capability to detect low levels of methylation.

FFPE Material Validation:

- To verify the assay's performance on FFPE material from a GBM, twenty replicates of unmethylated DNA purified from FFPE samples were analyzed using the EpiDirect[®] *MGMT* Methylation qPCR Assay.
- The purpose of this analysis was to confirm that all replicates would be correctly identified as unmethylated by the assay, based on the LOD's Δ Ct cut-off value.

Verification of LOD in FFPE Material:

- To further verify the LOD in FFPE material, twenty replicates of 3% methylated DNA were created by mixing fully methylated DNA with purified unmethylated FFPE samples.
- This allowed for the assessment of the assay's ability to detect low levels of methylation in FFPE material, reinforcing its LOD in this specific context.

These steps and validations are essential to understand the assay's sensitivity and specificity, especially in the context of detecting DNA methylation in challenging FFPE samples from GBMs.

2.8 Validation cohort

The validation cohort for this study comprised patients whose data were retrospectively selected from the database of the Oncology Institute of Southern Switzerland (IOSI), EOC, in Switzerland, spanning the period from 2004 to 2021. All patient samples included in the study were anonymized, and the research had received ethical approval (approval code Ref. EC 3721 - BASEC 2020-01939, granted on 16 October 2020).

Patients included in the validation cohort met the following criteria:

- Age greater than or equal to 18 years.
- Histology-proven diagnosis of a brain tumor, which could be glioblastoma, oligodendroglioma, or astrocytoma.
- Availability of leftover tumor tissue or extracted DNA for the validation of the assay.

Patients were excluded from the cohort if they:

- Were under the age of 18 years.

- Had an insufficient amount of leftover tissue material or extracted DNA available for the validation process.

This comprehensive selection process ensured that the patient cohort met specific criteria and, at the same time, preserved the ethical standards and requirements for patient confidentiality and data protection.

In the validation cohort, a total of 50 tumor samples were initially available. Out of these, 42 samples contained a sufficient amount of material to perform all three analyses, and these 42 samples were used for the comparative study.

2.9 Comparator methods

In the study involving the validation cohort, the EpiDirect® Methylation qPCR assay was compared with two other methods for analyzing the methylation status of the *MGMT* promoter. These two comparator methods were:

Comparator Method 1 involved a methyl-specific PCR (MSP) assay followed by gel electrophoresis. It was designed by and used in the clinical routine at the Institute of Pathology of Locarno, EOC, Switzerland.

Comparator Method 2 was a quantitative real-time MSP assay known as the geneMAP® *MGMT* Methylation Analysis Kit (Genmark Sağlık Ürünleri, Istanbul, Turkey).

For each patient included in the study, the following procedure was followed:

- a. FFPE tumor tissue was assessed for quality and tumor content.
- b. Genomic DNA was extracted from three 8 µm-thick serial sections of each FFPE block using the QIAamp DNA FFPE tissue kit manufactured (Qiagen, Chatsworth, CA, USA). The extraction process followed the manufacturer's instructions.
- c. For the two comparator methods, the purified DNA was subjected to bisulfite treatment before the MSP analysis. Bisulfite treatment is a key step in DNA methylation analysis, as it converts unmethylated cytosines into uracil while leaving methylated cytosines unchanged.

- d. The concentration of the extracted DNA was quantified using a Nanodrop 1000 spectrophotometer (Witec, Littau, Switzerland).

These detailed steps ensured the proper preparation of DNA samples for methylation analysis using the EpiDirect® Methylation qPCR assay and the two comparator methods. It also allowed for a comparative evaluation of the results obtained by each method.

For Comparator Method 1, which utilized a methyl-specific PCR assay, the following steps were performed:

- a. Approximately 500 ng of DNA was subjected to bisulfite treatment using the EZ DNA Methylation-Gold kit (cat# D5005) from Zymo Research. Bisulfite treatment is a critical step for DNA methylation analysis, as it converts unmethylated cytosines into uracil while leaving methylated cytosines unaltered.
- b. Subsequently, 6 µL of the purified and bisulfite-treated DNA was used for MSP in duplicate reactions.
- c. The MSP reactions employed specific primers for the *MGMT* gene, one for the methylated (*MGMT*-M) state and another for the unmethylated (*MGMT*-UM) state. These primers are found in Table 3.

<i>MGMT</i> primers	Sequence 5' to 3'-end
<i>MGMT</i> -M-Fw	TTTCGACGTTCTAGGTTTTCGC
<i>MGMT</i> -M-Rev	GCACTCTTCCGAAAACGAAACG
<i>MGMT</i> -U-Fw	TTTGTGTTTTGATGTTTGTAGGTTTTTGT
<i>MGMT</i> -U-Rev	AACTCCACACTCTTCCAAAAACAAAACA

Table 3. Primers used in comparator method 1. Abbreviations: *MGMT*, O-6-methylguanine-DNA methyltransferase; *MGMT*-M-Fw, primer forward for methylation of *MGMT*; *MGMT*-M-Rev, primer reverse for methylation of *MGMT*; *MGMT*-U-Fw primer forward for unmethylated *MGMT*; *MGMT*-U-Rev, primer reverse for unmethylated *MGMT*.

- d. The PCR protocol included the following steps:
 - Initial denaturation at 94°C for 60 seconds.
 - Annealing at 55°C for *MGMT*-M or 57°C for *MGMT*-UM for 60 seconds.
 - Elongation at 72°C for 60 seconds.

- This cycle (denaturation, annealing, and elongation) was repeated for 40 times.
 - The reaction was concluded with a final elongation step at 72°C for 10 minutes.
- e. After the MSP reaction, the resulting PCR products were visualized by running them on a 3% agarose gel.
- f. The samples were identified as methylated or unmethylated based on the presence or absence of amplification products, which could be visually distinguished by comparing them to positive and negative controls.

This method allowed for the determination of the methylation status of the *MGMT* gene based on the presence or absence of PCR products after bisulfite treatment and MSP amplification, followed by gel electrophoresis.

For Comparator Method 2, the following steps were taken to analyze the DNA methylation status using the geneMAP[®] *MGMT* Methylation Analysis Kit:

- a. Approximately 200 ng of DNA was subjected to bisulfite conversion using the EZ DNA Methylation-Lightning Kit, cat# D5030, from Zymo Research. This conversion process is essential for DNA methylation analysis, as it modifies unmethylated cytosines into uracil, while leaving methylated cytosines unchanged.
- b. Five µL of the converted material was then analyzed using the geneMAP[®] *MGMT* Methylation Analysis Kit following the manufacturer's instructions.
- c. The analysis was carried out using a CFX Opus 96 Real-time PCR Instrument from Bio-Rad Laboratories, or a CFX96[®] instrument, also from Bio-Rad Laboratories.
- d. In accordance with the manufacturer's guidelines, a cut-off threshold of greater than 0.6% was applied to interpret the results. This cut-off value likely served to distinguish between methylated and unmethylated samples based on the proportion of methylation detected.

This method provided a quantitative assessment of DNA methylation status based on the manufacturer's recommended cut-off value, enabling the classification of samples as

methyated or unmethyated. The bisulfite conversion step was crucial for methylation analysis, as it is a common method for assessing DNA methylation levels.

The DNA samples obtained from each patient in the validation cohort were analyzed using the EpiDirect[®] *MGMT* Methylation qPCR Assay by following these steps:

- a. Five microliters (concentration ranging from 0.1 to 10 ng/ μ L) of purified DNA from each patient were added to the assay.
- b. The DNA was subjected to amplification according to the previously mentioned PCR program detailed in the method section. This amplification process was carried out using either the CFX Opus 96 Real-time PCR Instrument from Bio-Rad Laboratories or the CFX96[®] instrument, also from Bio-Rad Laboratories.
- c. The data obtained from the PCR amplification were analyzed based on the Δ Ct (cycle threshold) between the FAM[®] and HEX[®] channels. This analysis allowed for the calculation of an estimate of the percentage methylation. The equation derived from the assay verification studies was used to make this conversion.
- d. The technical LOD served as a cut-off for determining the methylation status of the samples. Samples were classified as methyated if they exceeded the technical LOD, and unmethyated if they fell below this threshold.

This approach utilized the EpiDirect[®] *MGMT* Methylation qPCR Assay to quantify the methylation percentage in patient samples based on Δ Ct values and the technical LOD, thereby determining the methylation status for each sample in the validation cohort.

2.10 Data analysis and statistics

All data analysis and statistical calculations were performed using R Studio, specifically version 1.3.1093, and R version 4.0.3. The analysis involved various aspects, including the determination of the T_m of DNA duplexes and the statistical comparison of T_m values. Here are some key details:

T_m Determination:

- The T_m of the DNA duplexes was determined based on the maximum value of the first negative derivative of the melt curves.

- This determination process was automated and conducted using the PCR software associated with the BaseTyper48.4 Quiet HRM Real-Time PCR System, which is provided by PentaBase A/S.
- Mean T_m values were reported, and the standard deviation (\pm) was used to denote the variability within the data.

Statistical Analysis:

- Differences in T_m values between various conditions or groups were calculated.
- These calculations included the use of 95% confidence intervals to assess the range of uncertainty.
- The statistical analysis assumed that the technical replicates followed a normal distribution, which is a common assumption for many statistical tests.

The use of R Studio and the described methodology allowed for comprehensive data analysis and statistical assessment in the study, ensuring the robustness and reliability of the results obtained from the various experiments and assays.

The PCR cycle threshold (C_t) values were determined in the CFX Maestro Software 2.0 (Bio-Rad Laboratories). The thresholds were manually set for both the FAM[™] and HEX[™] channels according to 10% of the maximum relative fluorescence units (RFU) of the positive control sample (25% methylated DNA). The ΔC_t between the two channels was calculated by the equation:

$$\Delta C_t = C_{t_{FAM}} - C_{t_{HEX}}$$

The PCR efficiency was calculated by the equation:

$$E = 10^{\frac{-1}{\text{slope}}} - 1$$

A significance level of 0.001 was chosen, giving a critical (Z_α) value of 2.576 for the LOB study. The mean value (μ_B) of the unmethylated replicates and the standard deviation (σ_B) was used to calculate the LOB using the equation:

$$LOB_{\Delta C_t} = \mu_B - Z_\alpha \cdot \sigma_B$$

The LOD at 95% certainty was calculated from the LOB using the following equation, with 19 degrees of freedom (f), as 20 replicates were used for the study.

$$LOD_{\Delta Ct} = LOB_{\Delta Ct} + \frac{1.645}{1 - \left(\frac{1}{4} \cdot f\right)} \cdot \sigma_B$$

The sensitivity and specificity of the assay were calculated by the following equations, respectively. The 95% confidence intervals were calculated using the Wilson score.

$$Sensitivity [\%] = \frac{True\ Positive}{True\ Positive + False\ Negative} \cdot 100$$

$$Specificity [\%] = \frac{True\ Negative}{True\ Negative + False\ Positive} \cdot 100$$

RESULTS

1. ABOUT miRNA EXPRESSION AND ITS CORRELATION WITH RESPONSE TO STANDARD THERAPY

1.1. General consideration

During the ten-year period spanning from January 2004 to December 2013, a total of 112 patients diagnosed with GBM, *IDH*-wildtype, WHO grade 4 tumors, were recruited.

MGMT Methylation Status:

- Among the evaluable cases, 39 out of 108 patients (36.1%) exhibited methylation of the *MGMT* gene promoter.
- The remaining 69 out of 108 patients (63.9%) were found to have an unmethylated *MGMT* gene promoter.

MGMT IHC status:

- Among the evaluable cases, 54 out of 98 patients (55.1%) tested positive for *MGMT* IHC.
- The remaining 44 out of 98 patients (44.9%) were negative for *MGMT* IHC (Fig. 3).

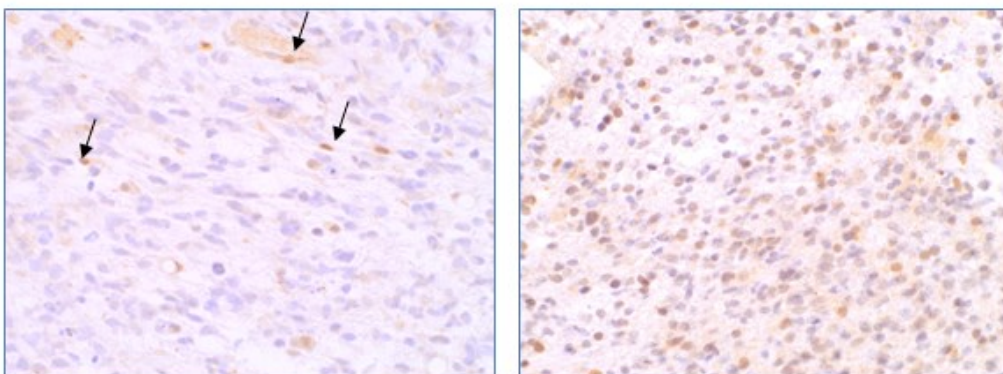


Figure 3. Two examples of *MGMT* expression evaluated by IHC. On the left side, an example of a GBM with negative staining of *MGMT* protein. The arrows indicate internal positive controls, namely inflammatory cells and endothelial cells. On the right side, an example of a GBM showing expression of *MGMT* protein

From the neurosurgical perspective, the extent of surgical resection was classified as follows among the patients:

- Gross Total Resection (GTR): this was achieved in 79 patients, which represents 70.5% of the cases. A GTR indicates that the surgical team successfully removed the entire tumor.
- Subtotal Resection (STR): an STR was performed in 17 patients, constituting 15.2% of the cases. In an STR, a portion of the tumor is intentionally left in place due to its location or other factors.
- Biopsy: in the remaining 16 cases (14.3%), the attending neurosurgeons opted for a biopsy. A biopsy involves taking a small sample of tissue from the tumor for diagnostic purposes without attempting to remove the entire tumor.

All of the clinicopathological and molecular data related to these surgical approaches and patient characteristics are summarized in Table 4.

Patient's Characteristics	
Age	
28–85 years	
	no. (%)
Sex	
Male	57/112 (50.9%)
Female	55/112 (49.1%)
Histologic Type	
GBM IDH-wt WHO grade 4	112/112 (100%)
MGMT promoter methylation (not evaluable in 4 cases)	
Methylated	39/108 (36.1%)
Unmethylated	69/108 (63.9%)
MGMT IHC (not evaluable in 14 cases)	
Positive	54/98 (55.1%)
Negative	44/98 (44.9%)
Neurosurgery	
GTR	79/112 (70.5%)
STR	17/112 (15.2%)
Biopsy	16/112 (14.3%)

Table 4. Patients' characteristics. Abbreviations: GTR, Gross total resection; IHC, Immunohistochemistry; STR, Subtotal resection.

Particularly, in 14 out of 112 cases (12.5%), the quality of the samples did not allow an adequate immunohistochemical evaluation of MGMT due to fixation artifacts. Similarly, in 4 out of 112 cases (3.6%), the quality and/or quantity of the DNA extracted from the samples did not permit methylation analysis.

1.2. miRNA expression

In the study, the data reported is based on a specific cut-off value of greater than 3 for the analysis. However, it is worth noting that results obtained using two other cut-off values were found to be nearly identical, indicating the consistency of the findings (Table 5).

miRNA	miRNA Expression Values		
	<0.333	0.333–3	>3
miR-181c	39/112 (34.8%)	62/112 (55.4%)	11/112 (9.8%)
miR-181d	38/112 (33.9%)	71/112 (63.4%)	3/112 (2.7%)
miR-21	1/112 (0.9%)	20/112 (17.9%)	91/112 (81.2%)
miR-195	19/112 (17%)	69/112 (61.6%)	24/112 (21.4%)
miR-196b	7/112 (6.2%)	10/112 (9%)	95/112 (84.8%)
miR-648	28/112 (25%)	77/112 (68.7%)	7/112 (6.3%)
miR-767.3p	47/86 (54.6%)	17/86 (19.8%)	22/86 (25.6%)

Table 5. miRNA distribution. Abbreviations: miRNA, microRNA.

In general, the analysis of miRNA expression revealed the following trends:

- Strong miRNA Overexpression (values > 3): this was notably observed for miR-21 and miR-196b.

- Down-Regulation (values < 0.33): miR-767.3 exhibited down-regulation, indicating a significant decrease in its expression.
- Normal Expression (values between 0.333 and 3): for the remaining four miRNAs, their expression levels fell within the range of 0.333 to 3 in the majority of cases, suggesting that their expression was relatively stable and within a normal range.

These observations provide insight into the expression patterns of various miRNAs in the study's cohort, and how they relate to different cut-off values, with miR-21, miR-196b, and miR-767.3 showing distinct patterns of expression.

A multivariate analysis was conducted to explore the relationship between the expression levels of various miRNAs and the positivity of MGMT IHC (Table 6).

		IHC MGMT		<i>p</i>
		Negative	Positive	
miR-181c	<0.333	10/98 (10.2%)	22/98 (22.5%)	0.0015
	0.333–3	24/98 (24.5%)	31/98 (31.6%)	
	>3	10/98 (10.2%)	1/98 (1%)	
miR-181d	< 0.333	11/98 (11.2%)	22/98 (22.4%)	0.0560
	0.333–3	30/98 (30.6%)	32/98 (32.7%)	
	>3	3/98 (3.1%)	0/98 (0%)	
miR-21	<0.333	0/98 (0%)	1/98 (1%)	0.7846
	0.333–3	7/98 (7.1%)	11/98 (11.2%)	
	>3	37/98 (37.8%)	42/98 (42.9%)	
miR-195	<0.333	6/98 (6.1%)	10/98 (10.2%)	0.0025
	0.333–3	21/98 (21.4%)	39/98 (39.8%)	
	>3	17/98 (17.4%)	5/98 (5.1%)	
miR-196b	<0.333	2/98 (2%)	4/98 (4.1%)	0.8216
	0.333–3	4/98 (4.1%)	4/98 (4.1%)	
	>3	38/98	46/98	

		(38.8%)	(46.9%)	
miR-648	<0.333	4/98 (4.1%)	17/98 (17.3%)	0.0230
	0.333–3	37/98 (37.8%)	35/98 (35.7%)	
	>3	3/98 (3.1%)	2/98 (2%)	
miR-767.3p	<0.333	12/98 (15.8%)	28/98 (36.8%)	0.0005
	0.333–3	11/98 (14.5%)	5/98 (6.6%)	
	>3	15/98 (19.7%)	5/98 (6.6%)	

Table 6. MGMT IHC and miRNA bivariate analysis. Abbreviations: IHC, immunohistochemistry; MGMT, O-6-methylguanine-DNA methyltransferase; miRNA, microRNA.

The analysis revealed statistically significant correlations between a positive MGMT IHC status and low expression of specific miRNAs, reported in bold in the table.

These findings suggest that there is a statistically significant relationship between the expression levels of these miRNAs and the positivity of MGMT IHC, indicating a potential molecular connection between MGMT promoter status and the expression of these specific miRNAs. The statistical significance of these correlations implies that these miRNAs may play a role in the regulation of MGMT expression or other related processes in the context of GBM.

The general expression pattern of miRNAs, when considered in relation to MGMT promoter methylation status, revealed interesting correlations. A multivariate analysis was conducted to examine the relationship between miRNA expression levels and MGMT methylation status (Table 7).

		MGMT		<i>p</i>
		Methylated	Unmethylated	
miR-181c	<0.333	10/108 (9.3%)	26/108 (24.1%)	0.4288
	0.333–3	24/108 (22.2%)	37/108 (34.3%)	
	>3	5/108 (4.6%)	6/108 (5.5%)	

miR-181d	<0.333	9/108 (8.3%)	26/108 (24.1%)	0.0245
	0.333–3	27/108 (25%)	43/108 (39.8%)	
	>3	3/108 (2.8%)	0/108 (0%)	
miR-21	<0.333	0/108 (0%)	0/108 (0%)	1.0000
	0.333–3	6/108 (5.6%)	12/108 (11.1%)	
	>3	33/108 (30.6)	57/108 (52.8%)	
miR-195	<0.333	3/108 (2.8%)	13/108 (12%)	0.2984
	0.333–3	26/108 (24.1%)	42/108 (38.9%)	
	>3	10/108 (9.3%)	14/108 (12.9%)	
miR-196b	<0.333	0/108 (0%)	4/108 (3.7%)	0.0060
	0.333–3	0/108 (0%)	10/108 (9.3%)	
	>3	39/108 (36.1%)	55/108 (50.9%)	
miR-648	<0.333	3/108 (2.8%)	23/108 (21.3%)	0.0035
	0.333–3	34/108 (31.5%)	41/108 (37.9%)	
	>3	2/108 (1.9%)	5/108 (4.6%)	
miR-767.3p	<0.333	14/83 (16.9%)	31/83 (37.3%)	0.8591
	0.333–3	6/83 (7.2%)	10/83 (12.1%)	
	>3	8/83 (9.6%)	14/83 (16.9%)	

Table 7. MGMT methylation and miRNA bivariate analysis. Abbreviations: MGMT, O-6-methylguanine-DNA methyltransferase.

Low Expression of miR-181d and miR-648: a statistically significant association was observed between cases with unmethylated *MGMT* promoter and low expression of miR-181d ($p = 0.02$) and miR-648 ($p = 0.004$). This suggests that these miRNAs are more likely to be expressed at low levels in cases where the *MGMT* promoter is unmethylated.

High Expression of miR-196b: conversely, high expression of miR-196b ($p = 0.006$) appeared to be associated with cases where the MGMT promoter was methylated. This indicates that miR-196b is more likely to be expressed at higher levels in cases with MGMT promoter hypermethylation.

The remaining four miRNAs did not show any statistically significant association with MGMT promoter hypermethylation. These findings provide insights into the potential relationships between miRNA expression and MGMT promoter methylation status, suggesting that specific miRNAs, such as miR-181d, miR-648, and miR-196b, may be linked to the epigenetic regulation of the MGMT gene in the context of GBM.

1.3. Overall survival

The OS has been considered for both groups of patients included in the study (methylated vs. unmethylated GBM).

The OS for methylated patients is significantly better ($p = 0.006$). The same statistical consideration has been performed for MGMT IHC. The results show that a negative MGMT IHC is significantly correlated to a longer OS ($p = 0.01$) (Fig. 4).

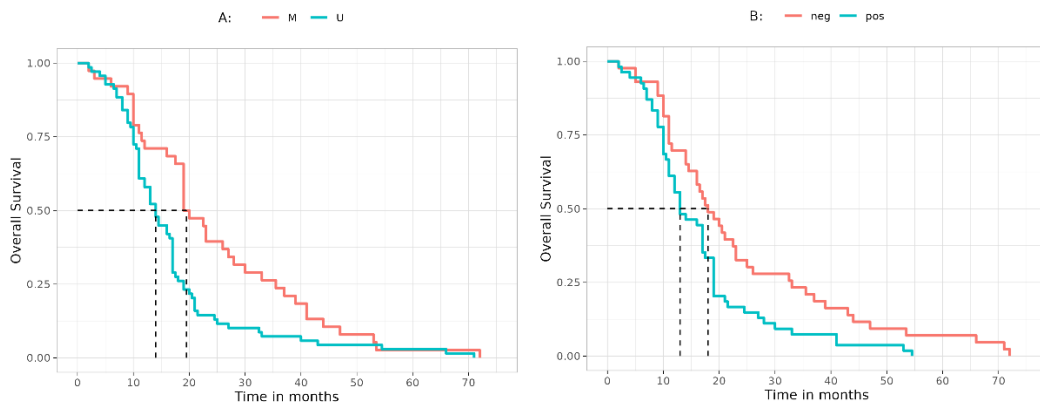


Figure 4. OS curves representing the survival of patients (in terms of months) on the basis of MGMT. On the left side (A), OS was evaluated on MGMT methylation status (M, methylated; U, unmethylated.). Median survival times are 19.5 months for methylated and 14.0 for unmethylated. On the right side (B), OS was evaluated on MGMT expression by IHC (neg, negative; pos, positive;). Median survival times are 18 months for negative and 13 months for positive groups.

Then we calculated the association of miRNA expression and OS. A significant correlation was found for miR-21 ($p = 0.006$), miR-195 ($p = 0.02$), miR-196b ($p = 0.008$) and miR-648 ($p = 0.02$) (Fig. 5; only the curves of the miRNAs associated to a significant result are reported).

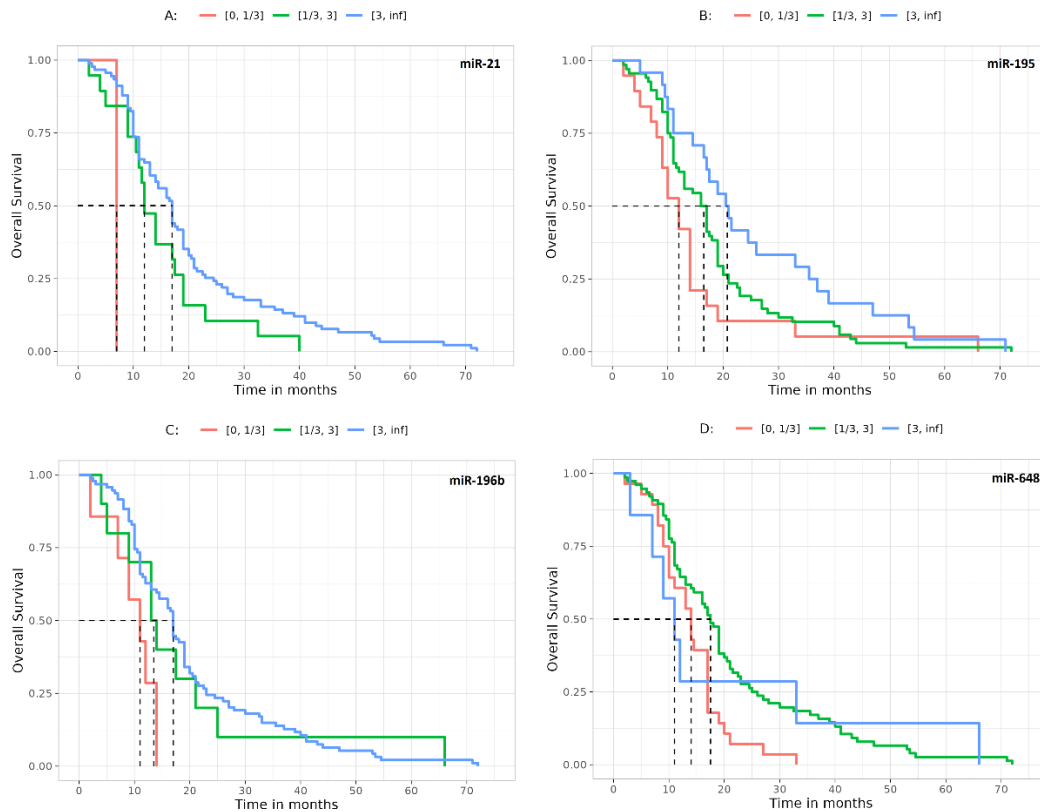


Figure 5. OS curves representing the survival of patients (in terms of months) on the basis of different miRNA expression. In (A), OS was evaluated on miR-21 expression. On dashed vertical lines, median survival times in months [0, 1/3]: 7, [1/3, 3]: 12, [3, inf]: 17. In (B), OS evaluated on miR-195 expression. On dashed vertical lines, median survival times in months [0, 1/3]: 12, [1/3, 3]: 16.5, [3, inf]: 20.8. In (C), OS evaluated on miR-196b expression. On dashed vertical lines, median survival times in months [0, 1/3]: 11, [1/3, 3]: 13.5, [3, inf]: 17. In (D), OS evaluated on miR-648 expression. On dashed vertical lines, median survival times in months [0, 1/3]: 14, [1/3, 3]: 17.5, [3, inf]: 11.

1.4. Progression free survival

Data have been analyzed also to define any significant relation with the PFS. A statistical correlation has been found between MGMT methylation status and PFS ($p = 0.03$) but also between GTR and PFS ($p = 0.04$) (Fig. 6).

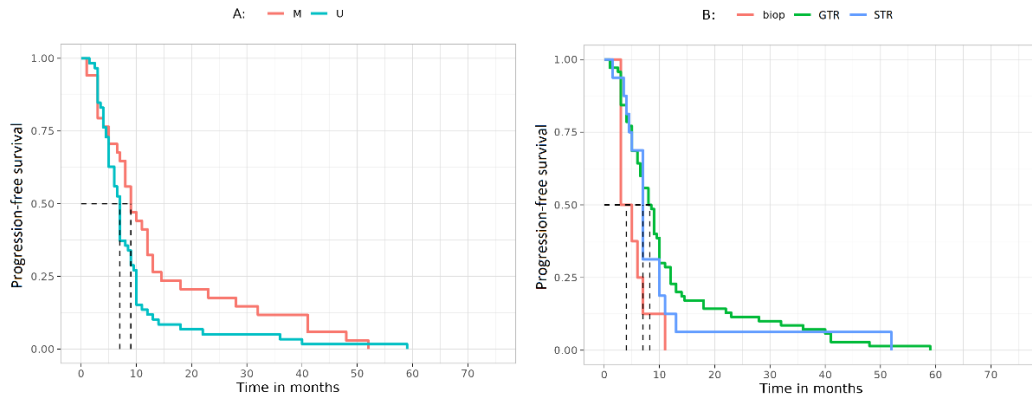


Figure 6. PFS curves representing the survival of patients (in terms of months) on the basis of MGMT methylation status. On the left side (A), PFS curves represented the survival of patients (in months) on the basis of MGMT methylation status (M, methylated; U, unmethylated). On dashed vertical lines, median survival times were 7 months for unmethylated and 9 months for methylated. On the right side (B), PFS curves representing the survival of patients (in months) on the basis of surgery type (biop, biopsy; GTR, Gross Total Resection; STR, Subtotal Tumor Resection). On dashed vertical lines, median survival times were 4 months for biopsied patients, 8.25 months for GTR, and 7 months for STR.

Contrary to the correlation with OS, we found no correlation between PFS and MGMT IHC; in addition, miRNA expression showed a trend, but never reached a statistically significant correlation with PFS.

2. ABOUT DIRECT PCR QUANTIFICATION OF METHYLATIONS USING UNTREATED DNA

2.1. Validation cohort

The composition of the cohort was as follows:

- Primarily consisting of GBM samples, which accounted for 83% of the samples.
- Approximately 57.1% of the samples were obtained from male patients.
- The age of patients at the time of biopsy ranged from 25 to 79 years, with an average age of 60.2 years for the entire set of samples.

The summarized data for the cohort of these 42 patients can be found in Table 8. This dataset forms the basis for the comparative analysis in the study.

	n (%)
Gender	
Male	24 (57.1)
Female	18 (42.9)
Age	
≥60	25 (59.5)
<60	17 (40.5)
Diagnosis	
Glioblastoma	35 (83.3)
Anaplastic Astrocytoma	1 (2.4)
Oligodendroglioma	2 (4.8)
Diffuse Astrocytoma	2 (4.8)
Pilocytic Astrocytoma	2 (4.8)
IDH1 status	
Mutated	5 (11.9)
Wildtype	37 (88.1)

Table 8. Patients’ characteristics.

2.2. Novel platform for direct methylation quantification

We tested an innovative PCR platform called EpiDirect[®], which enables the direct quantification of DNA methylation without the need for any DNA pre-treatment. Within this platform, we leverage the collaborative influence of cytosine methylation and our proprietary DNA technology, INA[®].

As illustrated in Fig. 7, an EpiPrimer[™] consists of three components: an anchor sequence, a loop segment, and a starter sequence, as depicted in the figure at the end of the paragraph. The anchor sequence comprises IPN molecules and covers the specific CpG region of interest. This anchor sequence binds with significantly greater thermal stability to a complementary methylated target as opposed to a complementary unmethylated target. The starter sequence is positioned at the 3'-end of the primer and is intentionally designed to possess low thermal stability. Consequently, it does not bind to the template DNA unless it receives support from the anchor sequence.

Since the anchor sequence forms stronger bonds with methylated DNA, it becomes possible to achieve a selective amplification of methylated DNA by conducting the PCR at an annealing temperature higher than the melting temperature (T_m) of the anchor sequence attached to unmethylated DNA.

In order to measure the methylation status of a specific sequence, we simultaneously amplify an independent reference sequence alongside the target sequence. These two sequences are detected in separate fluorescence channels. If both sequences reach the threshold at approximately the same PCR cycle (resulting in a low ΔC_t value between the methyl-specific assay and the internal reference assay), it indicates that the target DNA sequence is highly methylated in the region of interest.

Conversely, when there are no CpG methylations present in the targeted sequence, the EpiPrimer™ will exhibit minimal affinity for the DNA, leading to a significant ΔC_t value, as depicted in in the figure at the end of the paragraph.

The methylation pattern exclusively exists in the original DNA sample and is not transferred to the amplicons generated during PCR by the polymerase. Consequently, the anchor segment of the EpiPrimer™ exhibits limited binding affinity for the amplicons. To overcome this, we've incorporated a loop sequence that connects the anchor and starter sequences, allowing us to restore the affinity for sequences that initially contained DNA methylations.

It is important to note that the polymerase is unable to replicate over the IPN molecules. As a result, the anchor portion of the EpiPrimer™ will not be copied or replicated during the PCR process.

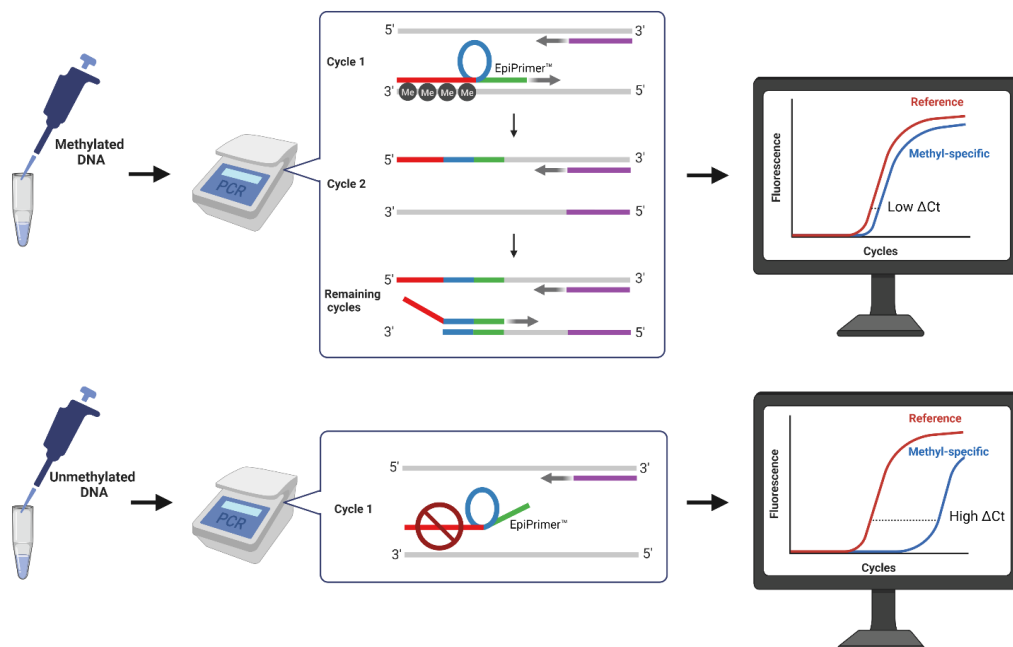


Figure 7. Principle of the EpiDirect® platform for selective amplification of methylated DNA.

2.3. Intercalating nucleic acids has increased thermal stability to DNA targets

We conducted an investigation to assess the impact of fluorescent INA® probes in comparison to DNA probes (referred to as "Ref") on the thermal stability of complementary oligonucleotides. Our study involved the use of two distinct IPN molecules, denoted as IPN 1 and IPN 2 (as illustrated in Fig. 8), which were integrated into a 14-nucleotide sequence located in the MGMT promoter region, specifically positioned 5' to the CpG sites of the sequence: 5'-CGTCCCGACGCCG-3'. R denotes a linker sequence, which binds the molecule to a phosphoramidite allowing for coupling into oligonucleotides. IPN molecules are composed of several conjugated double bonds and are thereby adding π -electrons to the DNA double helix. This increases the overall π -stacking energy of the DNA.

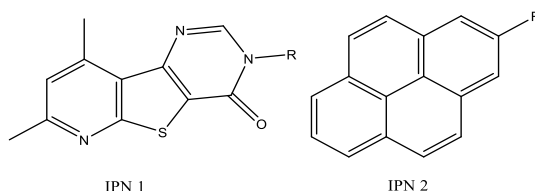


Figure 8. The skeletal structure of intercalating pseudo-nucleotide (IPN) type 1 and type 2.

We labeled the probe modified with IPN 1 as "INA-1" and the probe modified with IPN 2 as "INA-2". IPN molecules 1 and 2 were individually introduced into the sequence at each of the four CpG sites and then hybridized with a complementary unmethylated (UM) target, resulting in the formation of a probe/target duplex.

As a result of this hybridization, the melting temperature (T_m) increased by 7.3°C when utilizing INA-1 and 7.8°C when using INA-2 in comparison to the "Ref" probe. The specific T_m values are depicted in Table 9.

Probe	Mean T_m (°C)	+ T_m (°C) ^a	95% CI
Ref	64.6 ± 0.03	-	-
INA-1	72.4 ± 0.01	7.8	[7.8; 7.9]
INA-2	71.8 ± 0.25	7.3	[6.7; 7.9]

$$^a +T_m = T_m(\text{INA}) - T_m(\text{Ref})$$

Table 9. Melting temperature (T_m) of fluorescent oligonucleotide probes bound to an unmethylated complementary target. Abbreviations: CI, confidence interval; INA, Intercalating nucleic acid; T_m , melting temperature.

2.4. Methylated CpG sites increase the thermal stability of DNA

A fluorescent probe was synthesized with a FAMTM fluorophore (F) in the 5'-end and a black hole quencher 1 (BHQ[®]-1) in the 3'-end (as shown in Fig. 9). The probe covered a sequence found in the promoter region of *MGMT* comprising four CpG sites. The probe was hybridized to a complementary oligonucleotide being either unmethylated or methylated at all four cytosine nucleobases.

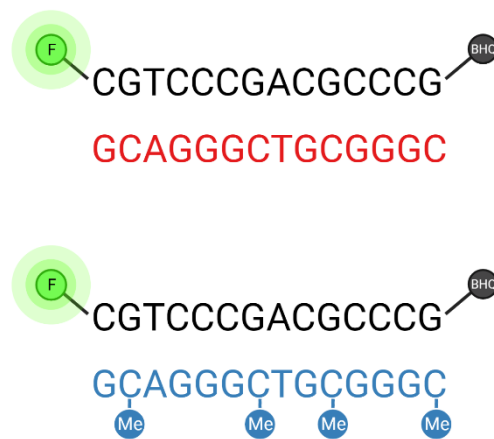


Figure 9. Sequences of the oligonucleotides used for the study.

The "Ref" probe was hybridized with both an unmethylated (UM) and a fully methylated (M) target, and the temperature was raised to determine the melting temperature (T_m). The T_m for the "Ref" probe was $64.6 \pm 0.03^\circ\text{C}$ when hybridized with the unmethylated target (UM) and $68.9 \pm 0.08^\circ\text{C}$ when hybridized with the fully methylated target (M).

This indicates that the presence of all four methylated CpG sites resulted in an approximate increase of 4.3°C (with a 95% confidence interval of [4.2; 4.5]) in T_m compared to unmethylated CpG sites (data shown in Fig. 10).

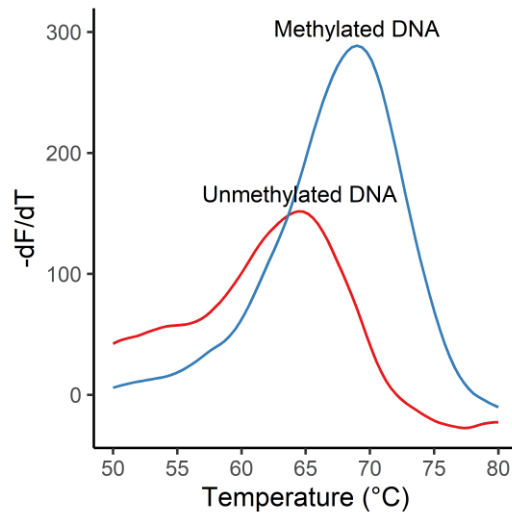


Figure 10. Thermal stability of the two duplexes.

2.5. Synergistic effect of intercalating nucleic acids and DNA methylations

As described in Fig. 11, IPN molecules, either type 1 or type 2, were coupled 5' to the G of the CpG sites, creating probe INA-1 and INA-2, respectively. The probes were hybridized to a complementary unmethylated oligonucleotide (UM), and a target methylated at all four CpG sites (M).

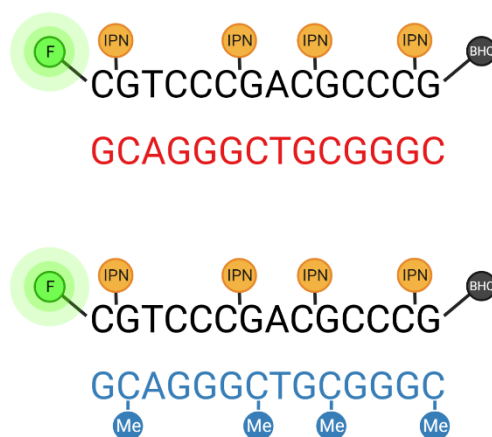


Figure 11. Sequences of the oligonucleotides used for the study.

As shown in Fig. 12, melt peaks of the methylated (blue, 82.8 ± 0.36 °C) and unmethylated (red, 71.9 ± 0.25 °C) target was hybridized to probe INA-2, giving a difference of 11.0 °C (95% CI [10.2; 11.7]).

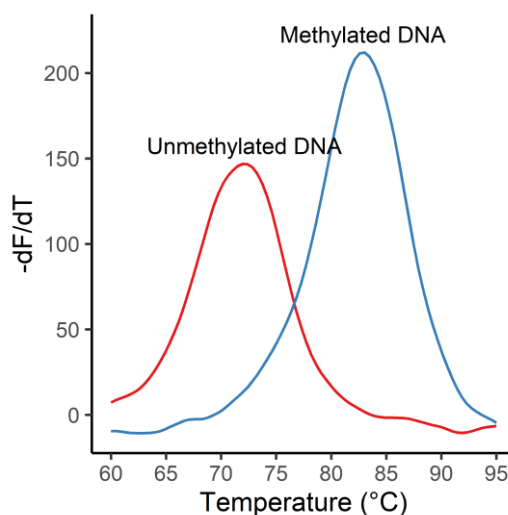


Figure 12. Melt peaks of methylated and unmethylated targets.

In Table 10 are described the melting temperature differences (ΔT_m) of fluorescent oligonucleotide probes bound to unmethylated (UM) or fully methylated (M) complementary target, respectively. INA-1 and INA-2 increased the ΔT_m compared to Ref.

Probe	Mean ΔT_m (°C) ^a	$+\Delta T_m$ (°C) ^b	95% CI
Ref	4.3 ± 0.1	-	-
INA-1	8.6 ± 0.1	4.2	[4.0; 4.5]
INA-2	11.0 ± 0.5	6.6	[5.5; 7.7]

^a $\Delta T_m = T_m(M) - T_m(UM)$

^b $+\Delta T_m = \Delta T_m(INA) - \Delta T_m(Ref)$

Table 10. Table of the melting temperature differences (ΔT_m) of fluorescent oligonucleotide probes bound to unmethylated (UM) or fully methylated (M) complementary target. Abbreviations: CI, confidence interval; INA, Intercalating nucleic acid; T_m , melting temperature.

2.6. Linear correlation between the number of methylated CpG sites and duplex stability

The introduction of the initial methyl group to any of the cytosines within the MGMT promoter sequence resulted in an increased binding affinity with the complementary Ref probe, raising the T_m by approximately 2.1 to 2.9°C. The extent of the increase depended on the specific position of the methyl group.

When utilizing INA-2, the comparative affinity enhancement was more substantial, with T_m increases ranging from 5.3 to 5.7°C, again depending on the methyl-group's location.

Subsequent additions of methyl groups (from the second to the fourth) further enhanced the affinity, resulting in an increment of approximately 0.6°C per 5mC when using the Ref probe and approximately 1.9°C per 5mC when using INA-2.

Fig. 13 shows the linear regression on the number of methylated CpG sites (one to four sites) and melting temperature of DNA duplexes using probe INA-2 (red), INA-1 (green), and Ref (blue).

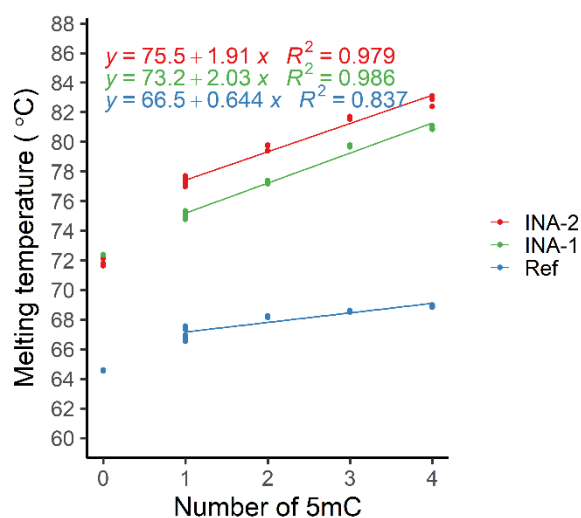


Figure 13. Linear regression on the number of methylated CpG sites using the different probes. Abbreviations: 5mC, 5-methylcytosine; INA, Intercalating nucleic acid.

2.7. EpiDirect[®] MGMT Methylation qPCR Assay verification

The EpiDirect[®] MGMT Methylation qPCR Assay exhibited a linear dynamic range spanning from 100% to 2.5% methylation. A linear regression analysis of the data points yielded the equation $y = 6 - 2.9x$, where y represents the ΔCt and x represents the logarithm (base 10) of the percentage of methylation. The fit of this equation produced an R^2 value of 0.976. Each sample was evaluated in 10 replicates from multiple PCR runs. The data is illustrated in Fig. 14.

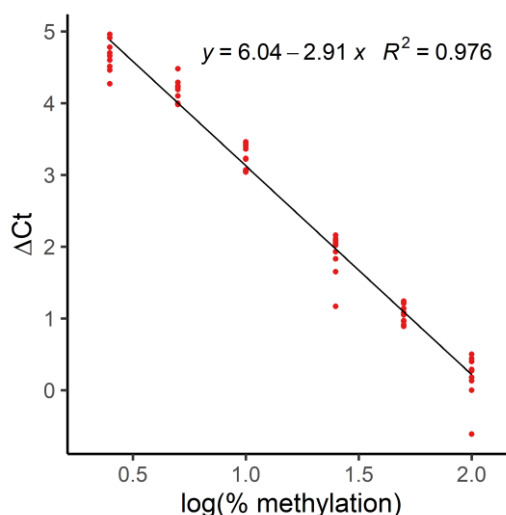


Figure 14. Performance study from the EpiDirect[®] MGMT Methylation qPCR Assay: linearity was observed from 100% to 2.5% methylation. Abbreviations: ΔCt : Differences between threshold cycles.

The percentage methylation can thus be calculated from the ΔCt value by the equation:

$$\% \text{ methylation} = 10^{\frac{\Delta Ct - 6}{-2.9}}$$

The assay was determined to have a consistent linear dynamic range when used with input DNA concentrations ranging from 0.1 to 10 ng/ μ L of the sample. This corresponds to an input range of 0.5 to 50 ng. Moreover, the PCR efficiency within this specified range was measured at 97.2% in both the FAM[™] and HEX[™] channels.

The LOB was calculated to be ΔCt 5.0, which corresponds to 2.3% methylation. From this value, the Technical LOD at a 95% confidence level was calculated to be ΔCt 4.9, equivalent

to 2.4% methylation. When tested at 3% methylation, nineteen out of twenty replicates resulted in ΔCt values below 4.9, demonstrating that the experimental LOD was confirmed to be 3% methylation.

The assay's methylation calling, based on twenty replicates, showed an average of $3.4\% \pm 0.78\%$.

For unmethylated DNA purified from FFPE, all twenty replicates had ΔCt values above the LOD of ΔCt 4.9, correctly indicating that they were unmethylated.

Furthermore, when 3% methylated DNA was diluted into DNA purified from FFPE material, nineteen out of twenty replicates were identified as methylated. The average percentage calling for these replicates was $3.9\% \pm 1.4\%$. Five ng of DNA was used as input for each replicate. The data is shown in Fig. 15.

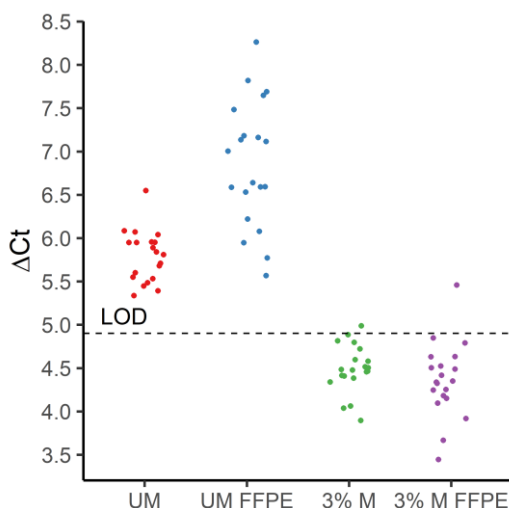


Figure 15. Performance study from the EpiDirect[®] MGMT Methylation qPCR Assay: experimental data for 20 replicates of unmethylated and 3% methylated DNA. Abbreviations: ΔCt , differences between threshold cycles; FFPE, formalin-fixed paraffin-embedded; LOD, limit of detection; M: MGMT methylated; UM: MGMT unmethylated.

2.8. EpiDirect[®] MGMT Methylation qPCR Assay validation

We conducted a comparison of the methylation calling performance of the EpiDirect[®] MGMT Methylation qPCR Assay with two comparator methods:

- a methyl-specific PCR assay followed by gel electrophoresis (comparator method 1);

- a quantitative real-time MSP Assay (comparator method 2).

This comparative analysis allowed us to assess the accuracy and reliability of the EpiDirect® assay in relation to these established comparator methods.

Out of the total 42 samples, 31 of them exhibited consistent results across all three methods. Six samples were identified as methylated, and 25 samples were determined to be unmethylated by all three methods, as shown in Fig. 16.

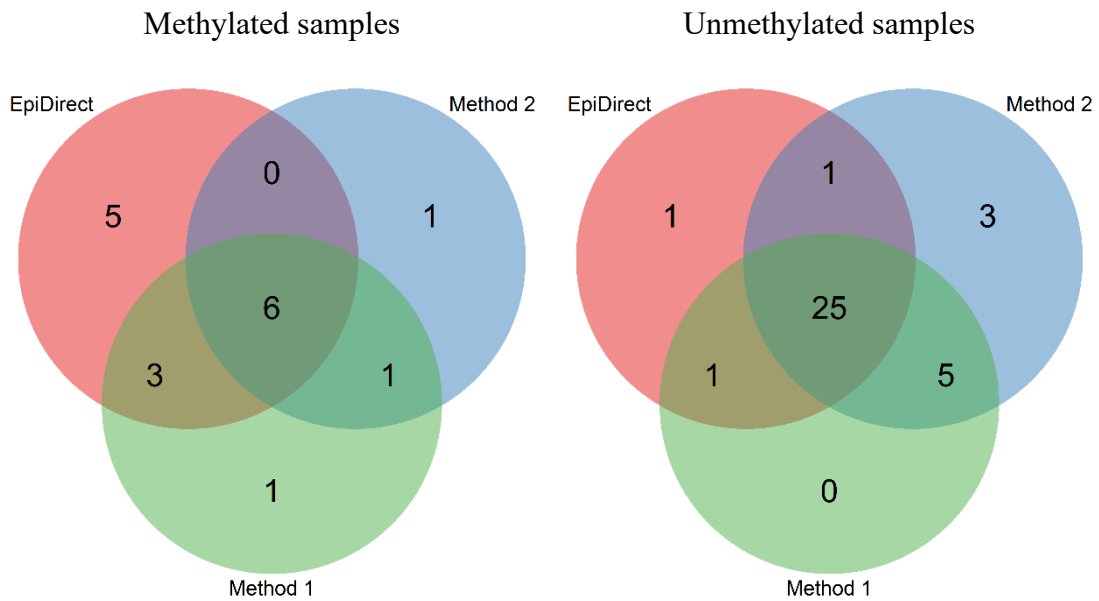


Figure 16. Validation data for the EpiDirect® MGMT Methylation qPCR Assay.

However, for the remaining 11 samples, there was not complete agreement among all three methods. Specifically, five samples displayed agreement between the EpiDirect® MGMT Methylation qPCR Assay and one of the other methods. Interestingly, the EpiDirect® Assay detected an additional five samples as methylated, while these same five samples were identified as unmethylated by the two comparator methods. According to the EpiDirect® analysis, these five samples exhibited methylation levels ranging from 2.4% to 6.5%. A visual representation of the percentage methylation calling by the EpiDirect® Assay and comparator method 2 is depicted in Fig. 17 (the dots are colored according to the methylation status of Method 1 and an identity line ($x = y$) is plotted as a black solid line).

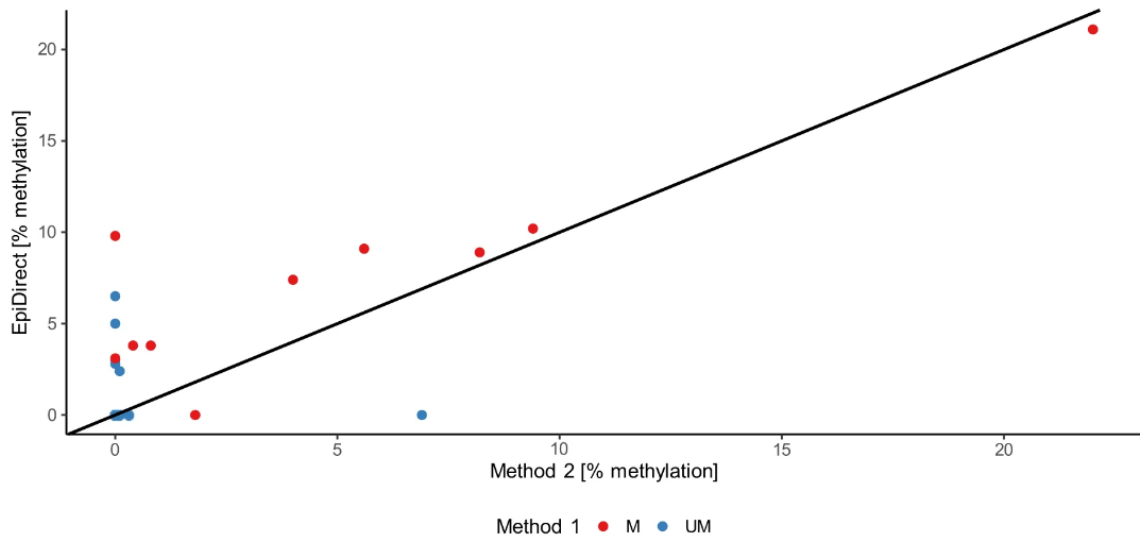


Figure 17. Scatter plot with the percentage methylation calling of EpiDirect plotted against the percentage methylation calling of Method 2. Abbreviations: M: MGMT methylated; UM: MGMT unmethylated.

When using comparative method 1 as a reference, the sensitivity of the EpiDirect[®] MGMT Methylation qPCR Assay was calculated to be 0.82 (95% Confidence Interval [CI] [0.52; 0.95]), and the specificity was found to be 0.84 (95% CI [0.41; 0.93]).

Alternatively, when using comparative method 2 as the reference, the sensitivity of the EpiDirect[®] Assay was determined to be 0.75 (95% CI [0.36; 0.96]), and the specificity was 0.76 (95% CI [0.60; 0.88]). These values provide insights into the assay's performance in relation to the two different reference methods.

DISCUSSION

1. ABOUT miRNA EXPRESSION AND ITS CORRELATION WITH RESPONSE TO STANDARD THERAPY

The ability to predict the effectiveness of available therapeutic options for managing GBM, particularly chemotherapy and radiotherapy following surgery, is of utmost importance for both clinicians and researchers.

Over the past decade, research has highlighted that specific molecular alterations can aid in the early identification of patients who may benefit from tailored chemotherapies. One such alteration is the analysis of MGMT promoter hypermethylation, which occurs in approximately 40% of GBMs. This molecular marker allows for the identification of GBM patients who are likely to respond positively to administration of TMZ. Indeed, it has been established that the presence of MGMT promoter hypermethylation is a favorable prognostic factor for GBM patients treated with TMZ [Stupp et al., 2005; Hegi et al., 2005; Śledzińska et al., 2021; Lee, 2016; Chen et al., 2018]. Nevertheless, it has been observed that there is still a subset of non-methylated tumors that can respond successfully to TMZ treatment. Therefore, the identification of this subgroup of patients is of particular significance [Chen et al., 2018].

This research proposal is situated within the broader context of investigating ways to predict the effectiveness of therapeutic approaches for managing GBM. Recent findings have indicated that small RNA molecules, known as miRNAs, can collectively downregulate the expression of the MGMT protein. This downregulation is not a result of direct interaction but rather involves one or several intermediate molecules. The outcome of this downregulation is similar to the effects of MGMT promoter hypermethylation [Kirstein et al., 2020; Hiddingh et al., 2014; Wang et al., 2019].

Moreover, it has been demonstrated that the presence of these specific miRNAs may be associated with a positive response to TMZ treatment [Kirstein et al., 2020]. However, existing research in this field has typically focused on the investigation of a single miRNA in a single patient cohort or in vitro experiments, which could introduce potential bias based on the unique characteristics of these cohorts. The available information on this topic is relatively fragmented and preliminary.

Therefore, our primary objective is to validate and build upon these promising and highly relevant findings by analyzing multiple miRNA molecules within a cohort of patients who have confirmed GBMs and have undergone treatment with chemo-radiotherapy following surgery, in accordance with the Stupp Protocol [Stupp et al., 2005]. This comprehensive approach aims to provide more robust and clinically applicable insights into the role of miRNAs in GBM therapy.

In our current research, we are investigating seven distinct miRNAs and their potential role in modulating MGMT.

Regarding these miRNAs, our observations have revealed that they do not all exhibit similar trends. Two miRNAs, specifically miR-21 and miR-196b, are generally found to be overexpressed in GBMs. In contrast, one miRNA, miR-767.3, is typically down-regulated in GBMs. The remaining four miRNAs do not show significant variations.

This diversity in miRNA expression patterns highlights the complexity of the regulatory mechanisms in GBMs and underscores the need for further investigation to understand how these miRNAs might collectively influence the modulation of MGMT.

One of the noteworthy findings from our research is the significant correlation observed between the reduced expression of four out of the seven miRNAs (miR-181c, miR-195, miR-648, and miR-767.3p) and the presence of MGMT protein expression, as assessed through IHC.

These findings align with previous research in the literature, which has reported that these particular miRNAs are downregulated in patients who do not respond well to TMZ treatment. These patients typically exhibit high MGMT expression as determined by IHC [Slaby et al., 2010]. Additionally, it is worth noting that these miRNAs generally play a role in inhibiting MGMT expression. Therefore, it is reasonable to infer that their reduced expression is associated with normal MGMT expression, as indicated by IHC [Kreth et al., 2013]. This correlation reinforces the significance of these miRNAs in the context of GBM treatment response.

A second significant finding is the confirmation of the correlation between miRNA expression and MGMT, as mentioned earlier, when examining MGMT methylation. In our analysis, specifically focusing on miR-648, which is the only miRNA exhibiting a

statistically significant association with both MGMT IHC and MGMT methylation, we found that it is associated with the absence of MGMT methylation.

This observation aligns with existing literature, and it reinforces the earlier data related to MGMT IHC. This is because MGMT IHC and methylation represent opposite situations [Lakomy et al., 2011; Kreth et al., 2013]. In other words, both low miRNA expression and the absence of MGMT methylation tend to lead to the expression of MGMT protein and, consequently, a positive result in MGMT protein detection.

However, it is important to note that all the other miRNAs that demonstrated a statistically significant association between their low expression and positive MGMT IHC (i.e., miR-181c, miR-195, and miR-767.3) did not exhibit a significant association with MGMT methylation. This discrepancy could be attributed to the fact that the miRNAs analyzed in this study do not directly interact with MGMT but rather regulate MGMT indirectly through other mediators. This indirect regulation may lead to different behaviors in relation to MGMT. Similarly, this explanation can account for the observations that miR-181d and miR196b expression are associated with MGMT methylation (miR-181d with low expression in unmethylated cases and miR-196b with methylated cases) but do not show a significant association with MGMT IHC.

Our study has yielded noteworthy findings in terms of clinical relevance of miRNA expression with respect to OS and PFS. Initially, we were able to reaffirm the positive correlation between improved OS and PFS ($p = 0.006$ and $p = 0.03$, respectively) and MGMT promoter hypermethylation. This confirmation supports the representativeness of our patient cohort.

Furthermore, our research has also taken into consideration the varying outcomes associated with different surgical approaches. Consistent with our previously published work and the existing literature, patients who underwent a GTR exhibited a more favorable clinical outcome in terms of PFS ($p = 0.04$) [Marchi et al., 2019]. This underscores the clinical significance of the extent of surgical resection.

Additionally, a better clinical outcome was observed in patients with negative IHC results ($p = 0.01$). This further validates the reliability of our analysis and underscores the inverse correlation between negative IHC results and the presence of MGMT methylation, reinforcing the clinical relevance of these molecular markers in predicting patient outcomes.

Significantly, our study also aimed to establish a meaningful relationship between miRNA expression and OS. In this regard, four out of the seven miRNAs analyzed exhibited statistically discernible associations with OS: miR-21, miR-195, miR-196b and miR-648. Interestingly, none of the miRNA analyzed displayed a statistical significant association with PFS.

These findings provide robust evidence that miRNAs indeed play a pivotal role in the modulation of MGMT and, consequently, have a substantial impact on the clinical outcomes of patients with GBM. This reinforces the clinical relevance of miRNAs as potential prognostic markers in GBM patient management.

2. ABOUT DIRECT PCR QUANTIFICATION OF METHYLATIONS USING UNTREATED DNA

MGMT promoter methylation is so important for the management of GBM patients, that it must be evaluated in every case. However, there are several issues, as it is an epigenetic alteration that does not lead to any mutation in the DNA sequence.

There are several methodologies available on the market for the analysis of MGMT methylation, none of them is considered the gold standard method, but all are characterized by positive and negative features. All the methodologies are characterized by the same requirement: the need of several hundreds of nanograms of DNA, a quantity that cannot be always reached when only small biopsies are available. Furthermore, the most diffused one, the methylation-specific PCR, requires DNA conversion of unmethylated cytosines to uracyl, a step that causes DNA damage leading a non-negligible portion of patients not evaluable. The other one, pyrosequencing, requires a dedicated instrument, therefore it is quite expensive and need trained operators, in addition to a modification step of the DNA.

Therefore, setting up a new procedure, faster than the current available, easy to be implemented in every diagnostic laboratory and which does not require any step of DNA modification, may represent a real improvement in the diagnostic workflow for assessing MGMT promoter methylation.

This is what we have done, in collaboration with a Danish company.

We have introduced an innovative platform for the analysis of DNA methylation, which relies solely on qPCR technology. As far as our knowledge extends, this represents the first qPCR method that does not require any form of pre-treatment, including chemical or enzymatic conversion or digestion. This approach offers a novel and simplified way to assess DNA methylation, potentially streamlining the analytical process in this field.

In our study, we observed a significant increase in melting temperature (T_m) when transitioning from zero methylation sites to a single methylation site, with the T_m rising by 2.1-2.9°C in our non-INA[®]-modified setup. This increase was greater than the approximately 1.6°C increase reported in 2015 by Nardo et al. Similarly, as the number of methylation sites increased from one to four, the T_m showed a rise of approximately 0.6°C per additional methylation, which was again higher than the roughly 0.3°C increase per methylation reported by Nardo et al. In 2021, another study by Tsuruta et al. reported an increase in T_m of approximately 1°C per methylation. These variations can be attributed to factors such as the buffer used for melt studies and the sequence itself, which can affect the T_m and account for differences among these studies.

Nonetheless, a common observation from both our study and that of Nardo et al. is that the T_m is more significantly influenced when transitioning from no methylations to one methylation compared to the addition of further methylation sites, even though different setups and sequences were employed [Grunau et al, 2001]. In our case, the use of INA[®] technology allowed us to achieve a substantial increase in T_m , up to 5.3-5.7°C, by introducing a single methylated cytosine into our target sequence compared to an unmethylated target. Additionally, we observed an increase of 1.9°C per additional added methylation, a finding that has not been previously reported.

In addition to the advantages we have discussed, it is important to acknowledge some limitations related to the PCR conditions of the EpiDirect[®] assay. The MGMT sequence used in this study requires a high annealing temperature of 76°C to achieve the highest specificity towards the methylated target. Furthermore, the anchor sequence that anneals to the CpG sites of interest is 14 nucleotides long. If it were longer or had a higher CpG content, the annealing temperature for the PCR would be even higher.

To address the challenge of extreme PCR conditions, we included a single mismatch in the anchor sequence, which effectively reduces the annealing temperature. Without this

mismatch, the optimal annealing temperature was around 80°C, which posed significant challenges for the PCR design. This strategy was employed to make the assay more feasible and reliable under these demanding conditions, but it is important to be aware of the influence of these design choices on the assay's performance.

The clinical validation of the assay revealed some variations between the methods, particularly in cases where the methylation degree was low (less than 10%) according to the EpiDirect® MGMT Methylation qPCR Assay and/or comparator method 2, which also provides semi-quantitative results. Several reasons could explain these discrepancies:

- Differences in analyzed CpG sites: one key factor is that comparator method 1 and EpiDirect® do not analyze the same CpG sites. Furthermore, the specific CpG sites analyzed in comparator method 2 are unknown. The choice of CpG sites can influence the results.
- Variability in cut-off values: EpiDirect® used a cut-off corresponding to the technical LOD of 2.4% methylation, while comparator method 2 used a cut-off of >0.6%. In contrast, comparator method 1 detected methylation by visual inspection of the gel, and no specific cut-off in terms of the percentage of methylation was set. The selection of cut-off values can have a significant impact on the interpretation of results.
- Lack of global consensus: it is important to note that there is no global consensus on the optimal cut-off for predicting the efficacy of TMZ and prognosis. A survey published in 2019 found that the cut-off values used by various laboratories ranged from 3% to 30% methylation when using pyrosequencing. This variability is indicative of the lack of standardized criteria.
- Influence of DNA factors: bisulfite treatment, a key step in DNA methylation analysis, can be influenced by various factors related to the DNA itself, such as quantity and quality. These factors can contribute to variability in results.
- Treatment protocols: additionally, due to the severe nature of the disease, most patients are typically treated with the same protocol, often following the Stupp protocol, regardless of the status of MGMT promoter methylation. In many cases, the MGMT methylation status is primarily used to predict the duration of treatment efficacy rather than to guide treatment decisions.

These considerations emphasize the complexity and variability in the interpretation of MGMT promoter methylation data and highlight the challenges in establishing standardized cut-off values for clinical decision-making in GBM management.

CONCLUSION AND FUTURE PERSPECTIVES

As regards the first part of our work, the present study marks one of the pioneering scientific attempts to investigate the expression of several miRNAs within the same cohort. As there are currently no firmly established methods for the assessment of miRNA expression in malignancy, including GBM, it is plausible to assume a potential bias when different miRNAs are assessed in separate cohorts. We believe that the true clinical relevance of miRNA expression may become evident through studies similar to the one presented here, where multiple miRNAs are evaluated simultaneously. This approach can provide a more comprehensive understanding of the role of miRNAs in malignancy.

Our findings remained consistent when we employed various cut-offs to assess miRNA expression, which enhances the robustness of our conclusions. These results further emphasize the clinical significance of miRNA expression as a potential alternative method for assessing promoter methylation and its regulatory role in MGMT expression.

If our observations are validated in other cohorts, including possibly larger series of GBM cases, our data suggest the potential for miRNA expression to play a future diagnostic role in predicting the efficacy of chemoradiation in GBM. This promising avenue could have a substantial impact on the management and treatment of GBM, with the potential to improve patient outcomes through more personalized and effective therapeutic strategies.

Regarding to EpiDirect[®], this innovative platform for DNA methylation analysis using qPCR technology represents a significant advancement. As per the available information, this is the first qPCR method that does not rely on any pre-treatment process, including chemical or enzymatic conversion or digestion. This approach stands out for its unique capability to analyze DNA methylation directly, streamlining the process and potentially offering a more efficient and simplified methodology for researchers and clinicians involved in DNA methylation analysis.

Our observations suggest that the integration of the EpiDirect[®] platform into diagnostic routine could offer significant advantages. This innovative platform has the potential to save valuable time in the laboratory, streamline the workflow, and eliminate the risk of

incomplete or over-conversion of DNA during the bisulfite treatment process, which can lead to inaccurate estimates of methylation percentages.

Moreover, the introduction of the EpiDirect[®] platform opens up possibilities for broader use of methylation analysis. It may enable smaller laboratories with limited resources to independently perform methylation analysis, thus expanding access to this valuable diagnostic tool, also for the evaluation of other epimutation in the context of tumorigenesis (i.e. MLH1 promoter methylation in sporadic microsatellite unstable tumors, including colorectal cancer and endometrial cancer). This not only enhances the efficiency and accuracy of DNA methylation analysis but also promotes the spreading of these advanced molecular techniques in clinical and research settings, even in emerging countries without substantial financial resources.

REFERENCES

- Barthel FP, Johnson KC, Varn FS, Moskalik AD, Tanner G, Kocakavuk E, Anderson KJ, Abiola O, Aldape K, Alfaro KD, Alpar D, Amin SB, Ashley DM, Bandopadhyay P, Barnholtz-Sloan JS, Beroukhir R, Bock C, Brastianos PK, Brat DJ, Brodbelt AR, Bruns AF, Bulsara KR, Chakrabarty A, Chakravarti A, Chuang JH, Claus EB, Cochran EJ, Connelly J, Costello JF, Finocchiaro G, Fletcher MN, French PJ, Gan HK, Gilbert MR, Gould PV, Grimmer MR, Iavarone A, Ismail A, Jenkinson MD, Khasraw M, Kim H, Kouwenhoven MCM, LaViolette PS, Li M, Lichter P, Ligon KL, Lowman AK, Malta TM, Mazor T, McDonald KL, Molinaro AM, Nam DH, Nayyar N, Ng HK, Ngan CY, Niclou SP, Niers JM, Noushmehr H, Noorbakhsh J, Ormond DR, Park CK, Poisson LM, Rabadan R, Radlwimmer B, Rao G, Reifenberger G, Sa JK, Schuster M, Shaw BL, Short SC, Smitt PAS, Sloan AE, Smits M, Suzuki H, Tabatabai G, Van Meir EG, Watts C, Weller M, Wesseling P, Westerman BA, Widhalm G, Woehrer A, Yung WKA, Zadeh G, Huse JT, De Groot JF, Stead LF, Verhaak RGW; GLASS Consortium. Longitudinal molecular trajectories of diffuse glioma in adults. *Nature*. 2019 Dec;576(7785):112-120. doi: 10.1038/s41586-019-1775-1. Epub 2019 Nov 20. PMID: 31748746; PMCID: PMC6897368.
- Bautista-Sánchez D, Arriaga-Canon C, Pedroza-Torres A, De La Rosa-Velázquez IA, González-Barrios R, Contreras-Espinosa L, Montiel-Manríquez R, Castro-Hernández C, Fragoso-Ontiveros V, Álvarez-Gómez RM, Herrera LA. The Promising Role of miR-21 as a Cancer Biomarker and Its Importance in RNA-Based Therapeutics. *Mol Ther Nucleic Acids*. 2020 Jun 5;20:409-420. doi: 10.1016/j.omtn.2020.03.003. Epub 2020 Mar 13. PMID: 32244168; PMCID: PMC7118281.
- Bogaerts, K.; Komarek, A.; Lesaffre, E. *Survival Analysis with Interval-Censored Data*; Chapman & Hall CRC: New York, NY, USA, 2018
- Braganza MZ, Kitahara CM, Berrington de González A, Inskip PD, Johnson KJ, Rajaraman P. Ionizing radiation and the risk of brain and central nervous system tumors: a systematic review. *Neuro Oncol*. 2012 Nov;14(11):1316-24. doi: 10.1093/neuonc/nos208. Epub 2012 Sep 5. PMID: 22952197; PMCID: PMC3480263.
- Brell M, Ibáñez J, Tortosa A. O6-Methylguanine-DNA methyltransferase protein expression by immunohistochemistry in brain and non-brain systemic tumours: systematic review and meta-analysis of correlation with methylation-specific polymerase chain reaction. *BMC Cancer*. 2011 Jan 26;11:35. doi: 10.1186/1471-2407-11-35. PMID: 21269507; PMCID: PMC3039628.
- Calin GA, Dumitru CD, Shimizu M, Bichi R, Zupo S, Noch E, Aldler H, Rattan S, Keating M, Rai K, Rassenti L, Kipps T, Negrini M, Bullrich F, Croce CM. Frequent deletions and down-regulation of micro-RNA genes miR15 and miR16 at 13q14 in chronic lymphocytic leukemia. *Proc Natl Acad Sci U S A*. 2002 Nov 26;99(24):15524-9. doi: 10.1073/pnas.242606799. Epub 2002 Nov 14. PMID: 12434020; PMCID: PMC137750.
- Calin GA, Sevignani C, Dumitru CD, Hyslop T, Noch E, Yendamuri S, Shimizu M, Rattan S, Bullrich F, Negrini M, Croce CM. Human microRNA genes are frequently located at fragile sites and genomic regions involved in cancers. *Proc Natl Acad Sci U S A*. 2004 Mar

2;101(9):2999-3004. doi: 10.1073/pnas.0307323101. Epub 2004 Feb 18. PMID: 14973191; PMCID: PMC365734.

Cao VT, Jung TY, Jung S, et al. The correlation and prognostic significance of MGMT promoter methylation and MGMT protein in glioblastomas. *Neurosurgery*. 2009 Nov;65(5):866-75; discussion 875. DOI: 10.1227/01.neu.0000357325.90347.a1. PMID: 19834398.

Capper D, Jones DTW, Sill M, Hovestadt V, Schrimpf D, Sturm D, Koelsche C, Sahm F, Chavez L, Reuss DE, Kratz A, Wefers AK, Huang K, Pajtler KW, Schweizer L, Stichel D, Olar A, Engel NW, Lindenberg K, Harter PN, Braczynski AK, Plate KH, Dohmen H, Garvalov BK, Coras R, Hölsken A, Hewer E, Bewerunge-Hudler M, Schick M, Fischer R, Beschorner R, Schittenhelm J, Staszewski O, Wani K, Varlet P, Pages M, Temming P, Lohmann D, Selt F, Witt H, Milde T, Witt O, Aronica E, Giangaspero F, Rushing E, Scheurlen W, Geisenberger C, Rodriguez FJ, Becker A, Preusser M, Haberler C, Bjerkvig R, Cryan J, Farrell M, Deckert M, Hench J, Frank S, Serrano J, Kannan K, Tzirigos A, Brück W, Hofer S, Brehmer S, Seiz-Rosenhagen M, Hänggi D, Hans V, Rozsnoki S, Hansford JR, Kohlhof P, Kristensen BW, Lechner M, Lopes B, Mawrin C, Ketter R, Kulozik A, Khatib Z, Heppner F, Koch A, Jouvet A, Keohane C, Mühleisen H, Mueller W, Pohl U, Prinz M, Benner A, Zapatka M, Gottardo NG, Driever PH, Kramm CM, Müller HL, Rutkowski S, von Hoff K, Frühwald MC, Gnekow A, Fleischhack G, Tippelt S, Calaminus G, Monoranu CM, Perry A, Jones C, Jacques TS, Radlwimmer B, Gessi M, Pietsch T, Schramm J, Schackert G, Westphal M, Reifenberger G, Wesseling P, Weller M, Collins VP, Blümcke I, Bendszus M, Debus J, Huang A, Jabado N, Northcott PA, Paulus W, Gajjar A, Robinson GW, Taylor MD, Jaunmuktane Z, Ryzhova M, Platten M, Unterberg A, Wick W, Karajannis MA, Mittelbronn M, Acker T, Hartmann C, Aldape K, Schüller U, Buslei R, Lichter P, Kool M, Herold-Mende C, Ellison DW, Hasselblatt M, Snuderl M, Brandner S, Korshunov A, von Deimling A, Pfister SM. DNA methylation-based classification of central nervous system tumours. *Nature*. 2018 Mar 22;555(7697):469-474. doi: 10.1038/nature26000. Epub 2018 Mar 14. PMID: 29539639; PMCID: PMC6093218.

Capper D, Stichel D, Sahm F, Jones DTW, Schrimpf D, Sill M, Schmid S, Hovestadt V, Reuss DE, Koelsche C, Reinhardt A, Wefers AK, Huang K, Sievers P, Ebrahimi A, Schöler A, Teichmann D, Koch A, Hänggi D, Unterberg A, Platten M, Wick W, Witt O, Milde T, Korshunov A, Pfister SM, von Deimling A. Practical implementation of DNA methylation and copy-number-based CNS tumor diagnostics: the Heidelberg experience. *Acta Neuropathol*. 2018 Aug;136(2):181-210. doi: 10.1007/s00401-018-1879-y. Epub 2018 Jul 2. PMID: 29967940; PMCID: PMC6060790.

Cardia A, Epistolio S, Zaed I, Sahnane N, Cerutti R, Cipriani D, Barizzi J, Spina P, Stefanini FM, Cerati M, Balbi S, Mazzucchelli L, Sessa F, Pesce GA, Reinert M, Frattini M, Marchi F. Identification of MGMT Downregulation Induced by miRNA in Glioblastoma and Possible Effect on Temozolomide Sensitivity. *J Clin Med*. 2023 Mar 6;12(5):2061. doi: 10.3390/jcm12052061. PMID: 36902848; PMCID: PMC10004383.

Chen L, Voronovich Z, Clark K, Hands I, Mannas J, Walsh M, Nikiforova MN, Durbin EB, Weiss H, Horbinski C. Predicting the likelihood of an isocitrate dehydrogenase 1 or 2

mutation in diagnoses of infiltrative glioma. *Neuro Oncol.* 2014 Nov;16(11):1478-83. doi: 10.1093/neuonc/nou097. Epub 2014 May 23. PMID: 24860178; PMCID: PMC4201069.

Chen TC, Chan N, Minea RO, Hartman H, Hofman FM, Schönthal AH. Rare Stochastic Expression of O6-Methylguanine- DNA Methyltransferase (MGMT) in MGMT-Negative Melanoma Cells Determines Immediate Emergence of Drug-Resistant Populations upon Treatment with Temozolomide In Vitro and In Vivo. *Cancers (Basel).* 2018 Sep 28;10(10):362. doi: 10.3390/cancers10100362. PMID: 30274152; PMCID: PMC6209933.

Colella S, Shen L, Baggerly KA, Issa JP, Krahe R. Sensitive and quantitative universal Pyrosequencing methylation analysis of CpG sites. *Biotechniques.* 2003 Jul;35(1):146-50. doi: 10.2144/03351md01. PMID: 12866414.

DeWitt JC, Jordan JT, Frosch MP, Samore WR, Iafrate AJ, Louis DN, Lennerz JK. Cost-effectiveness of IDH testing in diffuse gliomas according to the 2016 WHO classification of tumors of the central nervous system recommendations. *Neuro Oncol.* 2017 Nov 29;19(12):1640-1650. doi: 10.1093/neuonc/nox120. PMID: 29016871; PMCID: PMC5716163.

Ellingson BM, Bendszus M, Boxerman J, Barboriak D, Erickson BJ, Smits M, Nelson SJ, Gerstner E, Alexander B, Goldmacher G, Wick W, Vogelbaum M, Weller M, Galanis E, Kalpathy-Cramer J, Shankar L, Jacobs P, Pope WB, Yang D, Chung C, Knopp MV, Cha S, van den Bent MJ, Chang S, Yung WK, Cloughesy TF, Wen PY, Gilbert MR; Jumpstarting Brain Tumor Drug Development Coalition Imaging Standardization Steering Committee. Consensus recommendations for a standardized Brain Tumor Imaging Protocol in clinical trials. *Neuro Oncol.* 2015 Sep;17(9):1188-98. doi: 10.1093/neuonc/nov095. Epub 2015 Aug 5. PMID: 26250565; PMCID: PMC4588759.

Forcella M, Mozzi A, Stefanini FM, Riva A, Epistolio S, Molinari F, Merlo E, Monti E, Fusi P, Frattini M. Deregulation of sialidases in human normal and tumor tissues. *Cancer Biomark.* 2018 Feb 14;21(3):591-601. doi: 10.3233/CBM-170548. PMID: 29278877.

Gharzeddine K, Hatzoglou V, Holodny AI, Young RJ. MR Perfusion and MR Spectroscopy of Brain Neoplasms. *Radiol Clin North Am.* 2019 Nov;57(6):1177-1188. doi: 10.1016/j.rcl.2019.07.008. PMID: 31582043.

Grunau C, Clark SJ, Rosenthal A. Bisulfite genomic sequencing: systematic investigation of critical experimental parameters. *Nucleic Acids Res.* 2001 Jul 1;29(13):E65-5. doi: 10.1093/nar/29.13.e65. PMID: 11433041; PMCID: PMC55789.

Hegi ME, Diserens AC, Gorlia T, Hamou MF, de Tribolet N, Weller M, Kros JM, Hainfellner JA, Mason W, Mariani L, Bromberg JE, Hau P, Mirimanoff RO, Cairncross JG, Janzer RC, Stupp R. MGMT gene silencing and benefit from temozolomide in glioblastoma. *N Engl J Med.* 2005 Mar 10;352(10):997-1003. doi: 10.1056/NEJMoa043331. PMID: 15758010.

Herman JG, Graff JR, Myöhänen S, Nelkin BD, Baylin SB. Methylation-specific PCR: a novel PCR assay for methylation status of CpG islands. *Proc Natl Acad Sci U S A.* 1996 Sep 3;93(18):9821-6. doi: 10.1073/pnas.93.18.9821. PMID: 8790415; PMCID: PMC38513.

Hiddingh L, Raktoc RS, Jeuken J, Hulleman E, Noske DP, Kaspers GJ, Vandertop WP, Wesseling P, Wurdinger T. Identification of temozolomide resistance factors in glioblastoma via integrative miRNA/mRNA regulatory network analysis. *Sci Rep*. 2014 Jun 11;4:5260. doi: 10.1038/srep05260. PMID: 24919120; PMCID: PMC4052714.

Hottinger AF, Stupp R, Homicsko K. Standards of care and novel approaches in the management of glioblastoma multiforme. *Chin J Cancer*. 2014 Jan;33(1):32-9. doi: 10.5732/cjc.013.10207. PMID: 24384238; PMCID: PMC3905088.

International Agency for Research on Cancer Working Group on the Evaluation of Carcinogenic Risks to Humans; World Health Organization. Non-ionizing radiation: static and extremely low-frequency (ELF) electric and magnetic fields. 2002. Accessed February 1, 2023. <https://publications.iarc.fr/Book-And-Report-Series/IarcMonographs-On-The-Identification-Of-Carcinogenic-Hazards-To-Humans/Non-ionizing-Radiation-Part-1-Static-And-Extremely-Low-frequency-ELF-Electric-And-Magnetic-Fields-2002>

ISO 14155:2020; Clinical Investigation of Medical Devices for Human Subjects—Good Clinical Practice. ISO: Geneva, Switzerland, 2020

Jonsson P, Lin AL, Young RJ, DiStefano NM, Hyman DM, Li BT, Berger MF, Zehir A, Ladanyi M, Solit DB, Arnold AG, Stadler ZK, Mandelker D, Goldberg ME, Chmielecki J, Pourmaleki M, Ogilvie SQ, Chavan SS, McKeown AT, Manne M, Hyde A, Beal K, Yang TJ, Nolan CP, Pentsova E, Omuro A, Gavrilovic IT, Kaley TJ, Diamond EL, Stone JB, Grommes C, Boire A, Daras M, Piotrowski AF, Miller AM, Gutin PH, Chan TA, Tabar VS, Brennan CW, Rosenblum M, DeAngelis LM, Mellinghoff IK, Taylor BS. Genomic Correlates of Disease Progression and Treatment Response in Prospectively Characterized Gliomas. *Clin Cancer Res*. 2019 Sep 15;25(18):5537-5547. doi: 10.1158/1078-0432.CCR-19-0032. Epub 2019 Jul 1. PMID: 31263031; PMCID: PMC6753053. Kint S, De Spiegelaere W, De Kesel J, Vandekerckhove L, Van Criekinge W. Evaluation of bisulfite kits for DNA methylation profiling in terms of DNA fragmentation and DNA recovery using digital PCR. *PLoS One*. 2018 Jun 14;13(6):e0199091. doi: 10.1371/journal.pone.0199091. PMID: 29902267; PMCID: PMC6002050.

Kirstein A, Schmid TE, Combs SE. The Role of miRNA for the Treatment of MGMT Unmethylated Glioblastoma Multiforme. *Cancers (Basel)*. 2020 Apr 28;12(5):1099. doi: 10.3390/cancers12051099. PMID: 32354046; PMCID: PMC7281574.

Körber V, Yang J, Barah P, Wu Y, Stichel D, Gu Z, Fletcher MNC, Jones D, Hentschel B, Lamszus K, Tonn JC, Schackert G, Sabel M, Felsberg J, Zacher A, Kaulich K, Hübschmann D, Herold-Mende C, von Deimling A, Weller M, Radlwimmer B, Schlesner M, Reifenberger G, Höfer T, Lichter P. Evolutionary Trajectories of IDH^{WT} Glioblastomas Reveal a Common Path of Early Tumorigenesis Instigated Years ahead of Initial Diagnosis. *Cancer Cell*. 2019 Apr 15;35(4):692-704.e12. doi: 10.1016/j.ccell.2019.02.007. Epub 2019 Mar 21. PMID: 30905762.

Korshunov A, Chavez L, Sharma T, Ryzhova M, Schrimpf D, Stichel D, Capper D, Sturm D, Kool M, Habel A, Kleinschmidt-DeMasters BK, Rosenblum M, Absalyamova O, Golanov A, Lichter P, Pfister SM, Jones DTW, Perry A, von Deimling A. Epithelioid glioblastomas stratify into established diagnostic subsets upon integrated molecular analysis.

Brain Pathol. 2018 Sep;28(5):656-662. doi: 10.1111/bpa.12566. Epub 2017 Oct 30. PMID: 28990704; PMCID: PMC7469088.

Korshunov A, Schrimpf D, Ryzhova M, Sturm D, Chavez L, Hovestadt V, Sharma T, Habel A, Burford A, Jones C, Zheludkova O, Kumirova E, Kramm CM, Golanov A, Capper D, von Deimling A, Pfister SM, Jones DTW. H3-/IDH-wild type pediatric glioblastoma is comprised of molecularly and prognostically distinct subtypes with associated oncogenic drivers. *Acta Neuropathol.* 2017 Sep;134(3):507-516. doi: 10.1007/s00401-017-1710-1. Epub 2017 Apr 11. PMID: 28401334.

Kreth S, Limbeck E, Hinske LC, Schütz SV, Thon N, Hoefig K, Egensperger R, Kreth FW. In human glioblastomas transcript elongation by alternative polyadenylation and miRNA targeting is a potent mechanism of MGMT silencing. *Acta Neuropathol.* 2013 May;125(5):671-81. doi: 10.1007/s00401-013-1081-1. Epub 2013 Jan 23. PMID: 23340988.

Labreche K, Kinnersley B, Berzero G, Di Stefano AL, Rahimian A, Detrait I, Marie Y, Grenier-Boley B, Hoang-Xuan K, Delattre JY, Idbaih A, Houlston RS, Sanson M. Diffuse gliomas classified by 1p/19q co-deletion, TERT promoter and IDH mutation status are associated with specific genetic risk loci. *Acta Neuropathol.* 2018 May;135(5):743-755. doi: 10.1007/s00401-018-1825-z. Epub 2018 Feb 19. PMID: 29460007; PMCID: PMC5904227. Lagos-Quintana M, Rauhut R, Lendeckel W, Tuschl T. Identification of novel genes coding for small expressed RNAs. *Science.* 2001 Oct 26;294(5543):853-8. doi: 10.1126/science.1064921. PMID: 11679670.

Lakomy R, Sana J, Hankeova S, Fadrus P, Kren L, Lzicarova E, Svoboda M, Dolezelova H, Smrcka M, Vyzula R, Michalek J, Hajduch M, Slaby O. MiR-195, miR-196b, miR-181c, miR-21 expression levels and O-6-methylguanine-DNA methyltransferase methylation status are associated with clinical outcome in glioblastoma patients. *Cancer Sci.* 2011 Dec;102(12):2186-90. doi: 10.1111/j.1349-7006.2011.02092.x. Epub 2011 Oct 12. PMID: 21895872.

Law I, Albert NL, Arbizu J, Boellaard R, Drzezga A, Galldiks N, la Fougère C, Langen KJ, Lopci E, Lowe V, McConathy J, Quick HH, Sattler B, Schuster DM, Tonn JC, Weller M. Joint EANM/EANO/RANO practice guidelines/SNMMI procedure standards for imaging of gliomas using PET with radiolabelled amino acids and [¹⁸F]FDG: version 1.0. *Eur J Nucl Med Mol Imaging.* 2019 Mar;46(3):540-557. doi: 10.1007/s00259-018-4207-9. Epub 2018 Dec 5. PMID: 30519867; PMCID: PMC6351513.

Lee RC, Feinbaum RL, Ambros V. The *C. elegans* heterochronic gene *lin-4* encodes small RNAs with antisense complementarity to *lin-14*. *Cell.* 1993 Dec 3;75(5):843-54. doi: 10.1016/0092-8674(93)90529-y. PMID: 8252621.

Lee SY. Temozolomide resistance in glioblastoma multiforme. *Genes Dis.* 2016 May 11;3(3):198-210. doi: 10.1016/j.gendis.2016.04.007. PMID: 30258889; PMCID: PMC6150109.

Leske H, Dalglish R, Lazar AJ, Reifenberger G, Cree IA. A common classification framework for histone sequence alterations in tumours: an expert consensus proposal. *J*

Pathol. 2021 Jun;254(2):109-120. doi: 10.1002/path.5666. Epub 2021 May 7. PMID: 33779999.

Liu Y, Siejka-Zielińska P, Velikova G, Bi Y, Yuan F, Tomkova M, Bai C, Chen L, Schuster-Böckler B, Song CX. Bisulfite-free direct detection of 5-methylcytosine and 5-hydroxymethylcytosine at base resolution. *Nat Biotechnol.* 2019 Apr;37(4):424-429. doi: 10.1038/s41587-019-0041-2. Epub 2019 Feb 25. PMID: 30804537.

Livak KJ, Schmittgen TD. Analysis of relative gene expression data using real-time quantitative PCR and the 2^{(-Delta Delta C(T))} Method. *Methods.* 2001 Dec;25(4):402-8. doi: 10.1006/meth.2001.1262. PMID: 11846609.

Louis DN, Aldape K, Brat DJ, Capper D, Ellison DW, Hawkins C, Paulus W, Perry A, Reifenberger G, Figarella-Branger D, Wesseling P, Batchelor TT, Cairncross JG, Pfister SM, Rutkowski S, Weller M, Wick W, von Deimling A. Announcing cIMPACT-NOW: the Consortium to Inform Molecular and Practical Approaches to CNS Tumor Taxonomy. *Acta Neuropathol.* 2017 Jan;133(1):1-3. doi: 10.1007/s00401-016-1646-x. PMID: 27909809.

Louis DN, Perry A, Reifenberger G, von Deimling A, Figarella-Branger D, Cavenee WK, Ohgaki H, Wiestler OD, Kleihues P, Ellison DW. The 2016 World Health Organization Classification of Tumors of the Central Nervous System: a summary. *Acta Neuropathol.* 2016 Jun;131(6):803-20. doi: 10.1007/s00401-016-1545-1. Epub 2016 May 9. PMID: 27157931.

Louis DN, Perry A, Wesseling P, Brat DJ, Cree IA, Figarella-Branger D, Hawkins C, Ng HK, Pfister SM, Reifenberger G, Soffietti R, von Deimling A, Ellison DW. The 2021 WHO Classification of Tumors of the Central Nervous System: a summary. *Neuro Oncol.* 2021 Aug 2;23(8):1231-1251. doi: 10.1093/neuonc/noab106. PMID: 34185076; PMCID: PMC8328013. Louis DN, Perry A, Wesseling P, et al. The 2021 WHO Classification of Tumours of the Central Nervous System: a summary. *Neuro Oncol.* 2021;23(8):1231-1251. doi:10.1093/neuonc/noab106

Louis DN, Wesseling P, Aldape K, Brat DJ, Capper D, Cree IA, Eberhart C, Figarella-Branger D, Fouladi M, Fuller GN, Giannini C, Haberler C, Hawkins C, Komori T, Kros JM, Ng HK, Orr BA, Park SH, Paulus W, Perry A, Pietsch T, Reifenberger G, Rosenblum M, Rous B, Sahm F, Sarkar C, Solomon DA, Tabori U, van den Bent MJ, von Deimling A, Weller M, White VA, Ellison DW. cIMPACT-NOW update 6: new entity and diagnostic principle recommendations of the cIMPACT-Utrecht meeting on future CNS tumor classification and grading. *Brain Pathol.* 2020 Jul;30(4):844-856. doi: 10.1111/bpa.12832. Epub 2020 Apr 19. PMID: 32307792; PMCID: PMC8018152.

Ly KI, Wen PY, Huang RY. Imaging of Central Nervous System Tumors Based on the 2016 World Health Organization Classification. *Neurol Clin.* 2020 Feb;38(1):95-113. doi: 10.1016/j.ncl.2019.08.004. Epub 2019 Nov 7. PMID: 31761063.

Malley DS, Hamoudi RA, Kocialkowski S, Pearson DM, Collins VP, Ichimura K. A distinct region of the MGMT CpG island critical for transcriptional regulation is preferentially methylated in glioblastoma cells and xenografts. *Acta Neuropathol.* 2011 May;121(5):651-61. doi: 10.1007/s00401-011-0803-5. Epub 2011 Feb 3. PMID: 21287394.

Malmström A, Grønberg BH, Marosi C, Stupp R, Frappaz D, Schultz H, Abacioglu U, Tavelin B, Lhermitte B, Hegi ME, Rosell J, Henriksson R; Nordic Clinical Brain Tumour Study Group (NCBTSG). Temozolomide versus standard 6-week radiotherapy versus hypofractionated radiotherapy in patients older than 60 years with glioblastoma: the Nordic randomised, phase 3 trial. *Lancet Oncol.* 2012 Sep;13(9):916-26. doi: 10.1016/S1470-2045(12)70265-6. Epub 2012 Aug 8. PMID: 22877848.

Mansouri A, Hachem LD, Mansouri S, Nassiri F, Laperriere NJ, Xia D, Lindeman NI, Wen PY, Chakravarti A, Mehta MP, Hegi ME, Stupp R, Aldape KD, Zadeh G. MGMT promoter methylation status testing to guide therapy for glioblastoma: refining the approach based on emerging evidence and current challenges. *Neuro Oncol.* 2019 Feb 14;21(2):167-178. doi: 10.1093/neuonc/noy132. PMID: 30189035; PMCID: PMC6374759.

Marchi F, Sahnane N, Cerutti R, Cipriani D, Barizzi J, Stefanini FM, Epistolio S, Cerati M, Balbi S, Mazzucchelli L, Sessa F, Pesce GA, Reinert M, Frattini M. The Impact of Surgery in IDH 1 Wild Type Glioblastoma in Relation With the MGMT Deregulation. *Front Oncol.* 2020 Jan 24;9:1569. doi: 10.3389/fonc.2019.01569. PMID: 32039032; PMCID: PMC6992596.

Melin BS, Barnholtz-Sloan JS, Wrensch MR, Johansen C, Il'yasova D, Kinnersley B, Ostrom QT, Labreche K, Chen Y, Armstrong G, Liu Y, Eckel-Passow JE, Decker PA, Labussière M, Idbaih A, Hoang-Xuan K, Di Stefano AL, Mokhtari K, Delattre JY, Broderick P, Galan P, Gousias K, Schramm J, Schoemaker MJ, Fleming SJ, Herms S, Heilmann S, Nöthen MM, Wichmann HE, Schreiber S, Swerdlow A, Lathrop M, Simon M, Sanson M, Andersson U, Rajaraman P, Chanock S, Linet M, Wang Z, Yeager M; GliomaScan Consortium; Wiencke JK, Hansen H, McCoy L, Rice T, Kosel ML, Sicotte H, Amos CI, Bernstein JL, Davis F, Lachance D, Lau C, Merrell RT, Schildkraut J, Ali-Osman F, Sadetzki S, Scheurer M, Shete S, Lai RK, Claus EB, Olson SH, Jenkins RB, Houlston RS, Bondy ML. Genome-wide association study of glioma subtypes identifies specific differences in genetic susceptibility to glioblastoma and non-glioblastoma tumors. *Nat Genet.* 2017 May;49(5):789-794. doi: 10.1038/ng.3823. Epub 2017 Mar 27. PMID: 28346443; PMCID: PMC5558246. Miller AM, Shah RH, Pentsova EI, Pourmaleki M, Briggs S, Distefano N, Zheng Y, Skakodub A, Mehta SA, Campos C, Hsieh WY, Selcuklu SD, Ling L, Meng F, Jing X, Samoila A, Bale TA, Tsui DWY, Grommes C, Viale A, Souweidane MM, Tabar V, Brennan CW, Reiner AS, Rosenblum M, Panageas KS, DeAngelis LM, Young RJ, Berger MF, Mellinghoff IK. Tracking tumour evolution in glioma through liquid biopsies of cerebrospinal fluid. *Nature.* 2019 Jan;565(7741):654-658. doi: 10.1038/s41586-019-0882-3. Epub 2019 Jan 23. PMID: 30675060; PMCID: PMC6457907.

Molinaro AM, Hervey-Jumper S, Morshed RA, Young J, Han SJ, Chunduru P, Zhang Y, Phillips JJ, Shai A, Lafontaine M, Crane J, Chandra A, Flanigan P, Jahangiri A, Cioffi G, Ostrom Q, Anderson JE, Badve C, Barnholtz-Sloan J, Sloan AE, Erickson BJ, Decker PA, Kosel ML, LaChance D, Eckel-Passow J, Jenkins R, Villanueva-Meyer J, Rice T, Wrensch M, Wiencke JK, Oberheim Bush NA, Taylor J, Butowski N, Prados M, Clarke J, Chang S, Chang E, Aghi M, Theodosopoulos P, McDermott M, Berger MS. Association of Maximal Extent of Resection of Contrast-Enhanced and Non-Contrast-Enhanced Tumor With Survival Within Molecular Subgroups of Patients With Newly Diagnosed Glioblastoma.

JAMA Oncol. 2020 Apr 1;6(4):495-503. doi: 10.1001/jamaoncol.2019.6143. Erratum in: JAMA Oncol. 2020 Mar 1;6(3):444. PMID: 32027343; PMCID: PMC7042822. Nardo L, Lamperti M, Salerno D, Cassina V, Missana N, Bondani M, Tempestini A, Mantegazza F. Effects of non-CpG site methylation on DNA thermal stability: a fluorescence study. *Nucleic Acids Res.* 2015 Dec 15;43(22):10722-33. doi: 10.1093/nar/gkv884. Epub 2015 Sep 9. PMID: 26354864; PMCID: PMC4678853.

Nygren AO, Ameziane N, Duarte HM, Vijzelaar RN, Waisfisz Q, Hess CJ, Schouten JP, Errami A. Methylation-specific MLPA (MS-MLPA): simultaneous detection of CpG methylation and copy number changes of up to 40 sequences. *Nucleic Acids Res.* 2005 Aug 16;33(14):e128. doi: 10.1093/nar/gni127. PMID: 16106041; PMCID: PMC1187824.

Oh JE, Ohta T, Nonoguchi N, Satomi K, Capper D, Pierscianek D, Sure U, Vital A, Paulus W, Mittelbronn M, Antonelli M, Kleihues P, Giangaspero F, Ohgaki H. Genetic Alterations in Gliosarcoma and Giant Cell Glioblastoma. *Brain Pathol.* 2016 Jul;26(4):517-22. doi: 10.1111/bpa.12328. Epub 2015 Dec 16. PMID: 26443480; PMCID: PMC8029477.

Ostrom QT, Cioffi G, Waite K, Kruchko C, Barnholtz-Sloan JS. CBTRUS Statistical Report: Primary Brain and Other Central Nervous System Tumors Diagnosed in the United States in 2014-2018. *Neuro Oncol.* 2021 Oct 5;23(12 Suppl 2):iii1-iii105. doi: 10.1093/neuonc/noab200. PMID: 34608945; PMCID: PMC8491279. Oz G, Alger JR, Barker PB, Bartha R, Bizzi A, Boesch C, Bolan PJ, Brindle KM, Cudalbu C, Dinçer A, Dydak U, Emir UE, Frahm J, González RG, Gruber S, Gruetter R, Gupta RK, Heerschap A, Henning A, Hetherington HP, Howe FA, Hüppi PS, Hurd RE, Kantarci K, Klomp DW, Kreis R, Kruiskamp MJ, Leach MO, Lin AP, Luijten PR, Marjańska M, Maudsley AA, Meyerhoff DJ, Mountford CE, Nelson SJ, Pamir MN, Pan JW, Peet AC, Poptani H, Posse S, Pouwels PJ, Ratai EM, Ross BD, Scheenen TW, Schuster C, Smith IC, Soher BJ, Tkáč I, Vigneron DB, Kauppinen RA; MRS Consensus Group. Clinical proton MR spectroscopy in central nervous system disorders. *Radiology.* 2014 Mar;270(3):658-79. doi: 10.1148/radiol.13130531. PMID: 24568703; PMCID: PMC4263653.

Radke J, Koch A, Pritsch F, Schumann E, Misch M, Hempt C, Lenz K, Löbel F, Paschereit F, Heppner FL, Vajkoczy P, Koll R, Onken J. Predictive MGMT status in a homogeneous cohort of IDH wildtype glioblastoma patients. *Acta Neuropathol Commun.* 2019 Jun 5;7(1):89. doi: 10.1186/s40478-019-0745-z. Erratum in: *Acta Neuropathol Commun.* 2019 Aug 14;7(1):131. PMID: 31167648; PMCID: PMC6549362.

Reifenberger G, Weber RG, Rieher V, Kaulich K, Willscher E, Wirth H, Gietzelt J, Hentschel B, Westphal M, Simon M, Schackert G, Schramm J, Matschke J, Sabel MC, Gramatzki D, Felsberg J, Hartmann C, Steinbach JP, Schlegel U, Wick W, Radlwimmer B, Pietsch T, Tonn JC, von Deimling A, Binder H, Weller M, Loeffler M; German Glioma Network. Molecular characterization of long-term survivors of glioblastoma using genome- and transcriptome-wide profiling. *Int J Cancer.* 2014 Oct 15;135(8):1822-31. doi: 10.1002/ijc.28836. Epub 2014 Mar 28. PMID: 24615357.

Schaff LR, Mellinshoff IK. Glioblastoma and Other Primary Brain Malignancies in Adults: A Review. *JAMA.* 2023 Feb 21;329(7):574-587. doi: 10.1001/jama.2023.0023. PMID: 36809318.

Shah N, Lin B, Sibenaller Z, Ryken T, Lee H, Yoon JG, Rostad S, Foltz G. Comprehensive analysis of MGMT promoter methylation: correlation with MGMT expression and clinical response in GBM. *PLoS One*. 2011 Jan 7;6(1):e16146. doi: 10.1371/journal.pone.0016146. PMID: 21249131; PMCID: PMC3017549.

Slaby O, Lakomy R, Fadrus P, et al. MicroRNA-181 family predicts response to concomitant chemoradiotherapy with temozolomide in glioblastoma patients. *Neoplasma*. 2010 ;57(3):264-269. DOI: 10.4149/neo_2010_03_264. PMID: 20353279.

Śledzińska P, Bebyn MG, Furtak J, Kowalewski J, Lewandowska MA. Prognostic and Predictive Biomarkers in Gliomas. *Int J Mol Sci*. 2021 Sep 26;22(19):10373. doi: 10.3390/ijms221910373. PMID: 34638714; PMCID: PMC8508830.

Stichel D, Ebrahimi A, Reuss D, Schrimpf D, Ono T, Shirahata M, Reifenberger G, Weller M, Hänggi D, Wick W, Herold-Mende C, Westphal M, Brandner S, Pfister SM, Capper D, Sahm F, von Deimling A. Distribution of EGFR amplification, combined chromosome 7 gain and chromosome 10 loss, and TERT promoter mutation in brain tumors and their potential for the reclassification of IDHwt astrocytoma to glioblastoma. *Acta Neuropathol*. 2018 Nov;136(5):793-803. doi: 10.1007/s00401-018-1905-0. Epub 2018 Sep 5. PMID: 30187121.

Stupp R, Hegi ME, Mason WP, van den Bent MJ, Taphoorn MJ, Janzer RC, Ludwin SK, Allgeier A, Fisher B, Belanger K, Hau P, Brandes AA, Gijtenbeek J, Marosi C, Vecht CJ, Mokhtari K, Wesseling P, Villa S, Eisenhauer E, Gorlia T, Weller M, Lacombe D, Cairncross JG, Mirimanoff RO; European Organisation for Research and Treatment of Cancer Brain Tumour and Radiation Oncology Groups; National Cancer Institute of Canada Clinical Trials Group. Effects of radiotherapy with concomitant and adjuvant temozolomide versus radiotherapy alone on survival in glioblastoma in a randomised phase III study: 5-year analysis of the EORTC-NCIC trial. *Lancet Oncol*. 2009 May;10(5):459-66. doi: 10.1016/S1470-2045(09)70025-7. Epub 2009 Mar 9. PMID: 19269895.

Stupp R, Mason WP, van den Bent MJ, Weller M, Fisher B, Taphoorn MJ, Belanger K, Brandes AA, Marosi C, Bogdahn U, Curschmann J, Janzer RC, Ludwin SK, Gorlia T, Allgeier A, Lacombe D, Cairncross JG, Eisenhauer E, Mirimanoff RO; European Organisation for Research and Treatment of Cancer Brain Tumor and Radiotherapy Groups; National Cancer Institute of Canada Clinical Trials Group. Radiotherapy plus concomitant and adjuvant temozolomide for glioblastoma. *N Engl J Med*. 2005 Mar 10;352(10):987-96. doi: 10.1056/NEJMoa043330. PMID: 15758009.

Stupp R, Taillibert S, Kanner A, Read W, Steinberg D, Lhermitte B, Toms S, Idbaih A, Ahluwalia MS, Fink K, Di Meo F, Lieberman F, Zhu JJ, Stragliotto G, Tran D, Brem S, Hottinger A, Kirson ED, Lavy-Shahaf G, Weinberg U, Kim CY, Paek SH, Nicholas G, Bruna J, Hirte H, Weller M, Palti Y, Hegi ME, Ram Z. Effect of Tumor-Treating Fields Plus Maintenance Temozolomide vs Maintenance Temozolomide Alone on Survival in Patients With Glioblastoma: A Randomized Clinical Trial. *JAMA*. 2017 Dec 19;318(23):2306-2316. doi: 10.1001/jama.2017.18718. Erratum in: *JAMA*. 2018 May 1;319(17):1824. PMID: 29260225; PMCID: PMC5820703. Taal W, Oosterkamp HM, Walenkamp AM, Dubbink HJ, Beerepoot LV, Hanse MC, Buter J, Honkoop AH, Boerman D, de Vos FY, Dinjens WN,

Enting RH, Taphoorn MJ, van den Berkmortel FW, Jansen RL, Brandsma D, Bromberg JE, van Heuvel I, Vernhout RM, van der Holt B, van den Bent MJ. Single-agent bevacizumab or lomustine versus a combination of bevacizumab plus lomustine in patients with recurrent glioblastoma (BELOB trial): a randomised controlled phase 2 trial. *Lancet Oncol*. 2014 Aug;15(9):943-53. doi: 10.1016/S1470-2045(14)70314-6. Epub 2014 Jul 15. PMID: 25035291.

Tandel SG, Biswas M, Kakde GO, Tiwari A, Suri SH, Turk M, Laird JR, Asare CK, Ankrah AA, Khanna NN, Madhusudhan KB, Saba L, Suri JS. A Review on a Deep Learning Perspective in Brain Cancer Classification. *Cancers (Basel)*. 2019 Jan 18;11(1):111. doi: 10.3390/cancers11010111. PMID: 30669406; PMCID: PMC6356431.

Touat M, Li YY, Boynton AN, Spurr LF, Iorgulescu JB, Bohrson CL, Cortes-Ciriano I, Birzu C, Geduldig JE, Pelton K, Lim-Fat MJ, Pal S, Ferrer-Luna R, Ramkissoon SH, Dubois F, Bellamy C, Currimjee N, Bonardi J, Qian K, Ho P, Malinowski S, Taquet L, Jones RE, Shetty A, Chow KH, Sharaf R, Pavlick D, Albacker LA, Younan N, Baldini C, Verreault M, Giry M, Guillerm E, Ammari S, Beuvon F, Mokhtari K, Alentorn A, Dehais C, Houillier C, Laigle-Donadey F, Psimaras D, Lee EQ, Nayak L, McFaline-Figueroa JR, Carpentier A, Cornu P, Capelle L, Mathon B, Barnholtz-Sloan JS, Chakravarti A, Bi WL, Chiocca EA, Fehnel KP, Alexandrescu S, Chi SN, Haas-Kogan D, Batchelor TT, Frampton GM, Alexander BM, Huang RY, Ligon AH, Coulet F, Delattre JY, Hoang-Xuan K, Meredith DM, Santagata S, Duval A, Sanson M, Cherniack AD, Wen PY, Reardon DA, Marabelle A, Park PJ, Idhah A, Beroukhim R, Bandopadhyay P, Bielle F, Ligon KL. Mechanisms and therapeutic implications of hypermutation in gliomas. *Nature*. 2020 Apr;580(7804):517-523. doi: 10.1038/s41586-020-2209-9. Epub 2020 Apr 15. PMID: 32322066; PMCID: PMC8235024.

Tsuruta M, Sugitani Y, Sugimoto N, Miyoshi D. Combined Effects of Methylated Cytosine and Molecular Crowding on the Thermodynamic Stability of DNA Duplexes. *Int J Mol Sci*. 2021 Jan 19;22(2):947. doi: 10.3390/ijms22020947. PMID: 33477917; PMCID: PMC7833394.

Vaubel RA, Tian S, Remonde D, Schroeder MA, Mladek AC, Kitange GJ, Caron A, Kollmeyer TM, Grove R, Peng S, Carlson BL, Ma DJ, Sarkar G, Evers L, Decker PA, Yan H, Dhruv HD, Berens ME, Wang Q, Marin BM, Klee EW, Califano A, LaChance DH, Eckel-Passow JE, Verhaak RG, Sulman EP, Burns TC, Meyer FB, O'Neill BP, Tran NL, Giannini C, Jenkins RB, Parney IF, Sarkaria JN. Genomic and Phenotypic Characterization of a Broad Panel of Patient-Derived Xenografts Reflects the Diversity of Glioblastoma. *Clin Cancer Res*. 2020 Mar 1;26(5):1094-1104. doi: 10.1158/1078-0432.CCR-19-0909. Epub 2019 Dec 18. PMID: 31852831; PMCID: PMC7056576.

Vijapura C, Saad Aldin E, Capizzano AA, Policeni B, Sato Y, Moritani T. Genetic Syndromes Associated with Central Nervous System Tumors. *Radiographics*. 2017 Jan-Feb;37(1):258-280. doi: 10.1148/rg.2017160057. Epub 2016 Dec 2. PMID: 27911673. Vuong HG, Nguyen TQ, Ngo TNM, Nguyen HC, Fung KM, Dunn IF. The interaction between TERT promoter mutation and MGMT promoter methylation on overall survival of glioma patients: a meta-analysis. *BMC Cancer*. 2020 Sep 21;20(1):897. doi: 10.1186/s12885-020-07364-5. PMID: 32957941; PMCID: PMC7504655.

Wang Z, Li Z, Fu Y, Han L, Tian Y. MiRNA-130a-3p inhibits cell proliferation, migration, and TMZ resistance in glioblastoma by targeting Sp1. *Am J Transl Res.* 2019 Dec 15;11(12):7272-7285. PMID: 31934277; PMCID: PMC6943444.

Wang Q, Hu B, Hu X, Kim H, Squatrito M, Scarpace L, deCarvalho AC, Lyu S, Li P, Li Y, Barthel F, Cho HJ, Lin YH, Satani N, Martinez-Ledesma E, Zheng S, Chang E, Sauvé CG, Olar A, Lan ZD, Finocchiaro G, Phillips JJ, Berger MS, Gabrusiewicz KR, Wang G, Eskilsson E, Hu J, Mikkelsen T, DePinho RA, Muller F, Heimberger AB, Sulman EP, Nam DH, Verhaak RGW. Tumor Evolution of Glioma-Intrinsic Gene Expression Subtypes Associates with Immunological Changes in the Microenvironment. *Cancer Cell.* 2017 Jul 10;32(1):42-56.e6. doi: 10.1016/j.ccell.2017.06.003. Erratum in: *Cancer Cell.* 2018 Jan 8;33(1):152. PMID: 28697342; PMCID: PMC5599156. Weed DL. Weed DL. Do Cell Phones Cause Brain Tumors? Another Piece of the Puzzle. *J Natl Cancer Inst.* 2022 May 9;114(5):643-644. doi: 10.1093/jnci/djac043. PMID: 35350076; PMCID: PMC9086749.

Weller M, Felsberg J, Hartmann C, Berger H, Steinbach JP, Schramm J, Westphal M, Schackert G, Simon M, Tonn JC, Heese O, Krex D, Nikkhah G, Pietsch T, Wiestler O, Reifenberger G, von Deimling A, Loeffler M. Molecular predictors of progression-free and overall survival in patients with newly diagnosed glioblastoma: a prospective translational study of the German Glioma Network. *J Clin Oncol.* 2009 Dec 1;27(34):5743-50. doi: 10.1200/JCO.2009.23.0805. Epub 2009 Oct 5. PMID: 19805672.

Weller M, Tabatabai G, Kästner B, Felsberg J, Steinbach JP, Wick A, Schnell O, Hau P, Herrlinger U, Sabel MC, Wirsching HG, Ketter R, Bähr O, Platten M, Tonn JC, Schlegel U, Marosi C, Goldbrunner R, Stupp R, Homicsko K, Pichler J, Nikkhah G, Meixensberger J, Vajkoczy P, Kollias S, Hüsing J, Reifenberger G, Wick W; DIRECTOR Study Group. MGMT Promoter Methylation Is a Strong Prognostic Biomarker for Benefit from Dose-Intensified Temozolomide Rechallenge in Progressive Glioblastoma: The DIRECTOR Trial. *Clin Cancer Res.* 2015 May 1;21(9):2057-64. doi: 10.1158/1078-0432.CCR-14-2737. Epub 2015 Feb 5. PMID: 25655102.

Wen PY, Weller M, Lee EQ, Alexander BM, Barnholtz-Sloan JS, Barthel FP, Batchelor TT, Bindra RS, Chang SM, Chiocca EA, Cloughesy TF, DeGroot JF, Galanis E, Gilbert MR, Hegi ME, Horbinski C, Huang RY, Lassman AB, Le Rhun E, Lim M, Mehta MP, Mellingshoff IK, Minniti G, Nathanson D, Platten M, Preusser M, Roth P, Sanson M, Schiff D, Short SC, Taphoorn MJB, Tonn JC, Tsang J, Verhaak RGW, von Deimling A, Wick W, Zadeh G, Reardon DA, Aldape KD, van den Bent MJ. Glioblastoma in adults: a Society for Neuro-Oncology (SNO) and European Society of Neuro-Oncology (EANO) consensus review on current management and future directions. *Neuro Oncol.* 2020 Aug 17;22(8):1073-1113. doi: 10.1093/neuonc/noaa106. PMID: 32328653; PMCID: PMC7594557.

Wen PY, Weller M, Lee EQ, Alexander BM, Barnholtz-Sloan JS, Barthel FP, Batchelor TT, Bindra RS, Chang SM, Chiocca EA, Cloughesy TF, DeGroot JF, Galanis E, Gilbert MR, Hegi ME, Horbinski C, Huang RY, Lassman AB, Le Rhun E, Lim M, Mehta MP, Mellingshoff IK, Minniti G, Nathanson D, Platten M, Preusser M, Roth P, Sanson M, Schiff D, Short SC, Taphoorn MJB, Tonn JC, Tsang J, Verhaak RGW, von Deimling A, Wick W, Zadeh G, Reardon DA, Aldape KD, van den Bent MJ. Glioblastoma in adults: a Society for

Neuro-Oncology (SNO) and European Society of Neuro-Oncology (EANO) consensus review on current management and future directions. *Neuro Oncol.* 2020 Aug 17;22(8):1073-1113. doi: 10.1093/neuonc/noaa106. PMID: 32328653; PMCID: PMC7594557. Wick W, Platten M, Meisner C, Felsberg J, Tabatabai G, Simon M, Nikkhah G, Papsdorf K, Steinbach JP, Sabel M, Combs SE, Vesper J, Braun C, Meixensberger J, Ketter R, Mayer-Steinacker R, Reifenberger G, Weller M; NOA-08 Study Group of Neuro-oncology Working Group (NOA) of German Cancer Society. Temozolomide chemotherapy alone versus radiotherapy alone for malignant astrocytoma in the elderly: the NOA-08 randomised, phase 3 trial. *Lancet Oncol.* 2012 Jul;13(7):707-15. doi: 10.1016/S1470-2045(12)70164-X. Epub 2012 May 10. PMID: 22578793.

Wirsching HG, Galanis E, Weller M. Glioblastoma. *Handb Clin Neurol.* 2016;134:381-97. doi: 10.1016/B978-0-12-802997-8.00023-2. PMID: 26948367.

Yang P, Zhang W, Wang Y, Peng X, Chen B, Qiu X, Li G, Li S, Wu C, Yao K, Li W, Yan W, Li J, You Y, Chen CC, Jiang T. IDH mutation and MGMT promoter methylation in glioblastoma: results of a prospective registry. *Oncotarget.* 2015 Dec 1;6(38):40896-906. doi: 10.18632/oncotarget.5683. PMID: 26503470; PMCID: PMC4747376.

Yin AA, Zhang LH, Cheng JX, Dong Y, Liu BL, Han N, Zhang X. The predictive but not prognostic value of MGMT promoter methylation status in elderly glioblastoma patients: a meta-analysis. *PLoS One.* 2014 Jan 13;9(1):e85102. doi: 10.1371/journal.pone.0085102. PMID: 24454798; PMCID: PMC3890309.

RINGRAZIAMENTI

Non è facile, dopo aver profuso tanto impegno, fare sintesi di situazioni e sentimenti che hanno attraversato, lungo questi anni, non solo questo percorso accademico, ma anche e soprattutto la concretezza dei giorni ordinari. Mi viene in aiuto una delle parole più significative in ogni lingua: grazie. Da questa prospettiva sarà un po' più semplice.

Ho un senso di gratitudine profonda per il Dott. Milo Frattini e per la Dott.ssa Samantha Epistolio: senza la loro professionalità, accompagnata da grande acume intellettuale, senso critico, limpidezza del pensiero, garbo dei modi e infinita pazienza, questo lavoro non avrebbe visto la luce.

Non riconosco in me l'afflato di dedizione tipico del ricercatore: anche per questo motivo la mia professione è quella del medico ospedaliero, che ai lunghi tempi della ricerca preferisce l'orizzonte della giornata, al termine della quale si raccoglie quanto speso anche per un solo paziente. In quest'ottica cerco di essere un buon patologo, guidato e ispirato dal Prof. Luca Mazzucchelli e dal Prof. Renzo Boldorini: il primo il mio attuale primario, l'altro il mio mentore negli anni della specializzazione; le loro sensibilità differenti, eppure unite dalla medesima passione, competenza ed esperienza mi hanno accompagnato e formato, permettendomi anche di intraprendere questo programma di dottorato di ricerca.

Volutamente cito soltanto i nomi più significativi, ma in questo momento sono numerosi i volti che tengo ben presenti: colleghi e professionisti di grande spessore, che continuano a ricordarmi perché valga la pena di vivere questa difficile professione nel migliore dei modi. Di non minore importanza sono le storie, le vite dei nostri pazienti: loro, loro soltanto costituiscono la motivazione profonda di ogni mio, nostro sforzo.

Per questo mi piace terminare queste pagine con poche righe che arrivano dall'altra parte del mondo, scritte da Kenji Miyazawa (1896-1933), poeta e agronomo giapponese: le solite coincidenze (che, forse, tali non sono) me le hanno ricordate al momento giusto:

Non lo vince la pioggia

Non lo vince il vento

Non lo vince la neve, o la calura dell'estate

Ride sempre di un sorriso tranquillo

Osserva attento, ascolta, capisce

E non dimentica

Se ad est c'è un bimbo malato, va a curarlo

Se ad ovest c'è una madre stanca, va a sorreggere il suo covone di riso

Se a sud c'è qualcuno vicino alla morte, gli va a dire che non serve aver paura

Se a nord c'è una lite o una disputa legale, esclama: smettetela con tali sciocchezze

In tempo di siccità versa le sue lacrime

Questa è la persona

Che voglio diventare